Sonic hedgehog promotes myogenic differentiation of multipotent mesenchymal stromal stem cells to vascular smooth muscle cells in vitro

A dissertation submitted for the degree of MSc

Maryam Alshamrani, BSc, MSc.

Under the Supervision of Dr. Roya Hakimjavadi

Vascular Biology & Therapeutics Group

School of Biotechnology

Faculty of Science & Health

Dublin City University

Dublin 9, Ireland

December 2023

Declaration

I hereby certify that this material, which I now submit for assessment on the programme of study leading to the award of Master of Science is entirely my own work, and that I have exercised reasonable care to ensure that the work is original, and does not to the best of my knowledge breach any law of copyright, and has not been taken from the work of others save and to the extent that such work has been cited and acknowledged within the text of my work.

Signed: _ _ _____ ID No.: ___14210392_____ Date: _04/12/2023__

Acknowledgements

I would like to thank my supervisor for all of the help and guidance. I want to thank all my friends and colleagues for their support during my studies. Finally, I would like to thank my family for supporting and encouraging me over the last years at DCU.

Table of Contents

List of Figures

List of Tables

List of Abbreviations:

ABC- Adventitial progenitor cells

BCA - Bicinchoninic Acid

BSA – Bovine Serum Albumin

CNN – Calponin

CVD – Cardio Vascular Disease

DAPI - 4',6-diamidino-2-phenylindole

DES – Drug Eluting Stents

DMEM – Dulbecco's Modified Essential Medium

DMSO - Dimethyl Sulfoxide

DNA – Deoxyribose Nucleic Acid

EMEM – Eagle's Minimum Essential Medium

FBS – Fetal Bovine Serum

GFP – Green Fluorescent Protein

MSC – Mesenchymal Stem Cell

P/S – Penicillin-Streptomycin

PBS – Phosphate Buffer Saline

PCR – Polymerase Chain Reaction

RIPA - Radioimmunoprecipitation Assay

RT – Reverse transcriptase

RT – Room Temperature

SDS-PAGE - Sodium Dodecyl Sulfate Polyacrylamide Gel Electrophoresis

Shh – Sonic hedgehog

SMC – Smooth Muscle Cell

TEMED- Tetramethylethylenediamine

TGFβ – Transforming Growth Factor Beta

TMB - 3,3',5,5' Tetramethylbenzidine

αMEM – Minimal Essential Medium

Abstract

Author: Maryam Alshamrani

Thesis Title: Sonic hedgehog promotes myogenic differentiation of multipotent mesenchymal stromal stem cells to vascular smooth muscle cells in vitro

Introduction: Cardiovascular diseases (CVDs) are a major global health concern, often involving the dysfunction and remodelling of blood vessels. The sonic hedgehog (SHh) signalling pathway has been implicated in the regulation of vascular cell fate during development and disease. This study aimed to investigate the role of SHh signalling in the myogenic differentiation of mesenchymal stem cells (MSCs) and adventitial progenitor cells (APCs) into vascular smooth muscle cells (SMCs) in vitro.
Methods: Mouse bone marrow-derived MSCs and rat Sca1+ adventitial progenitor cells were cultured and treated with recombinant SHh (r-SHh) protein, as well as SHh pathway inhibitors cyclopamine, HPI-4, and anti-Patched1 antibody. Cell viability was assessed using the Alamar Blue assay. The expression of SMC differentiation markers calponin (CNN1) and myosin heavy chain 11 (MYH11) was evaluated by immunocytochemistry, Western blotting, and real-time qRT-PCR.
Results: Treatment with r-SHh significantly increased the expression of CNN1 and MYH11 in both MSCs and APCs, as demonstrated by immunocytochemistry and Western blot analysis. This effect was attenuated by the SHh pathway inhibitors cyclopamine, HPI-4, and anti-Patched1 antibody. Real-time qRT-PCR further confirmed the upregulation of the SHh target gene Gli1 and the SMC marker CNN1 in response to r-SHh, which was reduced by cyclopamine treatment.
Discussion and Conclusion: The results of this study indicate that SHh signalling plays a crucial role in promoting the myogenic differentiation of MSCs and APCs into vascular SMCs in vitro. Targeting the SHh pathway may offer a potential therapeutic strategy for the management of cardiovascular diseases characterized by aberrant vascular remodelling.

Chapter 1: Introduction

1.0 General Overview

Cardiovascular diseases (CVDs) are a collection of many heart illnesses that usually affect the functionality of the heart and blood vessels. CVD cases are prevalent in developing and developed countries such as Ireland and the United States. Exposure to risk factors such as cigarette smoke, high cholesterol levels, high blood pressure, and depression among others may lead to the development of heart disease. Blood vessels are the most affected by CVD since they facilitate the transportation of blood and essential material for metabolism to and from other body organs. The arteries are affected by arteriosclerosis, which is due to rupture of the inner walls of the vessels thereby leading to their blockage. The body provides mechanisms of repairing damaged or old intimal cells from numerous sources. Also, the treatment of arteriosclerosis is based on the genetic factors causing the disease in humans. The morphogen Hedgehog (Hh) signalling pathway components are significantly up-regulated within diseased arterial blood vessels of injured mice concomitant with enhanced accumulation of smooth muscle cells (SMCs); an effect that is attenuated in vivo following Hh receptor depletion. In this context, Hh signalling is an important regulator of stem cell self-renewal and differentiation to SMC in vitro.

1.1 CVD statistics in Ireland, the EU, and the US

Cardiovascular diseases (CVD) are widespread in the developed countries and economic blocs such as the United States, and European Union among others. According to Bennette (2007), the condition involves blood clot, structural problems, and diseased vessels of the heart. Also, other heart disorders related to CVD are ischemic and hemorrhagic stroke, heart valve problems, arrhythmia, and heart failure (Sanchis-Gomar et al., 2016). More than seventeen million patients die from CVDs per year whereby seven million are due to coronary

heart disease and six million due to stroke (Benjamin et al., 2017). The high mortality rate is due to exposure to risk factors such as diabetes and hypertension.

The diseases cause more than thirty percent of all global deaths that are linked to diseases (Luengo-Fernández et al., 2006). Stroke and heart disease are the major killers and challenges to Ireland's medical department. However, the mortality rate of heart disease has been reducing over the years with a gap of forty-seven percent due to increased rehabilitation programmes, seminars, and workshops to educate the public the dangers of cholesterol-rich products, blood pressure, and smoking to heart's health (Stock & Redberg, 2012). According to Bhatnagar et al. (2016), cases of cardiovascular diseases in the European Union have been increasing due to exposure to risk factors. Conversely, strategies are underway to overcome the challenge by establishing a mechanism to address the issue such as encouraging practices that eliminate risk factors. On the other hand, the United States faced high mortalities due to public use of risky products such as cholesterol oils for cooking (Benjamin et al., 2017). The country developed measures to prevent the disease such as educating the public on healthy lifestyles.

1.2 Major Causes of CVD

According to Leon and Maddox (2015), heart disease is the major cause of fatal deaths especially women and children in the middle class population. In fact, more than 90% of CVD-linked deaths are caused by a single risk factor. Causes of the diseases include smoking, depression, weight, family medical history, high blood pressure, diabetes, and high cholesterol levels (Wang, et al.,2010). Smoking is considered the major cause of heart diseases and high mortality since cigarettes, cigars, and pipes damage blood vessels, thus reducing the amount of oxygen that transmit through blood. According to Khan et al. (2015), cigarette smoke stick on artery walls, which increase chances of forming clots leading to heart attack or stroke.

High cholesterol levels are prevalent in arteries and they distort the normal flow of blood. Women are at a higher risk of developing a heart attack or brain disorder due to high LDL levels that lower the amount of oxygen in the heart (Anand, et al., 2015). Rosano et al. (2007) show that excessive body inactivity or lack of exercise increases weight around the stomach, which increase a risk of developing CVD. It is believed that women whose waist circumference measures more than eighty centimetres are at risk of developing a heart attack. Other factors that may lead to the development of heart diseases include menopause in women, ageing, polycystic ovary syndrome, ethnic background, and hypertension among others (Dosi et al., 2014).

1.3 Structure of the Vessel Wall

According to Moore et al. (2003), blood vessels are tubular and circular structures that transmit from one location to another in the body of living organisms. There are three types of blood vessels namely capillaries, veins, and arteries. The arteries transmit oxygen-rich blood from the heart to other body parts such as the stomach, brain, legs, liver, and kidney except for the pulmonary artery (Thijssen, Carter, & Green, 2016). Capillaries offer a large surface area of exchange of material between blood and other body organs and cells. Veins carry blood rich in waste products such as carbon (IV) oxide to the heart. The vessels have different structures and components based on their activities to enhance the increased functionality of the body (Hochauf, Sternitzky, & Schellong, 2007).

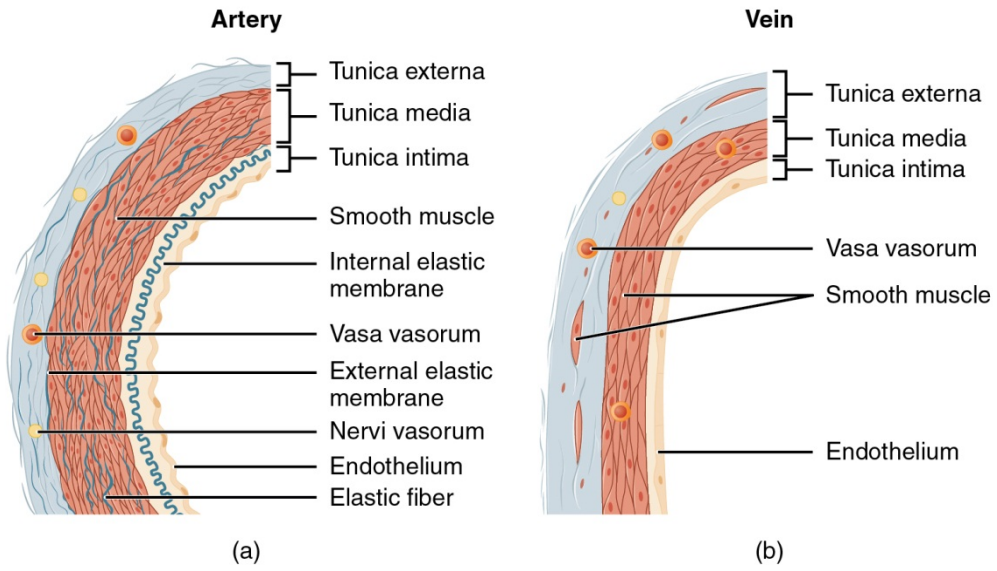

Figure 1: Structure of a typical blood vessel wall. The vessel wall consists of three main layers: (A) Tunica intima, the innermost layer, composed of endothelial cells and a thin layer of connective tissue; (B) Tunica media, the middle layer, primarily made up of smooth muscle cells and elastic fibres; and (C) Tunica externa (also called adventitia), the outermost layer, consisting mainly of connective tissue. This structure allows blood vessels to maintain blood pressure and regulate blood flow. (Taken from OpenStax, Anatomy & Physiology. OpenStax CNX. Aug 1, 2017 http://cnx.org/contents/14fb4ad7-39a1-4eee-ab6e-3ef2482e3e22@8.108 The Cardiovascular System: Blood Vessels and Circulation)

The artery wall is made up of three layers namely tunica intima, tunica media, and tunica externa (West, et al., 2010). Tunica intima is a squamous epithelium with connective tissues and elastic fibres at the basement membrane. Tunica adventitia is made up of elastic connective tissue with collagenous fibres. Tunica media is the thickest and consists of smooth muscles. On the other hand, the vein wall is composed of the tunica similar to the arteries. However, veins have thinner walls compared to arteries due to the absence of connective tissues and smooth muscles (Ramasamy, 2017). Thus, blood in veins has less pressure than in arteries but the wider space in veins make them hold more than seventy percent of blood at any given

time. Lastly, the capillaries link arteries to veins through the arterioles and venules respectively. Skeletal muscles and organs with increased metabolic activities have an extensive network of capillaries while connective tissue usually lacks capillaries (Pugsley & Tabrizchi, 2000). Figure 1, above, illustrates the typical structure of a blood vessel wall.

1.4 Aetiology of Arteriosclerosis and Atherosclerosis

Arteriosclerosis, also known as atherosclerosis, is a progressive and slow condition that develops from injuries of the inner walls of the arteries, thus causing them to thicken and stiffen (Bergheanu, Bodde, & Jukema, 2017). The stiffness slows down the flow of blood of the heart to other parts of the body, thus decreasing body cells oxygen required for significant metabolic activities (O`Connor, et al., 2011). Factors that cause the illness include high cholesterol levels, high blood pressure, triglycerides in the blood, insulin resistance, diabetes, smoking, inflammations, and obesity among others. Andrus, et al. (2015) show that cholesterol particles in the blood accumulate on the walls of arteries causing the development of plaques, which affects cell population in the vessels. It is believed that prolonged plaque formation without treatment may lead to their rupture and form blood clots that prevent the flow of blood. Figure 2 illustrates the difference between a normal artery and one affected by atherosclerosis.

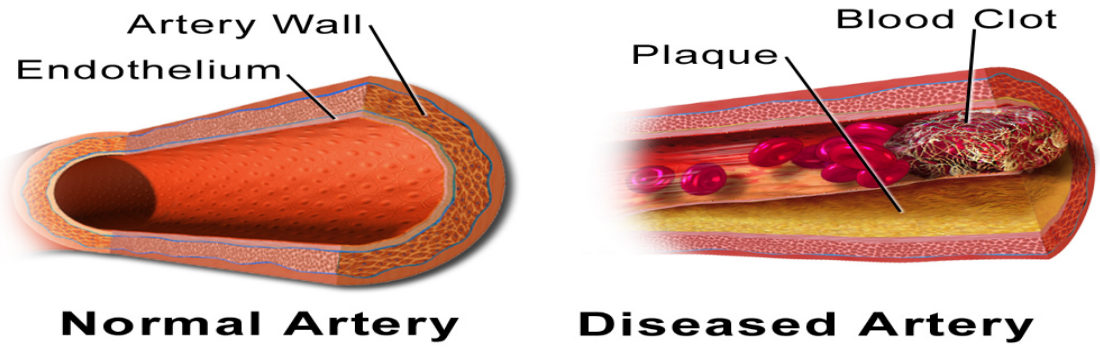

Figure 2: Comparison between a normal human artery (left) and an artery affected by atherosclerosis (right). In the normal artery, blood flows freely through a clear lumen. The atherosclerotic artery shows significant narrowing due to the build-up of plaque, which consists of cholesterol, fatty substances, cellular waste products, calcium, and fibrin. This

narrowing restricts blood flow and can lead to serious cardiovascular events. (Taken from Blausen.com staff (2014). "Medical gallery of Blausen Medical 2014". WikiJournal of Medicine1 (2). DOI:10.15347/wjm/2014.010. ISSN 2002-4436. - Own work)

According to Hurst, Kendall, and Khandheria (2007), intimal-media thickening (IMT) is a marker of arteriosclerosis that is used to measure the thickness of tunica media and tunica intima. The IMT is measured through invasive ultrasound catheters, external ultrasound as well as several other imaging modalities. Yelle (2002) shows that IMT values that are higher than 75 percentile (ASE) or 0.9 mm (ESC) are abnormal and the individuals require an immediate checkup and diagnosis. On that note, carotid artery ultrasound scan provides reliable results for the treatment of patients with atherosclerosis. However, the scan leads to increased chance of development of familial hypercholesterolemia, rheumatoid arthritis, type 2 diabetes, air pollution, high-density lipoprotein cholesterol (HDL-C) triglycerides, and non-alcoholic fatty liver disease among others (Cobble & Bale, 2010).

The excessive accumulation of vascular smooth muscle cells (SMC) in arteries leads to the proliferation and worsening of heart diseases such as arteriosclerosis, pulmonary hypertension, inflammation, and restenosis among others (Simova, 2012). According to Rudijanto (2007), the vascular SMC-like cells conduct myosin-actin interactions, thus acting as stromal cells for regulating blood pressure and arterial contractile tonus. It is evident that VSMCs secrete insoluble extracellular matrix (ECM) that withstands blood pressure in the arteries (Chistiakov, Orekhov, & Bobryshev, 2015). VSMCs plasticity and chromatin remodelling change DNA accessibility to transcription factors, which involves myocardia, P300, Kruppel-like factor 4, and serum responsive factor (Bennett, Sinha, & Owens, 2016). Figure 3 provides a detailed view of the different cell populations within the vessel wall

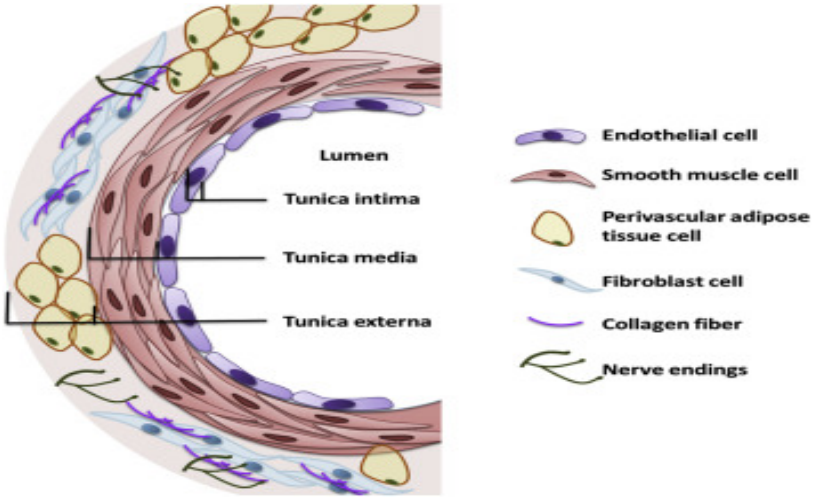

Figure 3: Cross-section of a vessel wall showing different cell populations. The diagram illustrates the three main layers of the vessel wall: intima, media, and adventitia. Key cell types are highlighted, including endothelial cells lining the lumen, smooth muscle cells in the media, and fibroblasts in the adventitia. The figure also shows the presence of vasa vasorum in the adventitia, which are small blood vessels that supply the vessel wall itself. (Taken from Zhao et al,Vascular nitric oxide: Beyond eNOS, Journal of Pharmacological Sciences,Volume 129, Issue 2, 2015, Pages 83-94, ISSN 1347-8613,

1.5 Stem Cells

1.5.1 General Overview

According to Biehl and Russell (2009), a stem cell is an undifferentiated cell of eukaryotes that give rise to cells of the same kind. They are essential in the development of tissues to repair the internal system and replenish other cells. The cell can remain as a stem cell or become a specialised one with specific functions such as red blood cell, muscle cell, or brain cell among others (Biehl & Russell, 2009). Stem cells are unspecialised and can renew themselves through cell division after a long inactivity period. According to Hotkar and Balinsky (2012), the cells can also be induced through certain conditions to become specific to organs or tissues.

It is important to note that the division of stem cells relies on the actual organs they are acting upon (Baker & Bruno, 2016). For instance, they are used to replace or repair damage to bone marrow and gut cells. They are also used in regenerating new cells in the pancreas and heart under special conditions (Faiella & Atoui, 2016). The ability of stem cells to divide plays a crucial role in enhancing growth and development of infants as well as increasing functionality of adult human cells in the body. According to Hotkar and Balinsky (2012), the inner cells of a blastocyst can give rise to any type of cells, tissue, or organ in the body such as lungs and heart among others.

1.5.2 Types of Stem Cells

There are numerous types of stem cells used in the regeneration of cells, tissues, and organs in living organisms (Baker & Bruno, 2016). The cells enhance growth and differentiation as well as the provision of cells that generate essential body organ, which usually grows up to adulthood (Faiella & Atoui, 2016). According to Hotkar and Balinsky (2012), essential stem cells include embryonic, the tissue-specific, mesenchymal, and induced pluripotent stem cells among others. First, the embryonic stem cells are acquired from the inner parts of a blastocyst. It is believed that the inner cells of a blastocyst divide and gives rise to new specialised cells that form organs and tissues of the body (Faiella & Atoui, 2016). However, the cells are grown in vitro conditions to maintain their properties, thus becoming stem cells. These cells are pluripotent but cannot give rise to umbilical cord and placenta (Biehl & Russell, 2009). They provide resources for understanding the development of diseases in humans and conducting therapeutic tests.

Second, the induced pluripotent stem cells (iPS) are cells developed in vitro to give rise to cells that behave the same way as embryonic stem cells (Faiella & Atoui, 2016). On that note, it is clear that the cells help in understanding disease prevalence, testing new drugs, and progression and development of ailments. According to Larijani et al. (2012), iPS cells can

give rise to any kind of cell in the body, which makes them crucial in medical treatments Figure 4 provides an overview of different types of stem cells and their potential applications in regenerative medicine and research. Third, the tissue-specific stem cells are also referred to as somatic stem cells and have specialised functions. According to Biehl and Russell (2009), the cells help in generating new cells in an organ in which they reside. For instance, hematopoietic stem cells in the bone marrow give rise to white and red blood cells as well as platelets.

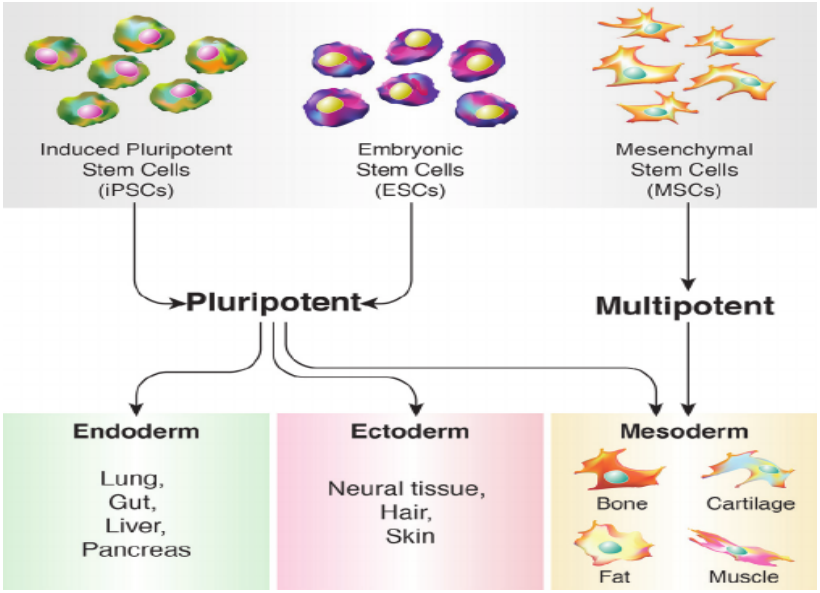

Figure 4: Overview of different types of stem cells and their potential applications. The figure illustrates the progression from totipotent stem cells (capable of forming all cell types including extra-embryonic tissues) to pluripotent stem cells (embryonic stem cells and induced pluripotent stem cells), and finally to multipotent stem cells (such as mesenchymal stem cells). Each type of stem cell is shown with its differentiation potential and possible therapeutic applications, including tissue regeneration, drug discovery, and disease modelling. (Taken from Stem cell therapies for treating osteoarthritis: prescient or premature?
Deanne J. Whitworth, Tania A. Banks Vet J. 2014 Dec; 202(3): 416–424)

Lastly, the mesenchymal stem cells (MSCs) are prevalent in a connective tissue that surrounds organs and tissues in the body called stroma (Sylvester & Longaker, 2004). It is clear

that bone marrow offered the first stromal cells, which are used in the regeneration of fat, cartilage, and bone cells. The cells are believed to have immunomodulatory properties and stem cell characteristics, which boosts their usage in the medical field for diagnosis and treatment of arterial infections (Watt & Driskell, 2010). According to Nguyen, Rhee, and Wu (2016), the MSCs differ based on their use, characteristics, origin, and impact on the body of living organisms. Therefore, the application requires ultimate care to ensure the selected cells meet the required goals.

1.5.3 Resident Vascular Stem Cells

The resident vascular stem cells are the MSCs that are prevalent in adult tissues and within blood vessels. According to Hotkar and Balinsky (2012), the common vascular stem cells (VSCs) populations include adventitial progenitor cells (APCs) and pericytes among others. The evidence of pericytes rely on pericyte-specific markers. However, the pericytes are sophisticated and functionally diversified to possess a large differentiation capacity (Sun et al., 2016).

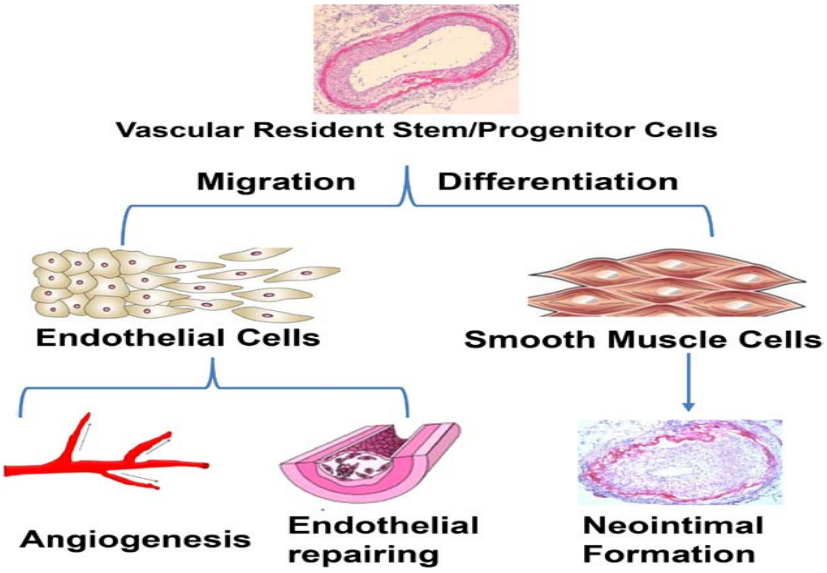

Figure 5: Illustration of vascular resident stem cell migration and differentiation. The figure shows how resident vascular stem cells, including pericytes and adventitial progenitor cells, can be activated in response to vascular injury or disease. These cells can migrate to the site of

injury and differentiate into various cell types including smooth muscle cells, endothelial cells, and fibroblasts, contributing to vascular repair and remodelling. The diagram also highlights the paracrine effects of these cells, which can influence the behaviour of surrounding cells and tissues. (Taken from Xie, Yao et al. "Vascular Regeneration by Stem/Progenitor Cells." *Arteriosclerosis, thrombosis, and vascular biology* 36 5 (2016): e33-40.)

On the contrary, APCs are more naïve functionally and tend to be the best MSCs. The cells are induced in *vitro* to divide into endothelial cells, SMCs, and MSCs (Faiella & Atoui, 2016). It is important to note that the resident VSCs have paracrine capacity that maintains tissue homeostasis and encourages differentiation and replication of MSCs. The vascular system is crucial in maintaining tissue homeostasis and response to injuries. The endothelial cells are heterogeneous in terms of cell surface expression, self-renewal, and proliferation capacity (Perin, 2006). Figure 5 illustrates the process of vascular resident stem cell migration and differentiation in response to vascular injury or disease.

1.6 Hedgehog Signalling

1.6.1 Morphogen, History, and Biology

According to Taipale et al. (2002), hedgehog signalling is a medical pathway that utilises morphogen such as sonic hedgehog to direct patterning, cell division, differentiation, and development of embryos. The morphogen is encoded for by sonic hedgehog gene (SHh), which is found in chromosome 7 in humans. According to Lee et al. (2001), the hedgehog gene (Hh) was discovered in *Drosophila melanogaster* in the early 1980s. The mammalian signalling pathway is composed of the SHh, deserat hedgehog (DHH), and Indian hedgehog (IHH). SHh is crucial in human organogenesis, which the Wolpert's model describes as the best morphogen (Varjosalo & Taipale, 2007; Bijlsma, et al., 2006; Pan & Zhou, 2012). The

model involves diffusing molecules that form a concentration gradient, which affects embryonic cells differently.

The ligand is translated as ~45kDa precursor that undergoes autocatalytic processing to release a ~20kDa N-terminal and a ~25kDa C-terminal (Rimkus et al., 2016; Choudhry, et al., 2014). It is important to note that SHh binds to Patched-1 (PTCH1) receptor, which inhibits the activity of the Smoothened (SMO) protein.

According to Lu, Wang, and Shen (2017); and Paulis et al., (2015), there are numerous Hh mechanisms that involve co-receptors, receptors, downstream Gli signalling, and adaptor proteins. Sonic hedgehog is the most studied ligand pathway present in most vertebrates. Figure 6 illustrates the key components and mechanisms of the Sonic Hedgehog signalling pathway

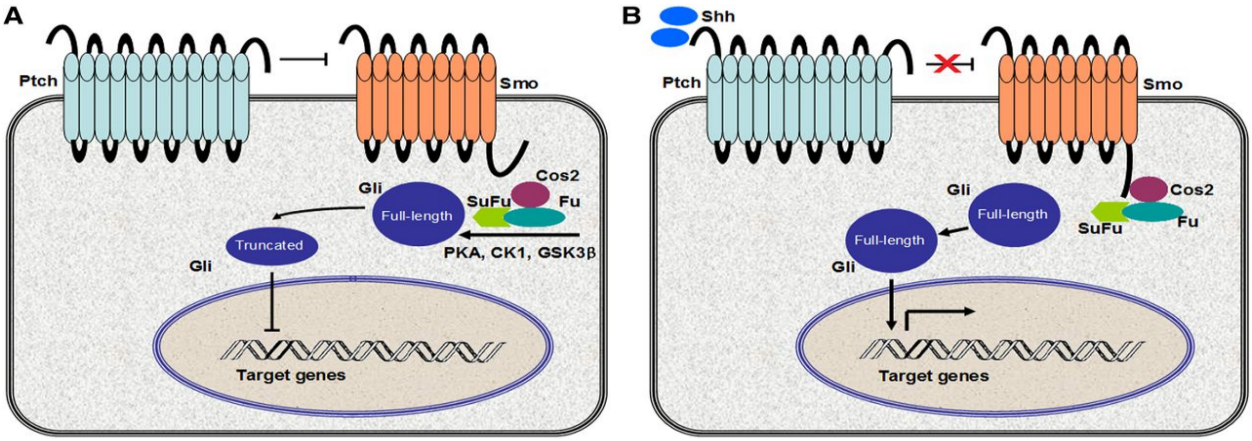

Figure 6: Schematic representation of the Sonic Hedgehog (Shh) signaling pathway. In the absence of Shh ligand (left panel), Patched (Ptch) inhibits Smoothened (Smo), leading to the proteolytic processing of Gli transcription factors into repressor forms (GliR). When Shh binds to Ptch (right panel), the inhibition on Smo is relieved, allowing it to activate full-length Gli proteins (GliA), which then enter the nucleus to activate target gene transcription. Key proteins involved in this pathway include Shh, Ptch, Smo, Suppressor of Fused (SuFu), and Gli1/2/3.(Taken from Hu et al, Molecular Pharmacology February1,2015, 87 (2) 174-182; DOI: https://doi.org/10.1124/mol.114.095141)

1.6.2 Importance to Vascular Development

Vascular development is the formation of blood vessels in humans, which is initiated by a primary capillary plexus to definitive vasculature (Hooper & Scott, 2005). It is believed that growth regulation and emergent of vascular development in a blood vessel is a complex mechanism, which is yet to be understood. Incardona, Gruenberg, and Roelink (2002) show that signalling pathways and growth factors are significant in the development of definitive vasculature. It is important to note that Hh signalling to certain parts such as cardiomyoblast and perivascular cells are essential for the growth and development of coronary veins and arteries respectively. In fact, Hh signalling is a conserved mechanism that addresses embryonic development in many organs and regeneration of cells and tissues after injuries (Lee, Zhao, & Ingham, 2016).

1.6.3 Signalling pathway and hedgehog signalling in CVD models

According to Pan and Zhou (2012), the Hh protein leads to the activation of classical ligand-dependent signalling transduction in the development of cardiovascular diseases. The inflammation and expression of hypoxia-induced factor-1 (HIF-1) in ischemic tissues usually activates the SHh signalling cascade in a Gli-dependent manner (Pan & Zhou,2012). The activation of the signalling pathway promotes EPCs, MSCs, and myocardial progenitors thereby differentiating into cardiomocytes. Resident stem cells play a crucial role in remodelling and vascular formation in physiological conditions. Vascular stem cells are inactive in their niches; however, they are activated to participate in SMCs accumulation and endothelial layer to form neointima (Zhang, et al., 2018). Figure 7 provides a detailed view of the Sonic Hedgehog receptors and co-receptors involved in initiating the signalling cascade.

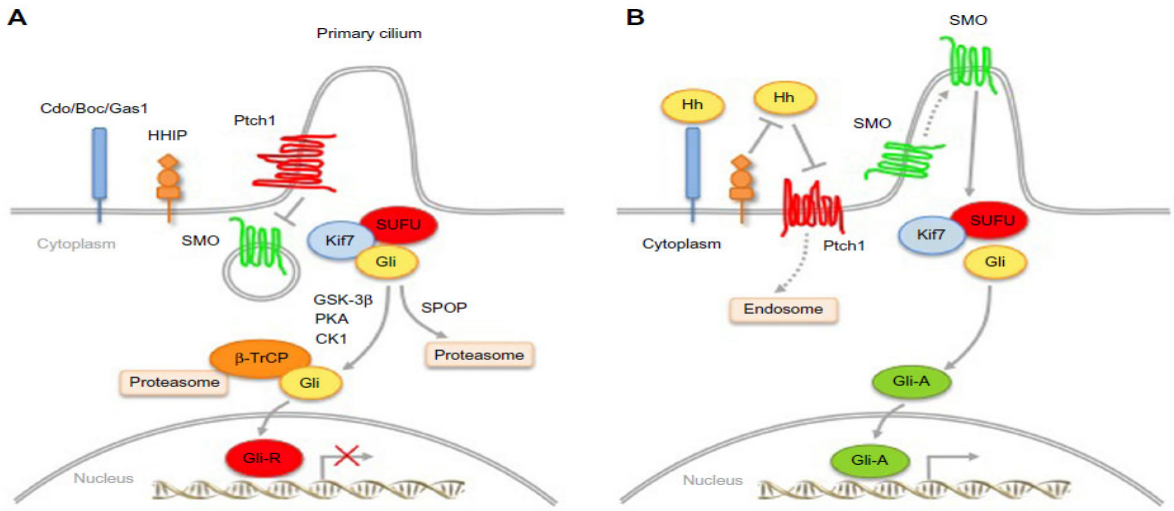

Figure 7: Diagram showing Sonic Hedgehog receptors and co-receptors. The primary receptor Patched1 (Ptch1) and co-receptors including Cell adhesion molecule-related/down-regulated by oncogenes (Cdo), Brother of Cdo (Boc), and Growth arrest-specific 1 (Gas1) are depicted. The figure illustrates how these receptors interact with the Sonic Hedgehog (Shh) ligand on the cell surface, initiating the signaling cascade that ultimately leads to the activation of Gli transcription factors and subsequent gene expression changes. (Taken from Pandolfi S, Stecca B. Cooperative integration between HEDGEHOG-GLI signalling and other oncogenic pathways: implications for cancer therapy. Expert Reviews in Molecular Medicine. 2015;17:e5.

1.6.4 Hedgehog Control of Stem Cell Fate

The Hh pathway is a crucial morphogen regulator of activities during embryo development and regulation of stem cell self-renewal (Tigges, Komatsu, & Stallcup, 2013). It is evident that the establishment of adventitious progenitors and resident multipotent vascular stem cells enhanced the understanding of origin of vascular smooth muscle cells during lesion formation, repair of injured or worn out vessels, and cardiovascular disease progression (Mooney, et al., 2015). The components of Notch and Hh signalling pathways have a putative role in the differentiation of vascular stem cells to vascular lineages. According to Mooney, et

al. (2015), the Hh pathway is a transcriptional machinery that enhances ischemia-induced postnatal neovascularisation, early vascular development, as well as the formation of muscularised blood vessels.

According to Infante et al. (2015), Hh signalling is advantageous in the treatment of cancer due to its aberrant activation capabilities. The activation of SMO downstream Hh signalling and drug resistance influences the inactivation of SMO inhibitors (Villavicencio, Walterhouse, & Iannaccone, 2000; Hui & Angers, 2011). Also, the targeting of glioma-associated oncogenes (Gli) proteins, which are isolated from the glioblastoma cells in humans, determines the cell fate in Hh signalling pathway. Aza-Blanc et al. (2000) show that the Gli effectors offer a promising and futuristic strategy in the fight against cancer tumours that depend on the hedgehog pathway. In addition, the recognition and determination of the structural requirements of the interaction between DNA and Gli factors in humans are crucial in drug discovery and treatment of cardiovascular diseases (Ruiz et al., 2002; Lovrics et al., 2014).

According to Jiang et al. (2006), the Gli transcription factors translate the concentration gradient of SHh to different fates through a complex regulatory network. The Gli factors bind to Gli responsive genes and interact with the new transcription complex, thus facilitating the inhibition or activation of transcription in humans (Wang et al., 2010). It is important to note that transcription is initiated through the zinc finger domains in DNA that binds consensus sequences on specific genes to suppress of activating transcription (Merchant, et al.,2010; Jacob & Briscoe, 2003). Proteins that enable the Gli factors inhibition or activation of gene transcription include Missing in Metastasis (MIM/BEG4) and human TFIID TATA box-binding proteins. Lastly, the synergistic action of MIM and Gli proteins induces epidermal growth and Shh grafts (Passman et al., 2008).

According to Lavine, et al. (2008), a colocalisation of hedgehog responsive cells in the adventitial areas of vessels is in conjunction with recapitulation of Notch and Hh in the medial layer. The medial layer concomitant appears as stem cells arising from smooth muscle cells after an injury to the vessels. Huang and Kalderon (2014) show that a hedgehog-Nitch stem cell population regenerates neointimal muscle cells to support formation of neointimal and vascular remodelling as the disease progresses. Local inhibition of Hh-Notch axis attenuates the generation SMCs in CVD models of vascular injury and controls the fate of vascular cell after an injury (Wagers, 2012).

1.7 Source of Intimal Cells Following Injury

1.7.1 Dedifferentiation of Contractile Smooth Muscle Cells

Numerous molecular transitions characterise the differentiation of smooth muscle cells, which involves an increase in cytoskeletal proteins and contractile apparatus such caldesmon, calponin, myosin heavy chain, and alpha-smooth muscle actin (Chen et al., 2016a). The differentiation also leads to a decrease in the expression of proteins such as fibronectin splice variants with extra domains A (EDA) and B (EDB). The dedifferentiation of contractile SMCs offers new intimal cells after an injury to an artery (Chang, et al., 2014). The SMCs are found in the inner intima, which has high expressions of EDA and EDB as well as a low expression of contractile and cytoskeletal protein. The inner intima exhibits progressive intimal thickening that involves generation of new cells in areas of cytolytic necrosis (Chen et al., 2016b).

1.7.2 Bone Marrow-Derived Stem Cells that Undergo Myogenic Differentiation

Smooth muscle cells and SMC-like cells such as intimal cells can be regenerated through transdifferentiation of endothelial cells, vascular resident stem cells, bone marrow cells, and adventitial fibroblasts (Westerweel & Verhaar, 2008). Bone marrow (BM) progenitors have the capability of differentiating into SMC, which is essential for vascular remodelling and angiogenesis. The intimal cells are derived from SMC acquired from the bone

marrow and haematopoietic stem cells. Neointimal SMCs present in chimeric scenarios and transgenic bone marrow are derived from haematopoietic stem cells (Xynos et al., 2010). Galli, Vitale, & Vaccarezza (2014) show that lineage tracing and confocal studies indicate that some SMC-like cells from the bone marrow and atherosclerotic lesions do not have a haematopoietic origin.

1.7.3 Resident Vascular Stem Cell that Undergo Myogenic Differentiation

The intimal accumulation of SMCs favours progression and development of restenosis and atherosclerotic lesions. The resident vascular stem cell dedifferentiates, migrate, and proliferate from the tunica media to the intima (Lin & Lue, 2013). Stem antigen-expressing cells are abundant in the vascular lesions, which are not easy to detect in the tunica media. Therefore, it is clear that resident stem cells may be accumulated in the neointima, whereby they may cause lesions. The contribution of vascular stem cells in remodelling has positive as well as negative effects on plaque stabilization (Lin & Lue, 2013). Resident vascular stem cell undergoes myogenesis to regenerate cells and tissues that overcomes degenerative muscle diseases (Lin & Lue, 2013; Zhang et al., 2018). The stem cells reprogram their fate and usually enter a myogenic pathway that facilitates regeneration of new intimal cells after destruction.

1.7.4 Endothelial-mesenchymal Stem Cell Transition (EndMT) that Undergo Myogenic Differentiation

According to Dejana, Hirschi, and Simons (2017), the endothelial cells show crucial phenotypic variability prevalent in the cardiovascular system such as the plasticity of endothelial-to-mesenchymal transition (EndMT). The cells are crucial in the regeneration of intimal cells after a rupture, whereby they lose cell-cell junctions due to VE-cadherin, which leads to the acquisition of migratory and invasive properties (Lin, Wang, and Zhang, 2012). In addition, they gain mesenchymal markers and lose numerous endothelial markers (Coll-Bonfill, et al., 2015). EndMT undergoes myogenic differentiation, which leads to the formation

of neointimal cells. TGF-β signalling activation dedifferentiates the endothelial cells to acquire SMC-like and mesenchymal phenotype (Souilhol et al., 2018).

1.8 Treatment of Atherosclerosis

Arteriosclerosis is a life-threatening condition that affects blood flow in arteries and is indicated by decreased blood pressure in the affected areas, weak pulse in the arteries, as well as bruits on the vessels (Martínez-Rubio & Pamias, 2017). Treatment involves undergoing medical tests such as Doppler ultrasound, blood test, ankle-brachial index, stress test, electrocardiogram, angiogram, and cardiac catheterisation among others. According to Insull (2009), treatment for the disorder involves lifestyle changes such as regular exercising and healthy dieting and maintaining hand hygiene. Nonetheless, the medical specialist may prefer surgical or medical procedure based on the severity of the condition.

According to Klingenberg and Hansson (2009), the medication involves prescription of drugs that may lower or reverse the effects of the disorder. Essential drugs include cholesterol medications, beta-blocker, anti-platelet, calcium channel blockers, diuretics, and angiotensin-converting enzyme inhibitors among others. Cholesterol medications lower the low-density lipoprotein (LDL) cholesterol and enhance the high-density lipoprotein (HDL) cholesterol (Muhlestein, 2003). Lowering LDL levels promote reversing the fatty deposits in the vessels through the use of drugs such as fibrates and statins, which prevents atherosclerosis. Anti-platelet drugs such as aspirin help in preventing clumping of platelets in arteries, thus lowering the risk of blood clot (Giacoppo et al.,2015). On the other hand, beta-blockers lower blood pressure and heart rate, thus reducing chances of developing heart rhythm problems and attack (Kalanuria, Nyquist, & Ling, 2012). In addition, the application of ACE inhibitors, calcium channel blockers, and water pills known as diuretics lowers the risk of developing high blood pressure (Spence, 2016).

It is important to note that some medical devices are used in the medication and surgeries for cardiovascular diseases (Lewis, 2009). Devices prevalent in the diagnosis and treatment of heart disease include imaging machines, implantable devices such as fit pacemakers, Cardioverter Defibrillators (ICDs) and cardiac resynchronisation therapy (CRT) devices, MRI scanners, and cardiac resynchronisation therapy (CRT) pacemakers among others (Riccioni & Sblendorio, 2012). Buccheri et al. (2016) show that the left ventricular assist devices (LVADs) are the mainly used devices for heart disease to support the functionality of the heart until a donor's heart is available for transplantation.

Restenosis is the continuous narrowing of blood vessels usually arteries thus restricting the flow of blood from the heart to other body parts (Byrne, Joner, & Kastrati, 2015). The treatment and management of in-stent restenosis (ISR) is a clinical challenge that is complicated by recurrences, thus leading to prolonged clinical treatments. According to Akin and Nienaber (2015), bare-metal ISR is used in the treatment but patients with drug-eluting stents (DES) also suffer from the ISR. Diagnosis and treatment are done through catheterisation and tests such as optical coherence tomography (OCT) and intravascular ultrasound (IVUS) (Hamid & Coltart, 2007). Also, angioplasty is an essential treatment technique for arteries as it widens the lumen and increases blood flow.

1.9 Genetics of Arteriosclerosis

Hedgehog signalling is a medical pathway that transmits information to cells for the division, differentiation, and growth (Wang et al., 2004; Sing, Stengård, & Kardia, 2003; Biros, Karan, & Golledge, 2008). It is important to note that different embryonic sections have different signalling proteins associated with numerous diseases such as basal cell carcinoma and cardiovascular diseases. According to Lander (2011), arteriosclerosis has multiple environmental and genetic contributions in causing stroke and artery diseases. There are genetic and non-genetic risk factors for heart disease, whereby family history is considered the

most crucial risk factor. Thus, diseases associated with CVD such as familial hypercholesterolemia (FH) avails little explanation on the susceptibility of heart disease (Holdt & Teupser, 2012).

According to Lusis et al. (2005), arteriosclerosis emerges from interactions of environmental and genetic factors, which usually cannot cause the disease as a single entity. More than ninety percent of Atrioventricular septal defects (AVSDs) cases require rapid and regular screening and surgery to overcome the detrimental effects of the condition. Peden et al. (2011) show that cilia-required sonic hedgehog (Shh) signalling drives atrioventricular septation. It is evident that the GLI family of transcription factors (TFs) transduces Hh signalling in patients with arteriosclerosis. According to Hansson (2005), the cardiogenic TF TBX5 and GLI TFs conduct a genetic interaction, which shows the activities of cardiogenic TFs and Hh signalling-dependent GLI TFs in gene regulatory of atrioventricular septation to determine the molecular basis of cardiovascular diseases.

In addition, Single Nucleotide Polymorphisms (SNPs) shows the alterations in DNA sequence at a single nucleotide position (Salazar et al., 2000). It is important to note that the alteration can be due to insertion, deletion, or changes in the base pairs, which is usually detected through recognition of restriction sites. SNP analysis of arteriosclerosis in arteries can be conducted through sequence-specific oligonucleotide (SSO) hybridization, hybridization array technologies, or reverse dot blot analysis (Musunuru & Kathiresan, 2010). The use of SNP helps in determination of ruptured arteries since they are numerous in mammalian genomes, easy to achieve robust multiplex amplification, and presence of many techniques of identifying SNPs (Wang et al., 2004; Kovacic & Bakran, 2012). This helps in the treatment and analysis of the genetic basis of cardiovascular diseases.

Aims of the study

The aims of the study are;

- To determine the effect of hedgehog inhibitors, cyclopamine and HPI-4 on bone marrow derived mesenchymal stem cells (MSCs) viability and growth *in vitro.*
- To determine the effects of recombinant sonic hedgehog on myogenic differentiation of bone marrow derived mesenchymal stem cells (MSCs) to SMC in *vitro* by examining the expression of SMC differentiation markers (calponin 1; Cnn1 and myosin heavy chain 11: Myh11) in the absence or presence of smoothened inhibitor (cyclopamine), Gli inhibitor (HPI-4) and an anti-ptch1 receptor antibody.
- To determine the effects of recombinant sonic hedgehog on myogenic differentiation of resident vascular stem cells (rat adventitial Sca1+ MSC-like cells) to SMC in *vitro* by examining the expression of SMC differentiation markers (calponin 1; Cnn1 and myosin heavy chain 11: Myh11) in the absence or presence of smoothened inhibitor (cyclopamine), Gli inhibitor (HPI-4) and an anti-ptch1 receptor antibody.

Chapter 2: Materials and Methods

2.1.1Materials

Materials supplementary document is attached separately.

2.1.2Methods

2.2 Cell Culture

Sterile Bio air 2000MAC laminar flow cabinet was used to carry out cell culture work.

2.2.1 Culture of Mouse mesenchymal stem cells (mMSC)

mMSC cell line was purchased from Invitrogen Gibco Cat No. S1502-100. The cells were cultured in MEM-alpha Gibco medium with GlutaMAX-1 supplemented with 10% fetal bovine serum (FBS) MSC Qualified, and Gentamicin 5µg/mL, and maintained in a 37°C humidified atmosphere of 5% CO2 /95% air using a Hera water jacketed cell culture incubator. The cells were cultured between passages 8-15 in 75cm2 and 25cm2 flasks and were routinely fed every 2-3 days. Sub-culturing of the cells was carried out at 80-90% confluency by using 25% dilution of TrypleE.

2.2.2 Culture of Rat Sca1+ Adventitial progenitor cells (rAPCs)

rAPC cells were isolated from the adventitial layer of the rat blood vessels. Sca1+ cells were isolated using EasySep™ Mouse SCA1 Positive Selection Kit.

2.2.3 Cell Counting:

Cell counting was carried out using haemocytometer in terms of obtaining the number of viable cells. 1:1 of cells suspension was mixed gently with Trypan Blue, so 20µl of cells suspension with 20µl of Trypan Blue. 20µl of that suspension was added slowly and deliberately into the counting chambers under the coverslip.

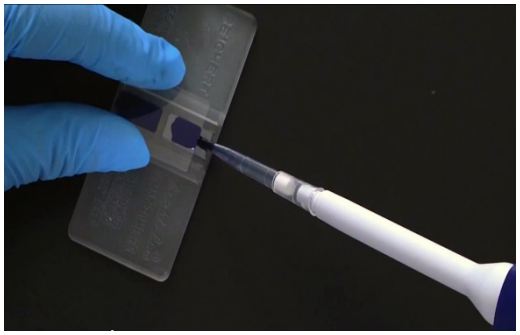

Figure 8: Haemocytometer cell counting slide.

Viable cells will appear bright under the microscope because they do not take up the dye. Four of the chambers were counted, and the total number was divided by 4, and that's number multiply by dilution factor and 10^4 to obtain the number of cells/mL.

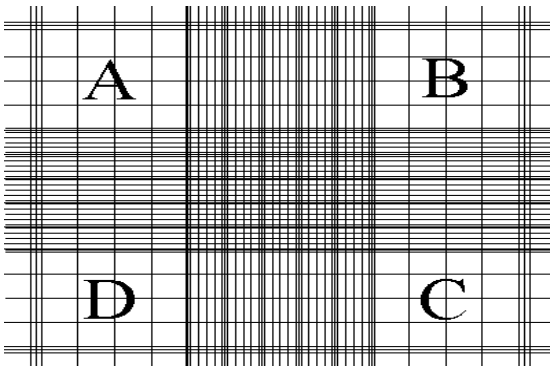

Figure 9: The 4 chambers of Haemocytometer cell counting slide

2.2.4 Cell Line Authentication and Mycoplasma Testing

The mMSC cell line (Invitrogen Gibco, Cat No. S1502-100) and rAPC cells were authenticated using Short Tandem Repeat (STR) profiling performed by ATCC's Cell Line Authentication Service. The STR profiles of these cell lines were compared to known profiles in the ATCC database to confirm their identity. Mycoplasma testing was performed monthly using the MycoAlert Mycoplasma Detection Kit (Lonza, Cat No. LT07-318). Briefly, 2 mL of

cell culture supernatant was centrifuged at 200 x g for 5 minutes. 100 µL of the supernatant was transferred to a luminescence-compatible 96-well plate, and the assay was performed according to the manufacturer's instructions. Luminescence was measured using a GloMax Navigator Microplate Luminometer (Promega). A ratio of B/A > 1 indicated mycoplasma contamination. All cell lines used in this study tested negative for mycoplasma contamination.

2.2.5 Cryogenic Cell Storage

Cells were stored in liquid nitrogen cryo-freezer unit -196°C for long-term maintenance. Cells were trypsinised from the flask, centrifuged for 5 minutes at 1000 rpm, and the pellet was resuspended in freeze down media which was consisted of fresh media, FBS and DMSO. The final concentration depends on companies' recommendation. The suspension was then transferred to sterile cryovials and frozen at -80°C at the rate of –1°C/minute using a Mr Freeze® cryo-freezing container overnight and later transferred to a cryo-freezer unit.

2.2.6 Recovery of Cells

Cells were thawed quickly at 37°C and resuspended in growth medium, centrifuge it for 5 minutes at 1000 rpm, and the cell pellet was resuspended in fresh medium and transferred to a culture flask.

2.3 Alamar Blue assay:

The Alamar Blue assay was used to assess cell viability and proliferation, based on the ability of metabolically active cells to reduce the Alamar Blue reagent, resulting in a colorimetric change that can be quantified.

2.3.1 Cell Seeding and Treatment

Cells (mMSCs or rAPCs) were seeded in 96-well plates at a density of 5×10^3 cells per well in 100 µL of complete growth medium. The plates were incubated at 37°C in a humidified atmosphere of 5% CO_2 for 24 hours to allow cell attachment. After 24 hours, the medium was replaced with fresh medium containing the test compounds or growth factors.

Control wells received an equivalent volume of the vehicle (0.1% DMSO) used to dissolve the test compounds. Each condition was tested in triplicate.

2.3.2 Alamar Blue Addition and Incubation

After 48 hours of treatment, 10 µL of Alamar Blue reagent (10% of the culture volume) was added to each well, including control wells containing medium only (no cells). The plates were gently shaken to ensure mixing and then incubated at 37°C in the dark for 4 hours.

2.3.3 Fluorescence Measurement

Following the 4-hour incubation, fluorescence was measured using a T-can plate reader (Tecan, Switzerland) with excitation at 540 nm and emission at 590 nm. The plate reader was set to read from the bottom of the plates with an optimal gain.

2.3.4 Data Analysis

The fluorescence values were exported to Microsoft Excel for analysis. The average fluorescence of the medium-only control wells was subtracted from all other values to account for background fluorescence. Cell viability was calculated as a percentage of the untreated control cells using the following formula: *% Viability = (Fluorescence of treated cells / Fluorescence of untreated control cells) × 100.* For proliferation studies, a standard curve was generated by plating known numbers of cells (ranging from 1×10^3 to 5×10^4 cells per well) and measuring their fluorescence after 4 hours of Alamar Blue incubation. This standard curve was used to estimate cell numbers in treated wells. Data from at least three independent experiments were analysed using Microsoft Excel. One-way ANOVA followed by Dunnett's multiple comparisons test was used to determine statistical significance between treated groups and the untreated control. P-values < 0.05 were considered statistically significant.

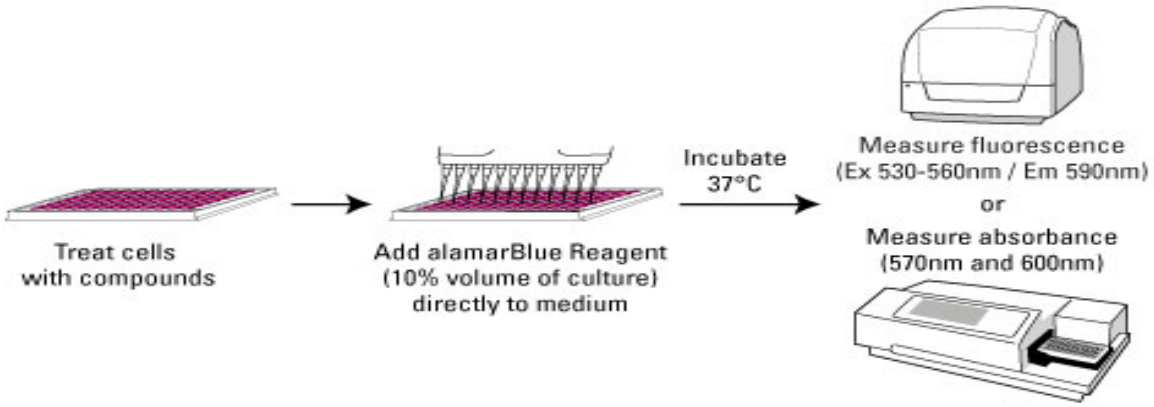

Figure 10: Schematic representation of the Alamar Blue assay procedure. (A) Cells are seeded in 96-well plates and treated with test compounds. (B) Alamar Blue reagent is added to the wells and incubated for 4 hours. (C) The plate is read using a fluorescence plate reader. (D) Representative fluorescence data showing the metabolic activity of treated cells for 48 hours. Data are presented as mean ± SEM of three independent experiments, each performed in triplicate. Statistical significance was determined by one-way ANOVA followed by Dunnett's multiple comparisons test. *$p < 0.05$, **$p < 0.01$ compared to untreated control. (Taken from Thermo scientific protocol).

2.4 Immunocytochemistry

Sterile coverslips were prepared by sterilizing them in IMS for 2 hours and washed up to 5 times in sterile PBS, and then they were placed into a 6-well plate, each coverslip in a well. For clear and best visualisation cells were seeded at low density (1-5,000 cells/well) the required volume of cells suspension was added on top of the sterile coverslip. The next day the medium was removed and the required medium which was composed of drugs, growth factors, peptide or maintenance medium was added to the seeded cells and left in the incubator for the long of period desired. After the treatment time was finished, the medium was removed and cells were washed with PBS, and fixed by using 3.7% of formaldehyde for 15 minutes at room temperature. Cells were permeabilized for intracellular staining using 0.025% Triton X-100 for

10-15 minutes. Cells were blocked for non-specific binding sites using blocking buffer which was composed of 5% BSA and 0.3M glycine in 1% Tween PBS solution for 1 hour at room temperature.

The primary antibody was prepared by diluting it in blocking buffer at the appropriate concentration depends on companies' recommendation, and added to the coverslips. 1mL of the dilution was sufficient to cover coverslips; however, 500µL was adequate as well. Cells were left overnight at 4°C to allow the primary antibody to bind. The next day, the primary antibody was removed and cells were washed up 3 times with PBS. The secondary antibody was diluted in the blocking buffer at the appropriate concentration, for (Alexa Fluor 488) dye labelling, 1:1000 concentration is sufficient. The secondary antibody was added to the wells and incubated for 1hr at room temperature. The secondary antibody was then removed and cells were washed up 3 times with PBS as per previous step. Cells nuclei were stained using DAPI with a concentration of (1:1000) and incubated for 15 minutes at room temperature. DAPI was removed and cells were washed up 3 times. The coverslips were mounted onto slides after applying mounting media to slides. 5 images were taken per sample at different magnifications.

Image Acquisition and Analysis

For each treatment condition, five random fields were imaged using a Nikon E100 Fluorescence Microscope, with images captured at 20x magnification using the following filter sets: DAPI (excitation 365 nm, emission 445/50 nm), and FITC (excitation 470/40 nm, emission 525/50 nm. For each field, z-stack images (0.5 µm intervals, 10 slices) were acquired to ensure all cellular structures were captured. Thereafter, the images were processed using ImageJ (NIH) software. For each treatment, at least 100 cells across the five fields were analysed for fluorescence intensity and morphological changes.

For ICC experiments, cells were seeded at a density of 1 x 10^4 cells/cm^2 on sterile glass coverslips in 6-well plates. Drug concentrations used for treatments were as follows: TGFβ1 (10 ng/mL), PDGF-BB (20 ng/mL), Cyclopamine (5 μM), HPI-4 (10 μM), and rShh (1 μg/mL). Image analysis was performed using ImageJ software (NIH, version 1.53c). For quantification, at least 100 cells per condition were analyzed across five random fields. The corrected total cell fluorescence (CTCF) was calculated using the formula: CTCF = Integrated Density - (Area of selected cell × Mean fluorescence of background readings). For morphological analysis, cell area and aspect ratio were measured using the 'Analyze Particles' function in ImageJ after appropriate thresholding.

2.5 SDS-PAGE and Western Blot Analysis

2.5.1 Preparation of Whole Cell Lysates – Protein Harvest

Radioimmunoprecipitation assay (RIPA) lysis buffer was used with 1/100 protease - Inhibitor for protein harvest. Cells were washed 2-3 times in ice cold PBS. Cells were scrapped by using cells scraper to detach the cells from the plate. The cells were transferred to 15mL falcon tube and centrifuged for 5 minutes at 1500rpm. An appropriate of RIPA buffer was added to the pellet. Usually, 80μL is sufficient for medium size pellet in terms to achieve a high concentration of protein. The cells pellet was re-suspended in the RIPA buffer using a pipette and was stored at -80°C.

2.5.2 Bicinchoninic acid (BCA) Assay

The Bicinchoninic acid (BCA) assay was used for protein quantification.

The assay depends on selective calorimetric detection of Cu+ ions by the bicinchoninic acid (BCA). Cu2+ reacts with protein under alkaline conditions and is reduced, producing the cuprous cation (Cu+), with selective colorimetric detection of Cu+ using a reagent containing BCA. The protein concentration is viewed by a colour change of the sample from yellow/ green

to purple. Complex absorbs light at a wavelength of 562 nm. The absorbance measures by using a spectrophotometer (Thermo Scientific). The bovine serum albumin (BSA) protein standards were used and added 25µL to a 96 well plate in triplicate as below:

	Vol of diluent	**BSA vol(µl)**	**BSA conc.(µg/µl)**
A	0	75 of stock	2000
B	37.5	112.5 of stock	1500
C	100	100 of stock	1000
D	50	50 of B	750
E	100	100 of C	500
F	100	100 of E	250
G	100	100 of F	125
H	80	20 of G	25
I	75	0	0

Table1: Serial Dilutions Table for BCA assay. 25µL of each concentration was added to each well.

The kit supplies two solutions, A and B. A is an alkaline bicarbonate solution and B is a copper sulphate solution. A dilution of 1:50 was made, B:A and protected from the light. 200µl of the solution was added to the protein cell lysate and BSA protein standards, protected from the light and incubated at 37°C for 30 minutes. After reading the absorbance, a standard curve was figured out. And an equation was given by the standard curve for example, y=0.6135x+0.3561. By working out the equation X value was given, which is the concentration of the protein.

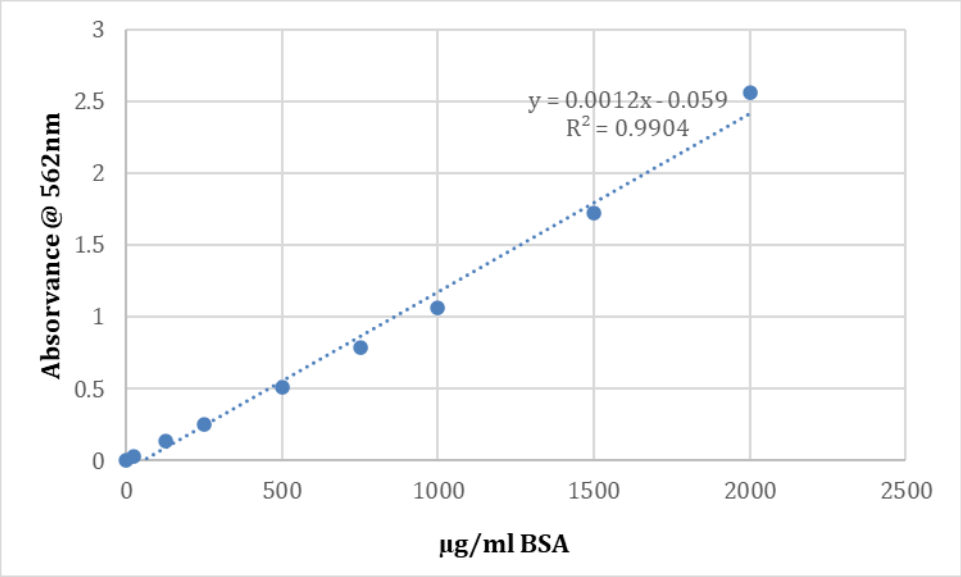

Figure 11: Represents the BCA assay performed to calculate the protein concentration

2.5.3 Western Blotting:

Polyacrylamide gels were prepared in two percentages 12.5% and 7%. The semi- dry Western blot method was used for the transfer process. In addition, nitrocellulose membrane was used.

Component	**12.5%Gel**	**7%Gel**
1.5M Tris-HCl pH8.8 (mL)	1.875mL	1.875mL
10% SDS (µL)	75µL	75µL
dH2O (mL)	2.385mL	3.8mL
10% APS (µL)	37.5µL	37.5µL
30% bis/acrylamide solution (mL)	3.12mL	1.7mL
TEMED	7.5µL	7.5µL

Table2: Resolving gel components

Component	**Stacking gel**
0.5M Tris-HCl	625µL

10% SDS (µL)	25µL
dH2O (mL)	1.54mL
10% APS (µL)	12.5µL
30% bis/acrylamide solution (mL)	325µL
TEMED	10µL

Table3: Stacking gel components

After BCA assay was performed, proteins concentration was determined. Therefore, equal amounts of protein were loaded into each well in the gel. Before that, the sample was prepared by mixing them with the loading buffer which was composed of 4X laemmli sample buffer diluted in β-mercaptoethanol as 3:1. Thereafter, the samples were boiled for 5 minutes at 95°C. The gel electrophoresed and the running buffer (0.025M Tris) was pouring into the electrophoreses rig at 15mA for each gel. It is recommended to pre-run gels for 30 minutes before loading samples to calibrate it. Page ruler plus pre-stained protein ladder was used as a signal for protein size, 10 µl of the page ruler ladder was loaded into the first well, and the 25µl of samples were loaded into the appropriate wells. The gels were run until the dye was at the bottom of the gels.

2.5.4 Transfer protein

Following gel electrophoresis, proteins were transferred from the gels to the membranes by taking out the gels from glass and wash them off with transfer buffer (Thermo scientific) for 30 minutes to remove electrophoresis salts and detergents. One sheet of Whatman (Life Sciences) nitrocellulose membrane was cut for each gel, and 4 sheets of Whatman gel filter paper (Sigma) were cut to fit the size of the gel and were soaked in transfer buffer for the transfer process. Protein transfer was carried out on a cassette PIERCE G2 Fast blotter (Thermo scientific) semi-dry automated system at 25V from 5-10 minutes depends on proteins

molecular weight. To confirm the transfer of the proteins to the membrane Ponceau S staining was used. 10 mL was added to the membrane and it was left on the blots for 3-5 minutes with constant agitation. Red bands on a white background refer to transferred proteins. The membrane then was washed using dH2O.

2.5.5 Immunological probing

Following proteins transfer, the membrane was blocked in a blocking buffer which composed of 0.5% BSA and 0.1% Tween in PBS, for one hour at room temperature. The membrane was washed 3 times with TBS-T washing buffer. Following this, the membrane was probing with the appropriate primary antibody diluted in blocking buffer at 4 °C overnight. The membrane was washed 3 times with TBS-T washing buffer to remove the primary antibody and prepare for the secondary antibody incubation. The secondary antibody (HRP-conjugated) was added to the membrane at the appropriate concentration for one hour at room temperature. The membrane then was washed 3 times. 3, 3',5,5'-Tetramethylbenzidine (TMB, Sigma) was added to cover the blot, to determine if the protein was present on the blot by observing dark blue bands. The membrane was then washed in dH2O to stop the reaction and background staining and the blot was photographed

Antibodies dilutions

Primary antibody	**Dilution**	**Secondary antibody**	**Dilution**
α-Actin (Sigma)	1:10000	HRP-Conjugated Anti-mouse IgG	1:10000
B-Actin (Sigma)	1:5000	HRP-Conjugated Anti-mouse IgG	1:10000
CNN1 (Sigma)	1:5000	HRP-Conjugated Anti-mouse IgG	1:10000
Myosin (Sigma)	1:1000	HRP-Conjugated Anti-mouse IgG	1:10000

Table4: Primary Antibody Dilutions for Immunocytochemistry

.

2.6 Polymerase Chain Reaction (PCR):

2.6.1 RNA isolation

Miniprep system protocol (Promega) was used for the first experiment. The cells were treated with the appropriate treatment. Following cells treatment, the cells were prepared for RNA isolation by scraping them very gently. The cells were centrifuge at 1500rpm for 5 minutes. 1 mL of PBS was added to the pellet and mixed very well. The suspension was centrifuge again at 1500rpm for 5 minutes. The same wash was repeated for the 3rd time but the last one was centrifuge for 1 minute. The pellet was then stored at -80 readies for RNA isolation. In Promega control, for best results, solutions and buffers have to be made immediately prior to use, as follows in the table.

DNase I	Add 80µl Nuclease-free water and gently mix by swilling (do not vortex) Store on ice (-20C long term)
BL+TG buffer	Add 32.5µL of 1-Thioglycerol to 3.25mL of BL buffer. Store between 2-10C
RNA wash solution	Add 20mL 95% ethanol to the bottle containing 11.8mL concentrated RNA wash solution. Store at room temp.
Column wash solution	Add 1.5mL95% ethanol to the bottle containing 1 mL concentrated column wash solution. Store at room temp.

Table 5: Promega protocol (z6010)

The required volume of BL+TG buffer was added to the frozen cell pellet and re-suspended. The cells suspension was collected in a 1.5mL centrifuge tube and it was mixed by vortexing for 30 seconds. Subsequently, the required volume of isopropanol was added and mixed by vortexing again for 5 seconds. 1x Minicolumn, 2x Collection tubes and 1x elution tube for each sample were unpacked and labelled properly. The Minicolumn was placed on the

Collection tube. The lysate was transferred then from the centrifuge tube to the Minicolumn and was centrifuged at 12,000-14,000 xg for 30 seconds at room temp. The Minicolumn and the flow-through were removed and discarded. A new Minicolumn was then replaced in the Collection tube. 500ul RNA wash solution was added to the Minicolumn and centrifuge at 12,000-14,000g for 30 seconds, and the flow-through was discarded. DNase I cocktail was prepared fresh as it is recommended by the company to mix these buffers prior to use.

Solution	**Volume**
Yellow Core Buffer	24µL
MnCl2 0.09M	3µL
DNase I	3µL

Thereafter, 30µl of DNase I incubation mix was added directly onto the Minicolumn membrane until the membrane was fully covered, and incubated for 15 minutes at room temp. 200µl of Column wash solution with ethanol was added to the Minicolumn and centrifuged at 12,000-14,000 xg for 15 seconds. 500µl of RNA wash solution was added and centrifuged at 12,000-14,000 xg for 30 seconds, afterwards, the wash solution and the Collection tube were discarded. The Minicolumn was placed in a new Collection tube, and 300µl of RNA wash solution was added and centrifuged at high speed for 2 minutes. The Minicolumn was transferred from the collection tube to an elution tube. 15µl of Nuclease-Free Water was added to the Minicolumn, and the Minicolumn along with elution tube was placed into the centrifuge with the elution tube lid facing out. Centrifuge at 12,000-14,000 for 1 minute. The Minicolumn was discarded and the elution tube containing the purified RNA was capped and stored at -20°C for long term storage.

2.6.2 Nanodrop samples

The concentration of mRNA obtained from the previous protocol was determined by using The NanoDrop® ND-1000 Spectrophotometer. The samples were kept on ice during measurement. The software for this measurement and analysis was ND 10000 V3.81. When the software was opened, Nucleic acid was choosing from the options, and RNA sample type was selected. 2µl of DEPC treated water was added as a blank, it was pipetted slowly and deliberately onto the end of a fibre optic wire. The second fiber optic wire was brought forward to be in contact with the sample. Afterwards, the sample was added and measured. The NanoDrop takes two absorbance readings at 260nm and 280nm and determines the ratio between them. The quantity of mRNA was showed as ng/µl.

2.6.3 Real time qRT-PCR

Real Time Rotor-GeneRG-3000TM light cycler was using to carry out quantitative PCR. The fundamental behind this is that the fluorescence measured is related to the amount of target gene in the sample, by using designated primer sets, all the primers used were from IDT. The kit used was SensiFAST SYBR No-ROX One-Step kit. The kit contains

Reagent	**100 x 20µl reactions**	**500 x 20µl reactions**
SensiFAST SYBR No-ROX One-Step mix (2x)	1 x 1mL	5 x 1mL
RiboSafe RNase inhibitor	1 x 40µL	1 x 200µL
Reverse Transcriptase	1 x 20µL	1 x 100µL
DEPC-H2O	1 x 1.8 mL	2 x 1.8mL

Table 6: SensiFAST SYBR No-ROX One-Step kit components.

20µl of the final reaction mix was made according to the recommended standard from the company.

Reagent	Volume	Final concentration
2x SensiFAST SYBR NO-ROX One-Step Mix	10µL	1x
10µM Forward Primer	0.8µL	400nM
10µM Reverse Primer	0.8µL	400nM
Reverse transcriptase	0.2µL	-
RiboSafe RNase inhibitor	0.4µL	-
H2O	Up to 16µL	
Template	4µL	
	20µL Final volume	

Table 7: Mastermix for the primers.

For each RT-qPCR experiment, samples were prepared in triplicate with reverse transcriptase (+RT), alongside a single negative control without reverse transcriptase (-RT) and a non-template control (NTC) to assess potential genomic DNA contamination and non-specific amplification, respectively. The thermal cycling program was optimized for each primer set and consisted of the following steps: an initial reverse transcription hold at 45°C for 10 minutes to synthesize cDNA, followed by a polymerase activation hold at 95°C for 2 minutes. The amplification stage comprised 40 cycles of denaturation at 95°C for 10 seconds, annealing at 68°C for 30 seconds, and elongation at 72°C for 30 seconds. Notably, a touchdown PCR approach was implemented during the annealing phase, where the temperature decreased by 1°C per cycle for the first 8 cycles, enhancing primer specificity and reducing non-specific amplification.

Fluorescence data were collected at the end of each elongation phase. Following amplification, a melting curve analysis was performed to confirm product specificity. The

comparative CT method (ΔΔCT) was employed for relative quantification of gene expression, as described by Livak and Schmittgen (2001). This method involves normalizing the CT values of target genes to a reference gene (typically GAPDH or β-actin) and then comparing the normalized values between treated and control samples to calculate fold changes in expression. To ensure reproducibility and statistical robustness, each experiment was performed in triplicate and repeated in three independent biological replicates. Data analysis included the calculation of means, standard deviations, and statistical significance using appropriate tests (e.g., Student's t-test or ANOVA) depending on the experimental design.

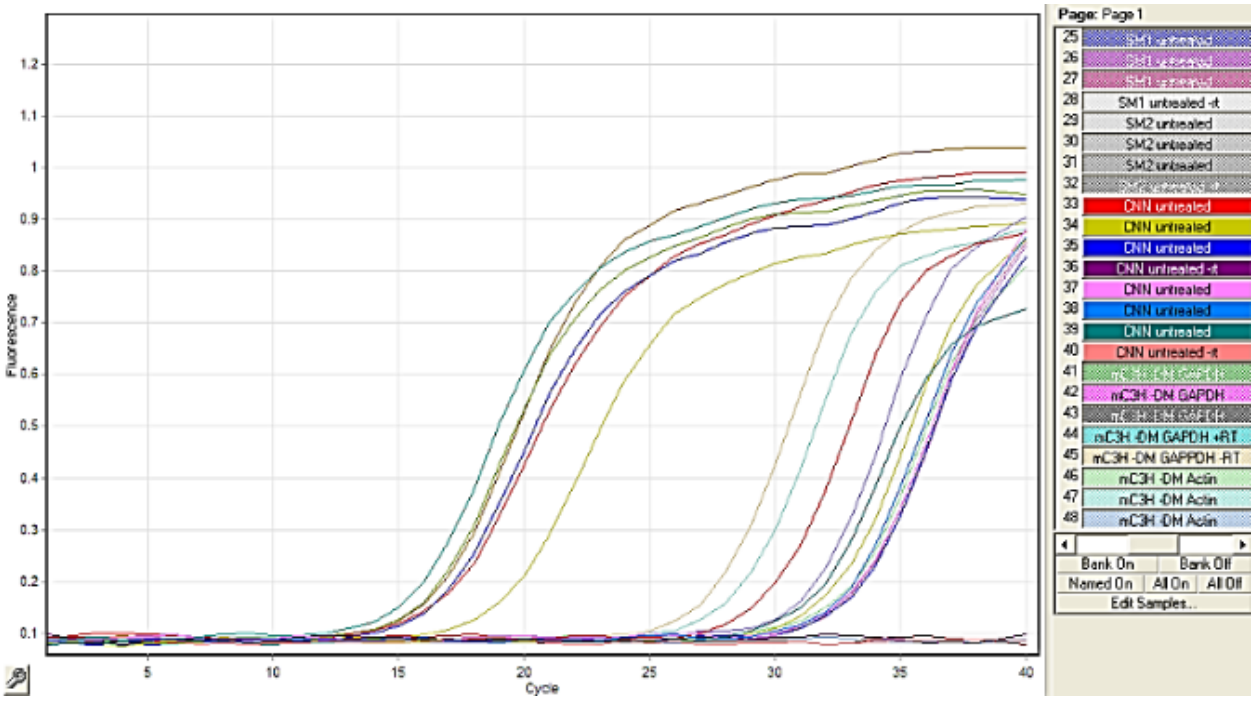

Figure 12: Representative amplification curves from RT-qPCR analysis. The graph shows the normalized fluorescence (ΔRn) plotted against the cycle number for a target gene (solid lines) and the reference gene GAPDH (dashed lines) in control (blue) and treated (red) samples. Each curve represents the mean of technical triplicates. The horizontal green line indicates the threshold for CT determination.

2.7 Statistical Analysis

All statistical analyses were performed using Microsoft Excel. Data are presented as mean ± standard error of the mean (SEM) from at least three independent experiments. For comparisons between two groups, two-tailed unpaired Student's t-tests were used. For multiple group comparisons, one-way ANOVA followed by Tukey's post-hoc test was employed. Two-way ANOVA was used for experiments with two independent variables, followed by Sidak's multiple comparisons test. P-values < 0.05 were considered statistically significant. The specific statistical test used for each experiment is indicated in the respective figure legend.

Chapter 3: Results

3.0 Mouse Mesenchymal Stem Cells

3.1 Effect of Sonic Hedgehog Inhibitors on Growth

3.1.1 Effect of Cyclopamine on mMSC Growth

Objective 1: To determine the cell viability of mMSC cells after treatments with Sonic hedgehog inhibitors, cyclopamine and HPI-4, by checking the growth rate of cells in response to drugs.

Cyclopamine treatment resulted in a dose-dependent decrease in mMSC metabolic activity (Figure 13). Compared to the 0.1% DMSO control, significant reductions in cell viability were observed at concentrations of 20 µM and above ($p < 0.05$, one-way ANOVA with Dunnett's post-hoc test). The IC50 of cyclopamine was approximately 35 µM under these conditions. At the highest concentration tested (100 µM), cyclopamine reduced metabolic activity to levels similar to those observed in the 0.5% serum low-growth control, suggesting a potent inhibitory effect on mMSC proliferation or viability.

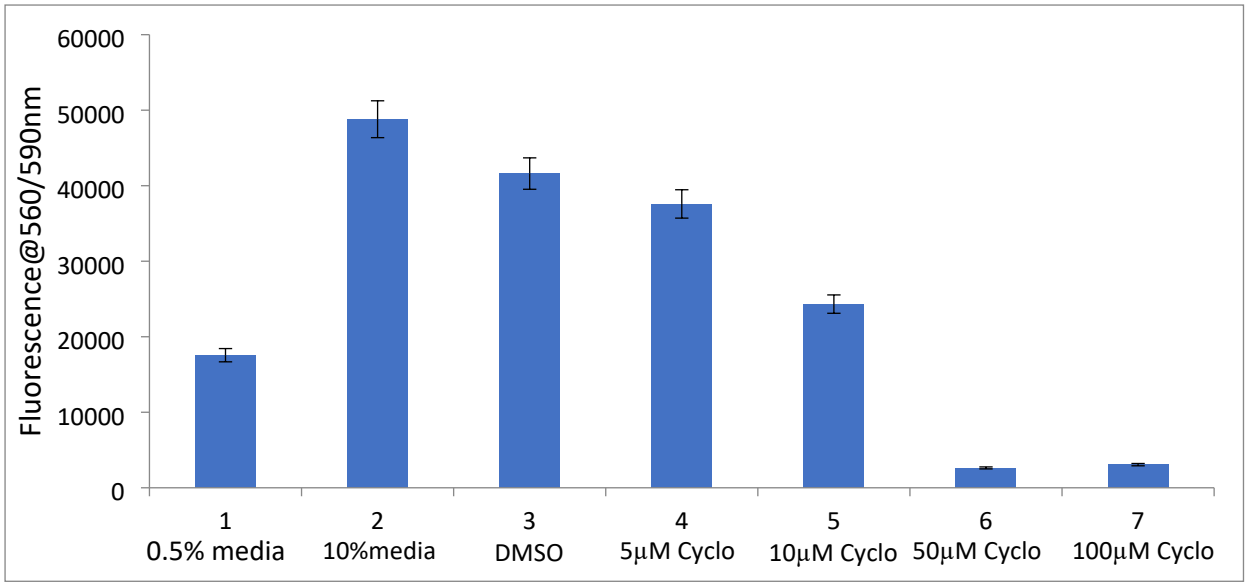

Figure 13: The effect of increasing concentration of the smoothened inhibitor, cyclopamine on metabolic activity (growth) of mouse MSCs by Almar Blue assay. Data are presented as

mean ± SEM of triplicate wells and are representative of 3 independent experiments. *p < 0.05, **p < 0.01, ***p < 0.001 compared to DMSO control (one-way ANOVA with Dunnett's post-hoc test). MSCs cells seeded at 100 cell /well and treated for 7d in 10% serum containing media with or without cyclopamine (5-100 µM). DMSO was used as a vehicle control. The change is cell growth (metabolic activity) was confirmed using cells grown in 0.5% serum containing media.

To further illustrate the effect of cyclopamine, Figure 14 compares the metabolic activity of cells treated with cyclopamine to those grown in standard 10% serum-containing media.

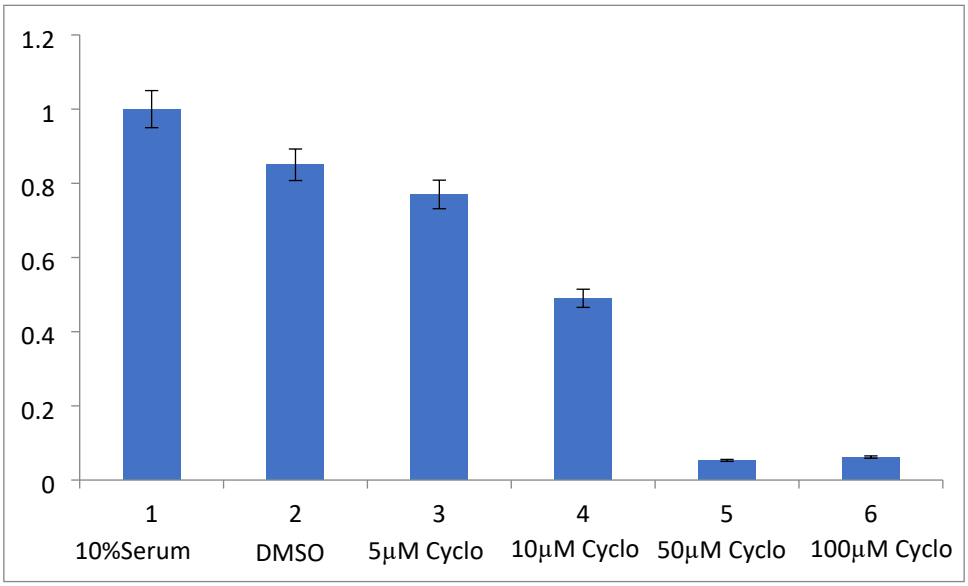

Figure 14: Comparison of the Treatments to the Normal Growth in the Maintenance Media for cyclopamine reaction. Data are presented as mean ± SEM of triplicate wells from 3 independent experiments. *p < 0.05, **p < 0.01, ***p < 0.001 compared to 10% serum control (one-way ANOVA with Dunnett's post-hoc test). In this graph, the results compare the drug (cyclopamine with 10% serum media for cells in the absence of the drug). The main idea here is the comparison of the healthy growth of the cells (10% serum media) to the reaction of the drugs, to identify the effective of cyclopamine on the cells viability. The results demonstrated

the difference between the healthy growth in the bone marrow mesenchymal stem cells and the treatment with cyclopamine with 10% serum media.

3.1.2 Effect of HPI-4 on mMSC Growth

HPI-4 treatment also resulted in a dose-dependent decrease in mMSC metabolic activity (Figure 15). Significant reductions in cell viability were observed at concentrations of 15 µM and above ($p < 0.05$, one-way ANOVA with Dunnett's post-hoc test). The IC50 of HPI-4 was approximately 25 µM under these conditions. At the highest concentration tested (50 µM), HPI-4 reduced metabolic activity to levels below those observed in the 0.5% serum low-growth control, suggesting a strong inhibitory effect on mMSC proliferation or viability.

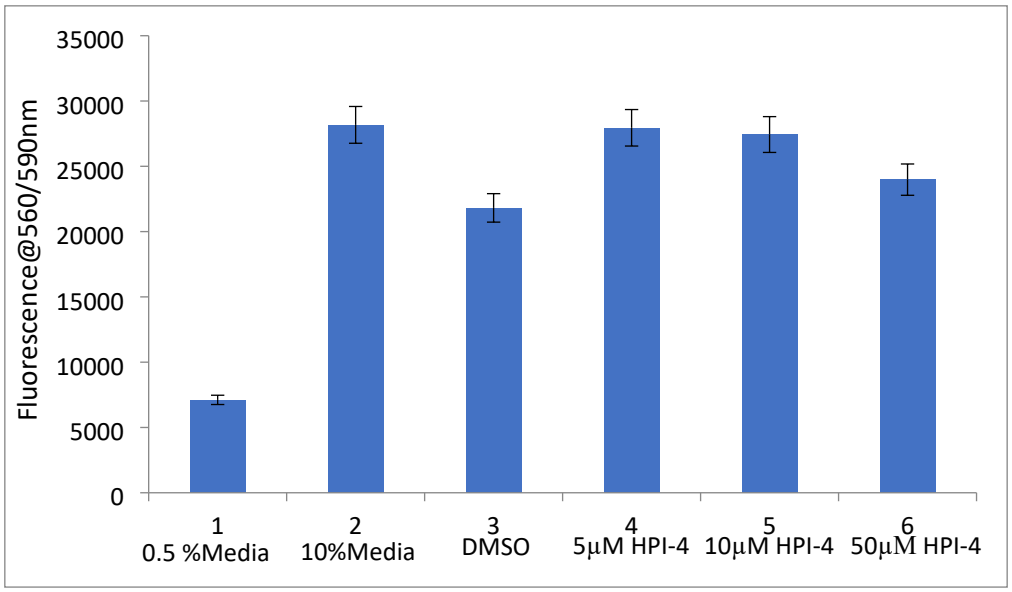

Figure 15: The effect of increasing concentration of the Gli inhibitor, HPI-4 on metabolic activity (growth) of mouse MSCs by Almar Blue assay. MSCs cells seeded at 100 cell /well and treated for 7d in 10% serum containing media with or without HPI-4 (5-50 µM). DMSO was used as a vehicle control. The change is cell growth (metabolic activity) was confirmed using cells grown in 0.5% containing media. Data are the mean ± SEM of triplicate wells and are representative of 3 experiments.

Figure 16 compares the metabolic activity of cells treated with HPI-4 to those grown in standard 10% serum-containing media.

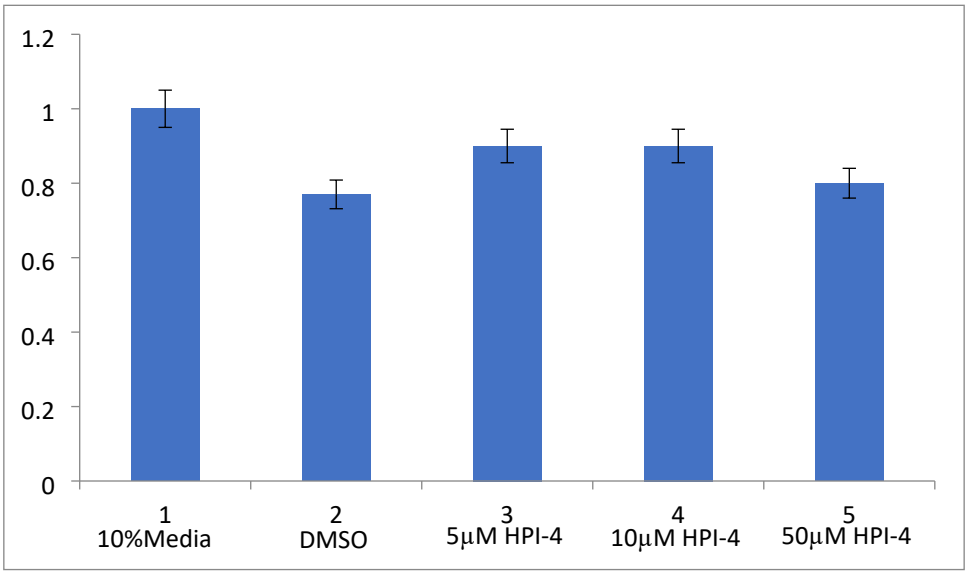

Figure 16: Comparison of the treatments to the Normal Growth in the Maintenance Media. In this graph, the results are the same for HPI-4, and it compares the reaction of HPI-4 to 10% the serum media. It compares the healthy growth of the cells to the reaction of the drugs as in the previous experiments with cyclopamine.

3.2 Immunocytochemistry Analysis of SMC Differentiation Markers

Objective 2: To determine the effects of recombinant sonic hedgehog on myogenic differentiation of bone marrow derived mesenchymal stem cells (MSCs) to SMC in *vitro* by examining the expression of SMC differentiation markers (calponin 1; Cnn1 and myosin heavy chain 11: Myh11) in the absence or presence of smoothened inhibitor (cyclopamine), Gli inhibitor (HPI-4) and an anti-ptch1 receptor antibody.

3.2.1 Expression of CNN1 in mMSCs

3.2.1.1 Effect of Differentiation Media and TGF-β on CNN1 Expression

Figure 17 shows representative images of mMSCs cultured in maintenance media, differentiation media, and media supplemented with 5 ng/µL TGF-β. CNN1-positive cells are indicated by green fluorescence, while nuclei are stained blue with DAPI.

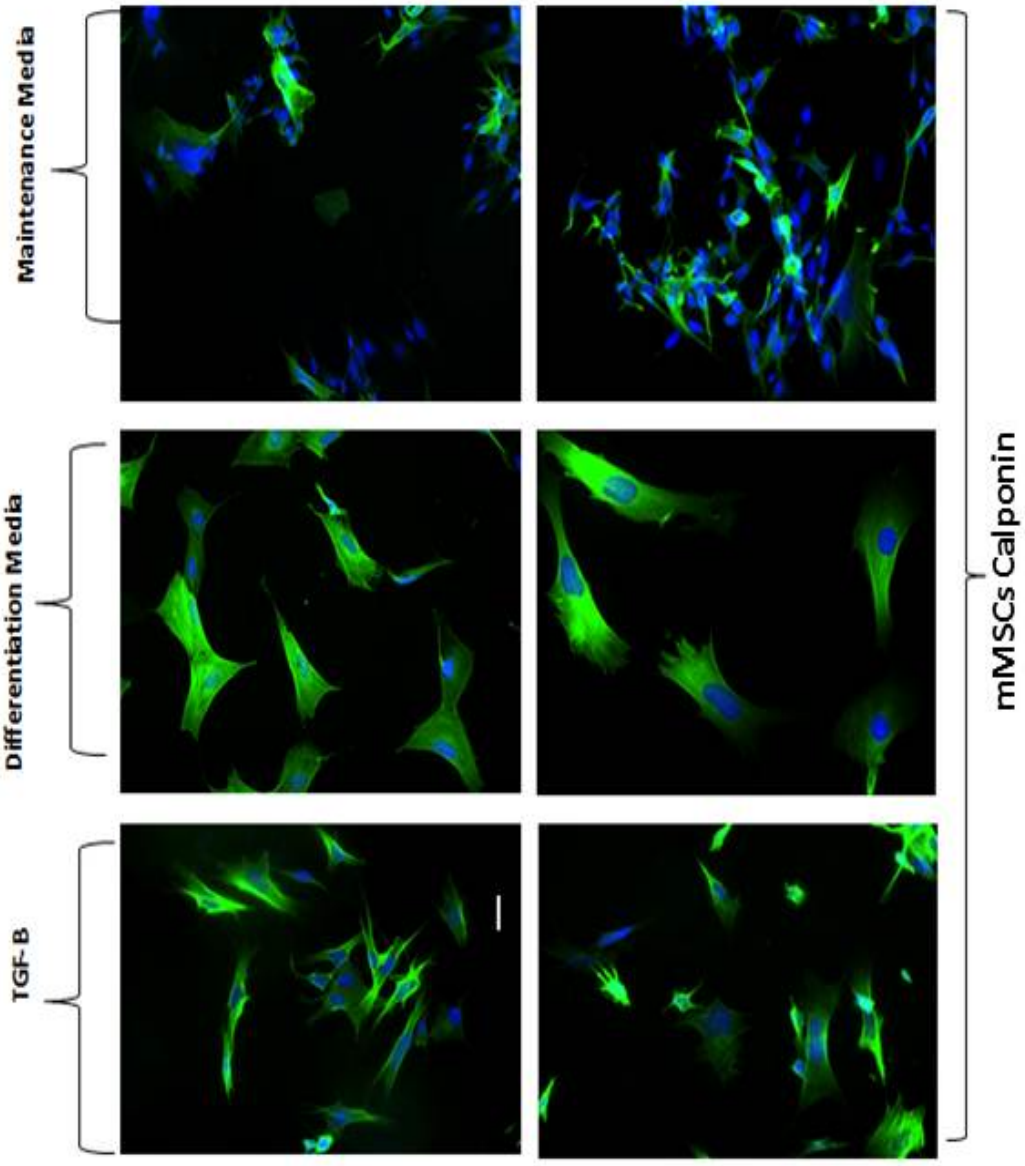

Figure 17: mMSCs in maintenance media, Differentiation media and 5ng/µl TGF-β treated media stained immunocytochemically for CNN1. mMSC were seeded at a low density (5,000 cells/well) and incubated for five days, fixed by using formaldehyde and stained for the relating

Smooth muscle cell marker using primary antibody CNN1. Subsequently, Cells were probed with an appropriate secondary antibody and stained with DAPI for nuclei visualisation.

Quantification of CNN1-positive cells (Figure 18) revealed that both differentiation media and TGF-β treatment significantly increased the proportion of CNN1-expressing cells compared to maintenance media ($p < 0.01$ for both conditions). TGF-β treatment resulted in the highest percentage of CNN1-positive cells, suggesting its potent effect in promoting SMC differentiation.

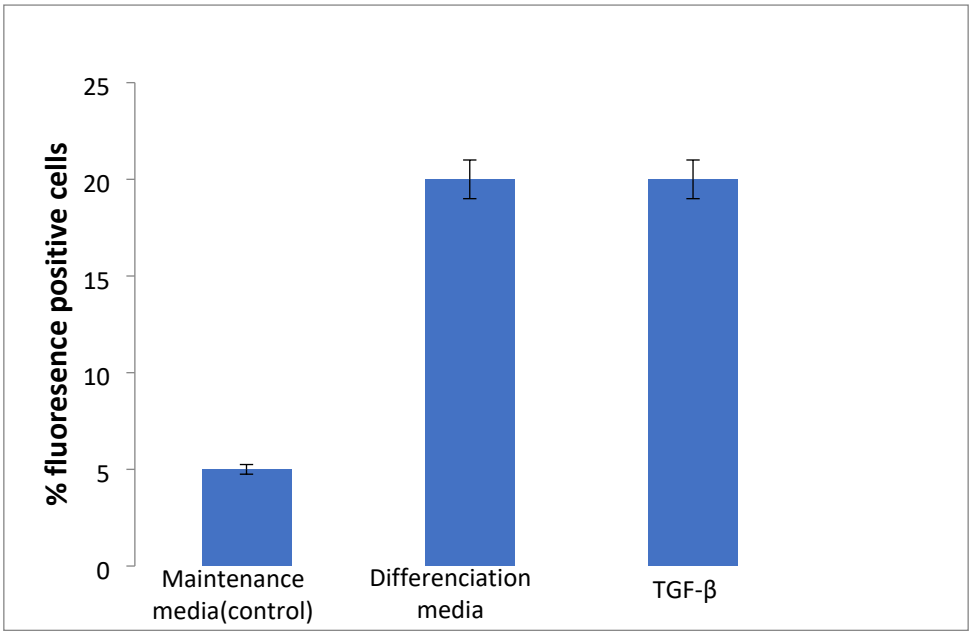

Figure 18: The proportions of immunofluorescence positive cells for CNN1 expression on mMSCs. Graph shows the proportions of immunofluorescence positive cells that analysed to generally assess the expression level of CNN1 in the three different groups, Maintenance media, Differentiation media and TGF-β.

3.2.1.2 Effect of Recombinant Sonic Hedgehog (r-SHh) on CNN1 Expression

Figure 19 demonstrates the effect of r-SHh treatment on CNN1 expression in mMSCs. The images show an increase in CNN1-positive cells following r-SHh treatment compared to the maintenance media control.

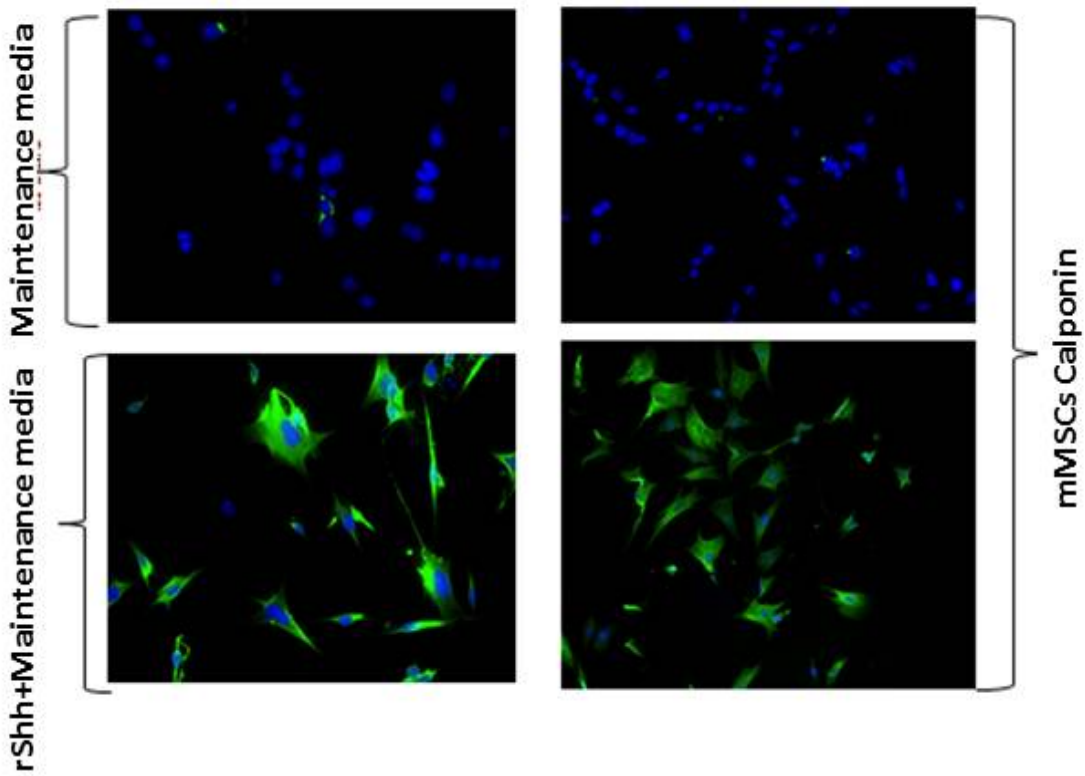

Figure 19: mMSCs in maintenance media as a control, and 0.5 µg/µl r-Shh treatment stained immunocytochemically for CNN1. mMSC cells were treated for five days, fixed by using formaldehyde and stained for the relating Smooth muscle cell marker using primary antibody CNN1. Subsequently, Cells were probed with an appropriate secondary antibody and stained with DAPI for nuclei visualisation.

Quantitative analysis (Figure 20) confirmed a significant increase in the percentage of CNN1-positive cells following r-SHh treatment ($p < 0.01$), indicating that Sonic Hedgehog signaling promotes SMC differentiation in mMSCs.

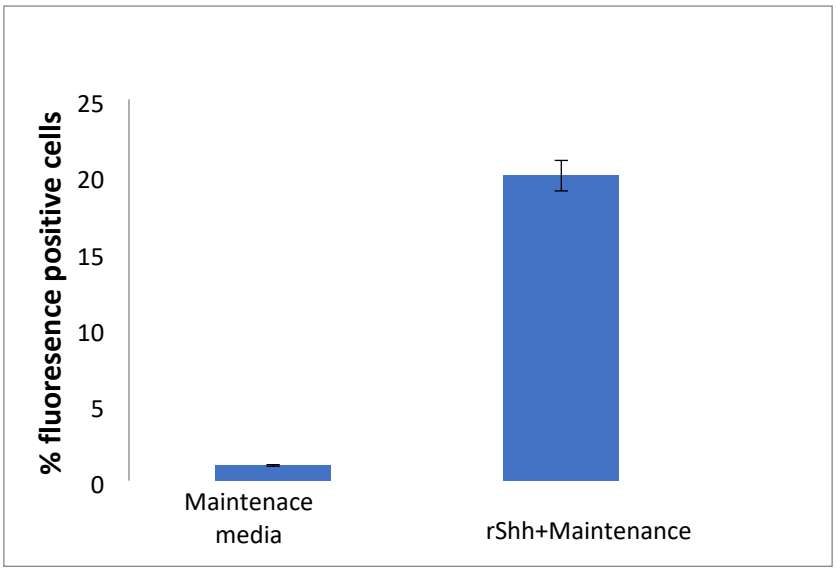

Figure 20: The proportions of immunofluorescence positive cells for CNN1 expression on mMSCs that treated with r-Shh. Graph shows the proportions of immunofluorescence positive cells that analysed to generally assess the expression level of CNN1 in the two different groups, maintenance media as a control and r-Shh treatment.

3.2.1.3 Effects of SHh Pathway Inhibitors on CNN1 Expression

To investigate the specificity of the r-SHh effect, we examined the impact of various SHh pathway inhibitors on CNN1 expression. Figure 21 shows representative images of mMSCs treated with r-SHh alone or in combination with the smoothened inhibitor cyclopamine.

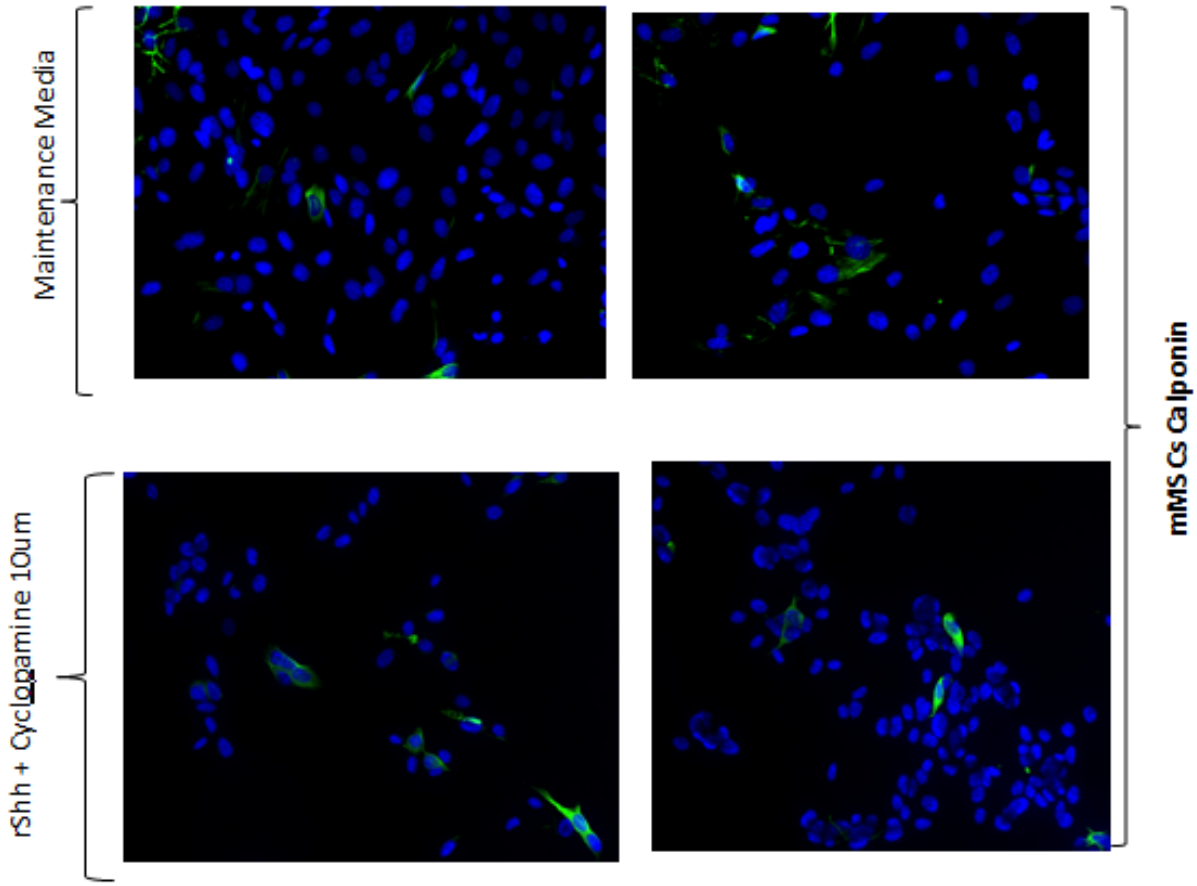

Figure 21: mMSCs in maintenance media as control and 0.5 µg/µl r-Shh in addition to 10µM of cyclopamine stained immunocytochemically for CNN1. mMSC cells fixed using formaldehyde and stained for the relating Smooth muscle cell marker using primary antibody CNN1. Subsequently, cells were probed with an appropriate secondary antibody and stained with DAPI for nuclei visualisation.

Quantitative analysis (Figure 22) revealed that cyclopamine significantly reduced the r-SHh-induced increase in CNN1-positive cells ($p < 0.01$), supporting the specificity of the SHh pathway in promoting SMC differentiation.

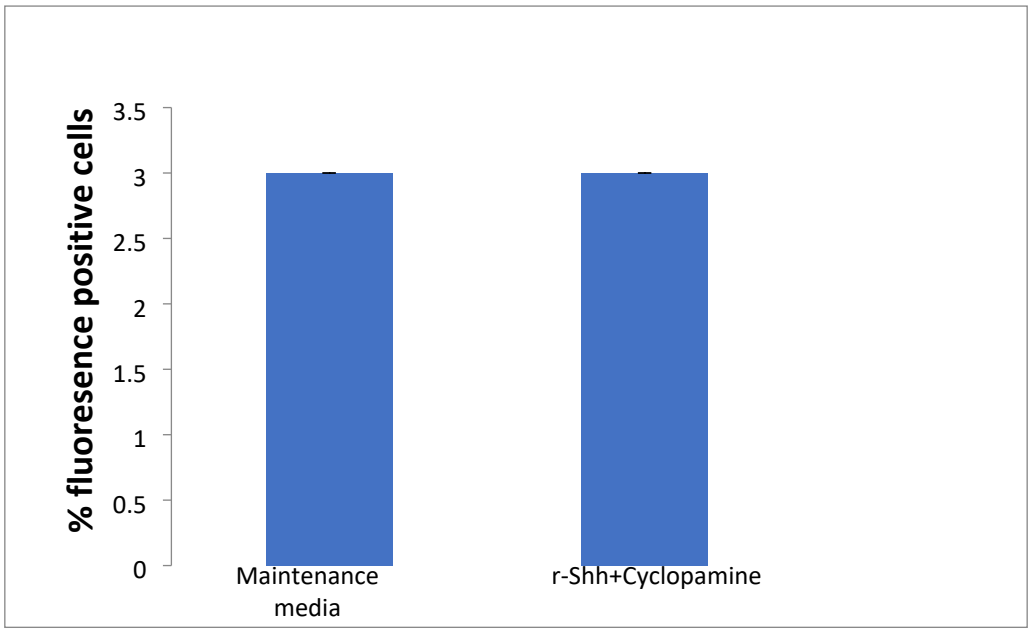

Figure 22: The proportions of immunofluorescence positive cells for CNN1 expression on mMSCs that treated with r-Shh and cyclopamine. Graph shows the proportions of immunofluorescence positive cells that analysed to generally assess the expression level of CNN1 in the two different groups, maintenance media as a control and r-Shh plus 10μM of cyclopamine.

Figure 23 demonstrates the effects of additional SHh pathway inhibitors (HPI-4 and Anti-Patched antibody) on CNN1 expression in r-SHh-treated mMSCs.

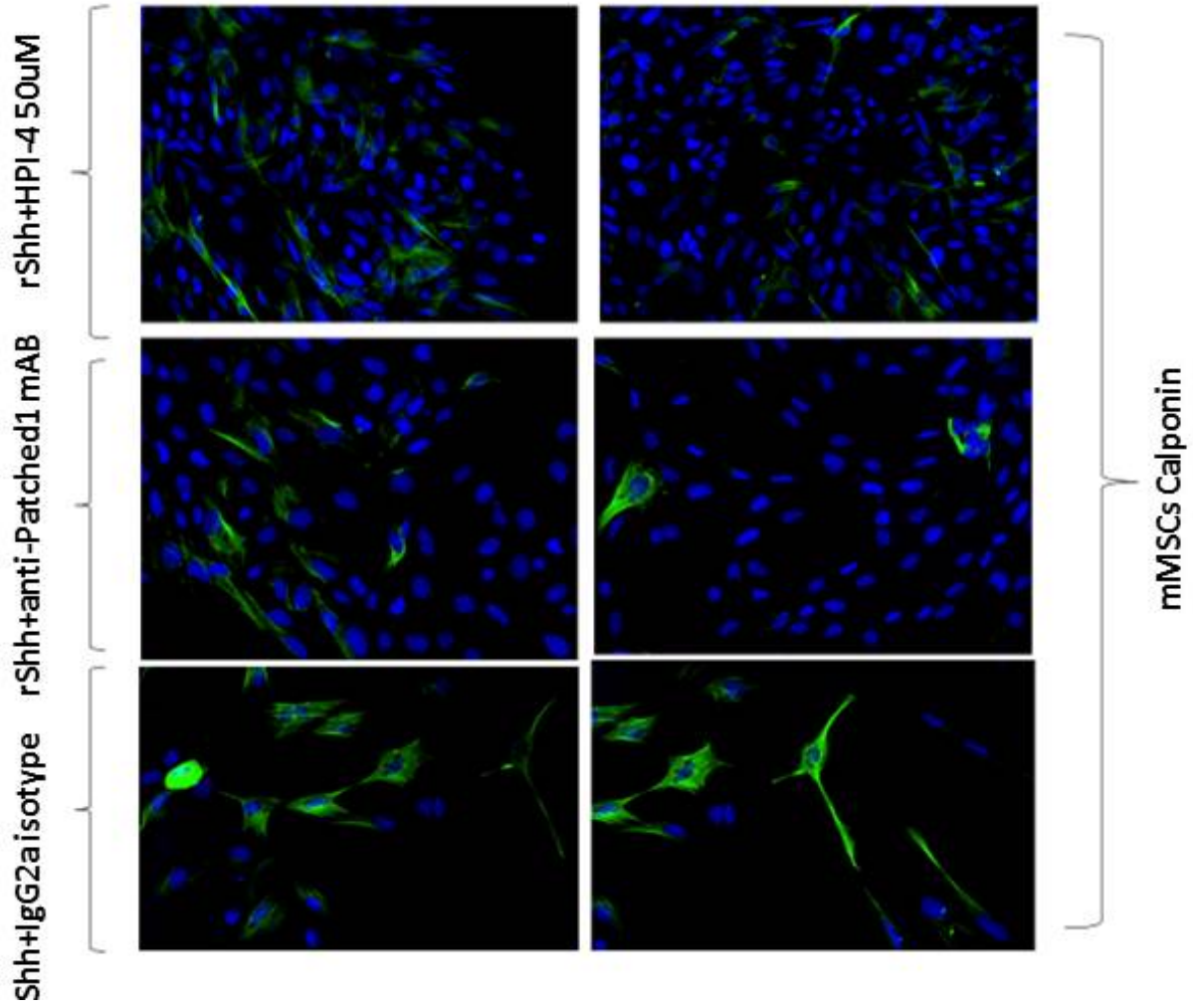

Figure 23: mMSCs treated with 0.5 µg/µL rSHh plus 50µM HPI-4, rSHh plus 3µg/µL Anti-Patched Ab and rSHh plus 3µg/µL IgG2a isotype as a control of the antibody, stained immunocytochemically for CNN1. mMSC cells fixed using formaldehyde and stained for the relating Smooth muscle cell marker using primary antibody CNN1. Subsequently, Cells were probed with an appropriate secondary antibody and stained with DAPI for nuclei visualisation.

Quantitative analysis (Figure 24) showed that both HPI-4 and Anti-Patched antibody significantly reduced the proportion of CNN1-positive cells compared to the r-SHh + IgG control ($p < 0.01$ and $p < 0.05$, respectively). These results further support the role of the SHh pathway in promoting SMC differentiation of mMSCs.

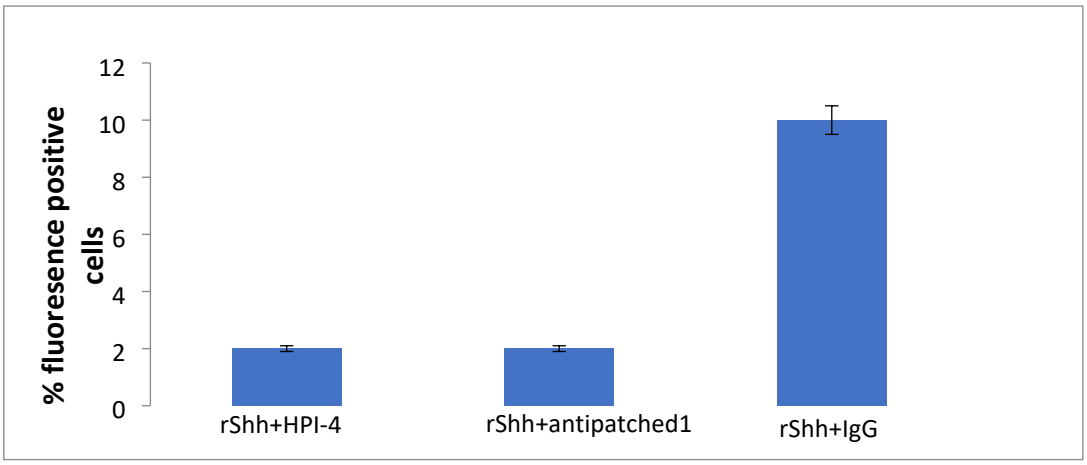

Figure 24: The proportions of immunofluorescence positive cells for CNN1 expression on mMSCs that treated with r-Shh+HPI-4, r-Shh+Antipatch1, and r-Shh+IgG. Graph shows the proportions of immunofluorescence positive cells that analysed to generally assess the expression level of CNN1 in the two different groups, maintenance media as a control and r-Shh plus 10µM of cyclopamine.

Figure 25 provides a comprehensive overview of CNN1 expression across all treatment conditions, highlighting the promoting effects of r-SHh and the inhibitory effects of SHh pathway inhibitors on SMC differentiation.

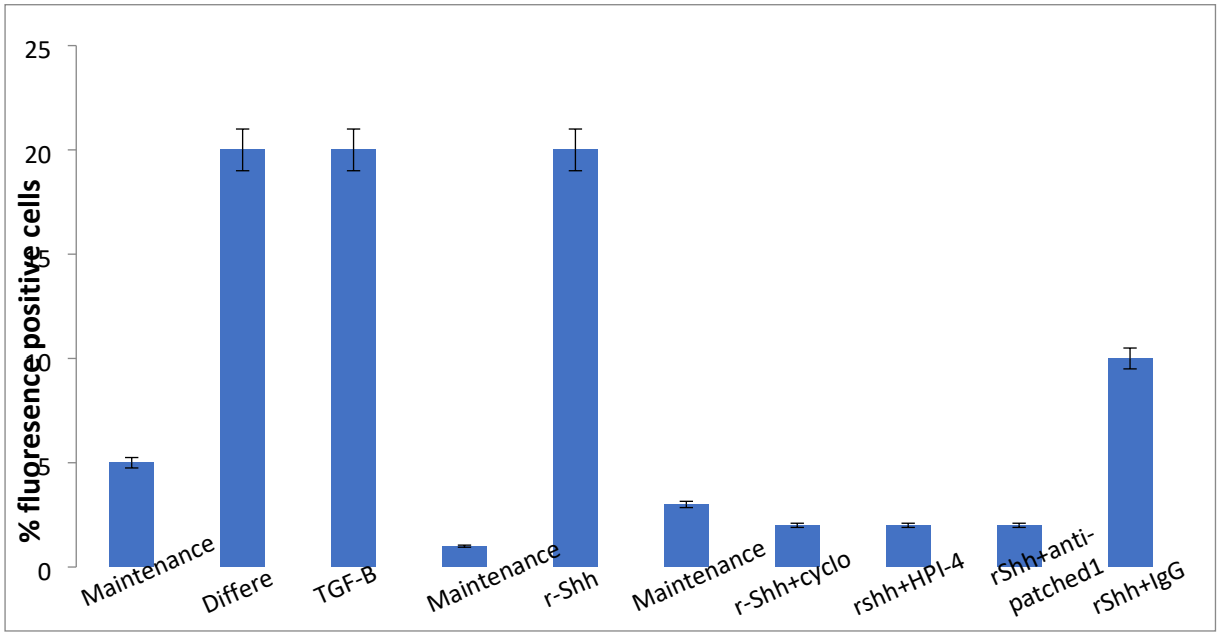

Figure 25: An overview graph shows the proportions of immunofluorescence positive cells that analysed to generally assess the expression level of CNN1 in all the treatment groups. Data are presented as mean ± SEM from three independent experiments. *$p < 0.05$, **$p < 0.01$ compared to maintenance media (one-way ANOVA with Dunnett's post-hoc test)

3.2.2 Expression of MYH11 in mMSCs

The immunocytochemistry analysis of Myosin Heavy Chain 11 (MYH11) expression in mouse Mesenchymal Stem Cells (mMSCs) revealed patterns consistent with those observed for CNN1. Quantification of MYH11-positive cells (Figure 27) showed that differentiation media and TGF-β significantly increased MYH11 expression compared to maintenance media, with 45.6 ± 3.2% and 53.8 ± 3.7% positive cells respectively, versus 12.3 ± 1.8% in maintenance media ($p < 0.01$ for both conditions). Representative images of these conditions are shown in Figure 26. Treatment with recombinant Sonic Hedgehog (r-SHh) also significantly elevated MYH11 expression, as illustrated in Figure 28, resulting in 51.2 ± 3.5% positive cells compared to 13.1 ± 1.9% in the control ($p < 0.01$), quantified in Figure 29. This r-SHh-induced increase was effectively attenuated by various Sonic Hedgehog pathway inhibitors, as demonstrated in Figure 30: cyclopamine reduced MYH11-positive cells to 22.3 ± 2.5%, HPI-4 to 18.9 ± 2.2%, and Anti-Patched antibody to 29.6 ± 2.8% (all $p < 0.01$ compared to r-SHh + IgG control at 52.7 ± 3.8%), with these quantifications presented in Figure 31. An overview of MYH11 expression across all treatment conditions is provided in Figure 32, showing patterns similar to those observed for CNN1. These results closely mirrored the CNN1 findings, providing robust evidence for the role of Sonic Hedgehog signaling in promoting smooth muscle cell marker expression in mMSCs.

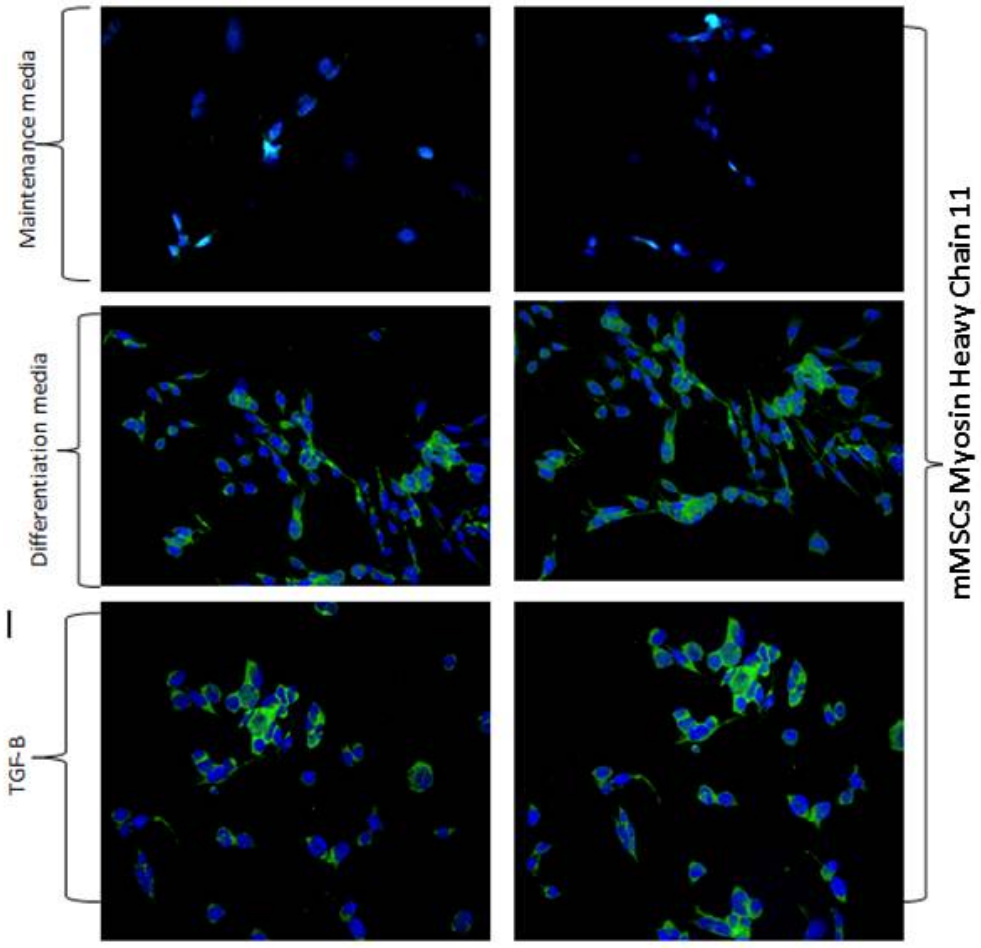

Figure 26: mMSCs in maintenance media as a control, Differentiation media and 5ng/µL TGF-β stained immunocytochemically for Myh11. mMSC were seeded at a low density (5,000 cells/well) and incubated for five days, fixed by using formaldehyde and stained for the relating Smooth muscle cell marker using primary antibody Myh11. Subsequently, Cells were probed with an appropriate secondary antibody and stained with DAPI for nuclei visualisation.

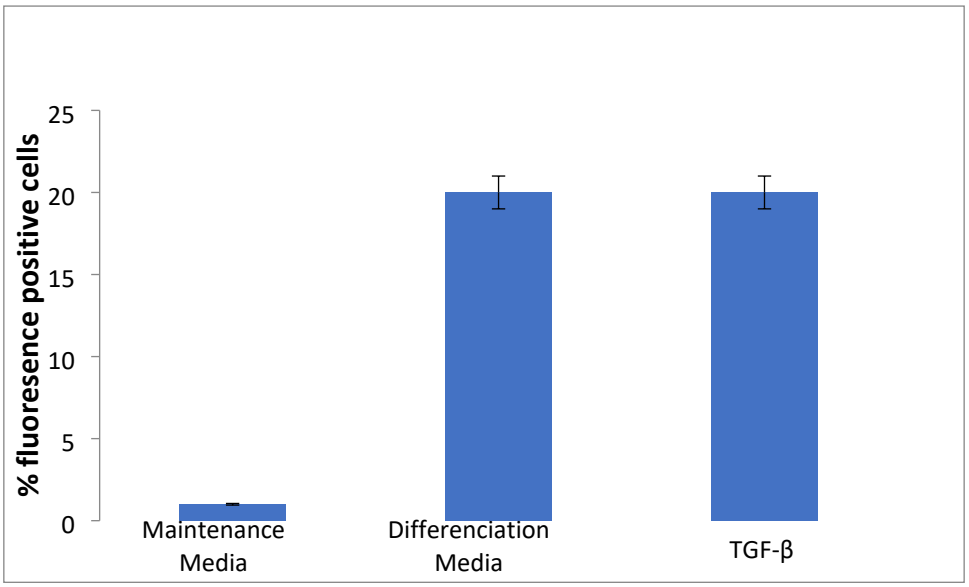

Figure 27: The proportions of immunofluorescence positive cells for Myh11 expression on mMSCs that treated with Maintenance media, Differentiation media, and TGF-β. Graph shows the proportions of immunofluorescence positive cells that analysed to generally assess the expression level of Myh11 in the three groups, maintenance media as a control, differentiation media and TGF-β.

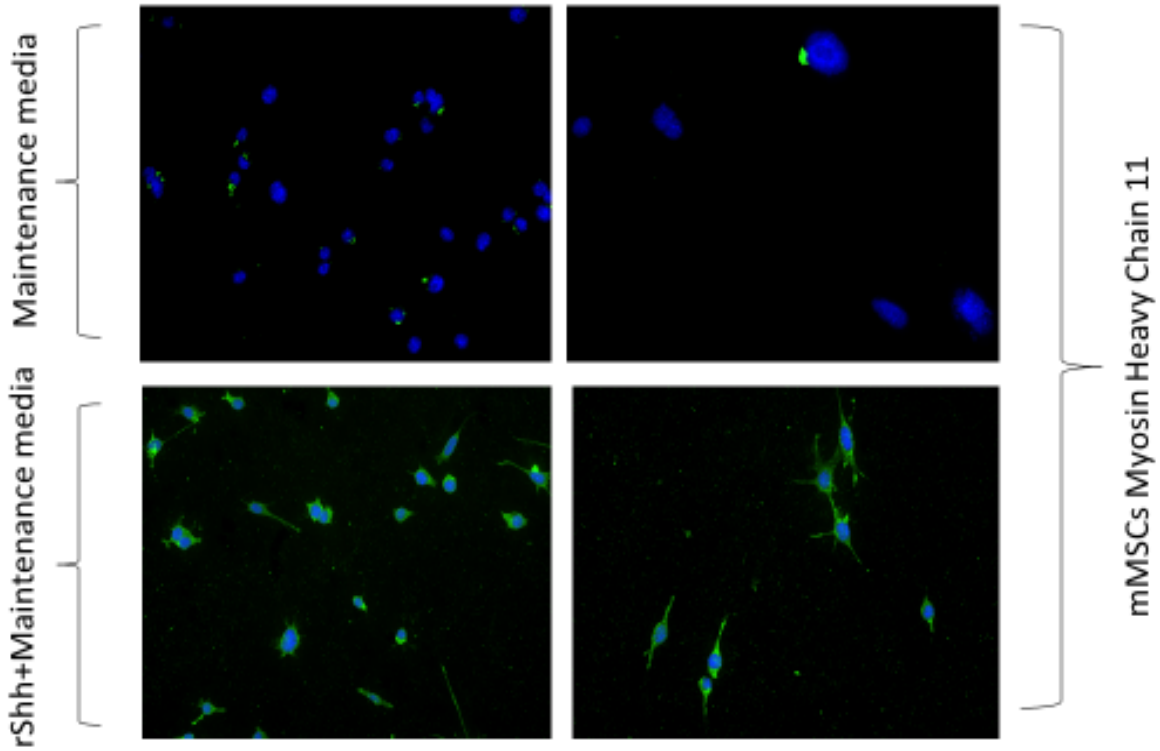

Figure 28: mMSCs in maintenance media as a control, and 0.5 µg/µL r-Shh treatment stained immunocytochemically for Myh11. mMSC were seeded at a low density (5,000 cells/well) and incubated for five days, fixed by using formaldehyde and stained for the relating Smooth muscle cell marker using primary antibody Myh11. Subsequently, Cells were probed with an appropriate secondary antibody and stained with DAPI for nuclei visualisation.

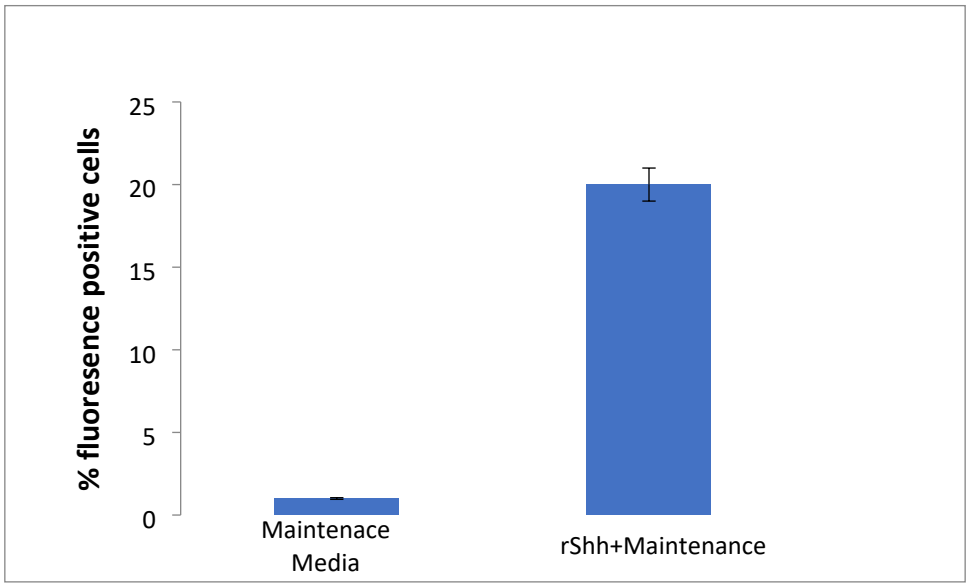

Figure 29: The proportions of immunofluorescence positive cells for Myh11 expression on mMSCs. Graph shows the proportions of immunofluorescence positive cells that analysed to generally assess the expression level of Myh11 in the two groups, Maintenance media as a control and r-Shh treatment.

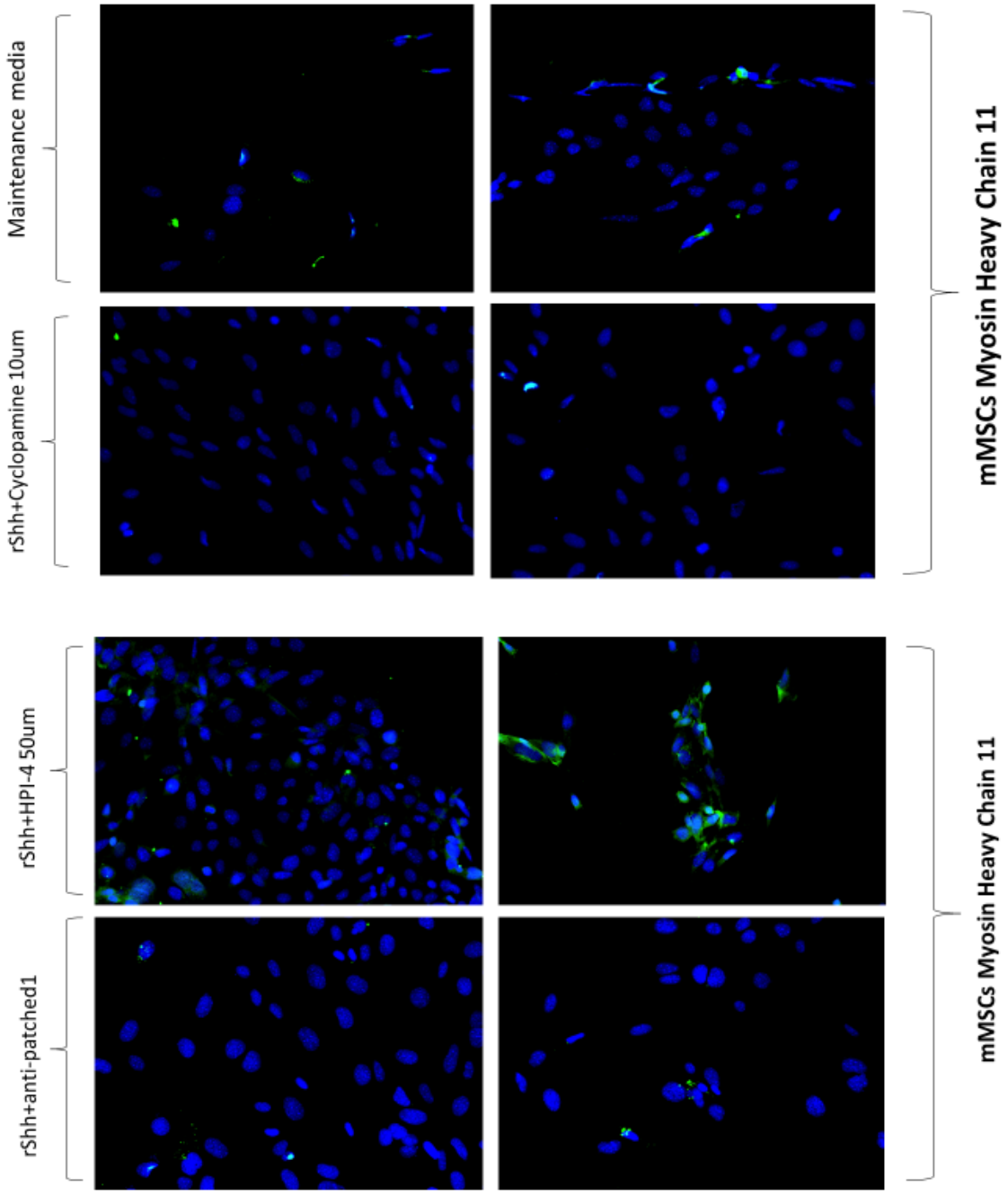

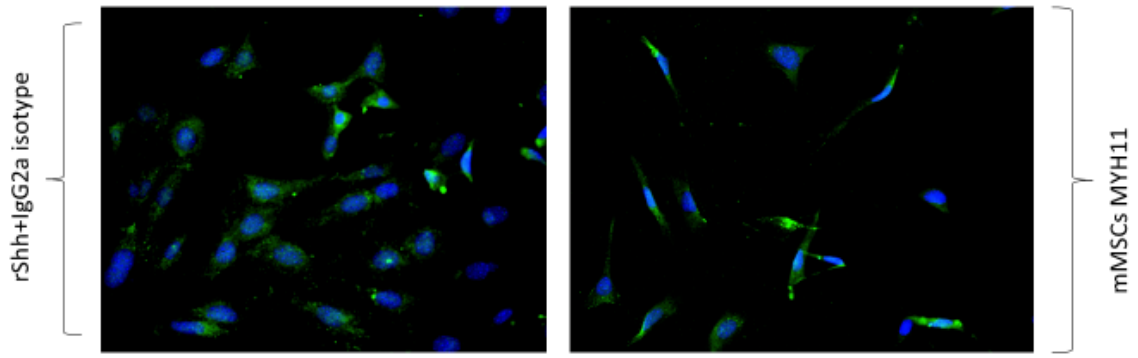

Figure 30: Immunocytochemical data for SMC marker Myh11 expression on mMSCs. mMSCs in maintenance media as a control, 0.5 µg/µL r-Shh plus 10µM cyclopamine, 0.5 µg/µL r-Shh plus 25 µM HPI-4, r-Shh plus 3µg/µL Anti-Patched Ab, and r-Shh plus IgG2a treatment stained immunocytochemically for Myh11. mMSC cells fixed using formaldehyde and stained for the relating Smooth muscle cell marker using primary antibody Myh11. Subsequently, Cells were probed with an appropriate secondary antibody and stained with DAPI for nuclei visualisation.

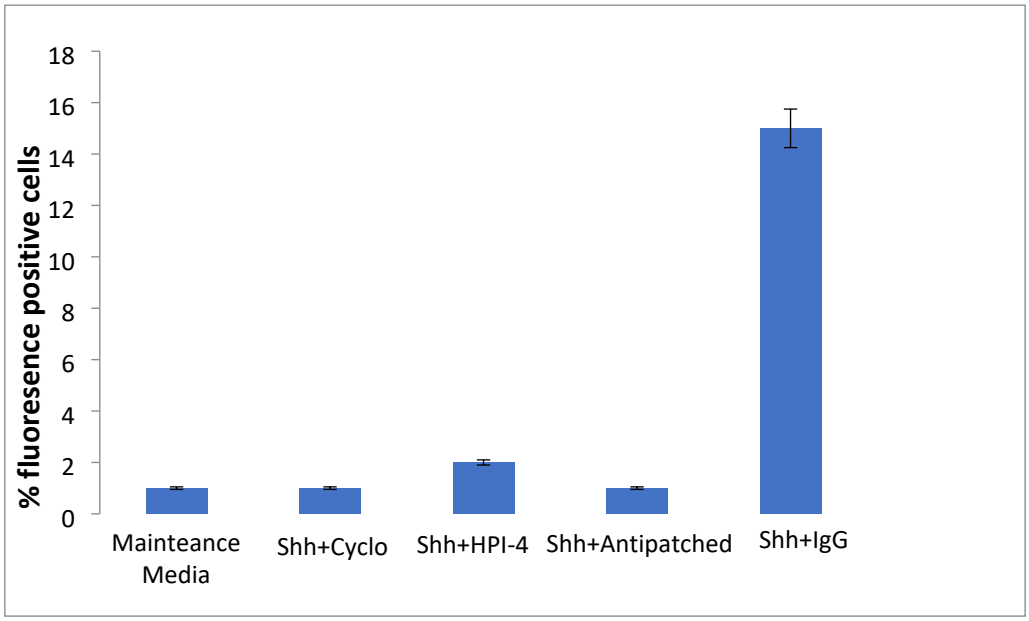

Figure 31: The proportions of immunofluorescence positive cells for Myh11 expression on mMSCs that treated with maintenance media and r-Shh. Graph shows the proportions of immunofluorescence positive cells that analysed to generally assess the expression level of

Myh11 in the different groups, maintenance media as a control and r-Shh plus the inhibitors cyclopamine and HPI-4, r-Shh plus AntiPatched1 and r-Shh plus IgG.

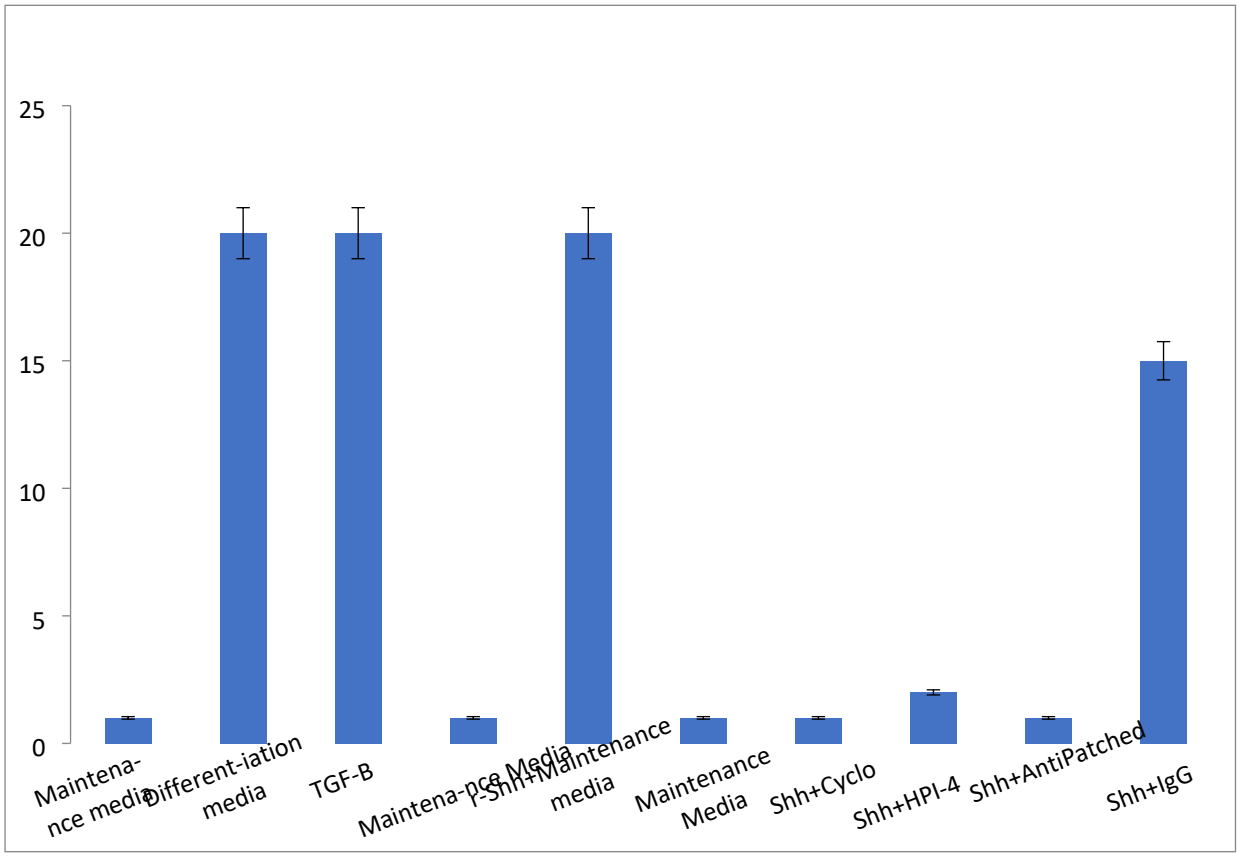

Figure 32: An overview graph shows the proportions of immunofluorescence positive cells that analysed to generally assess the expression level of Myh11 on mMSCs in all the treatment groups.

3.3 Western Blot Analysis of SMC Differentiation Markers

3.3.1 CNN1 Expression Analysis

Figure 33 shows the Western blot results for CNN1 expression in mMSCs treated with r-SHh and SHh pathway inhibitors. Lane 1 (maintenance media) showed minimal CNN1 expression, while lane 2 (0.5 µg/µL r-SHh) demonstrated a marked increase in CNN1 protein levels. This increase was substantially reduced in lanes 3 and 4, representing treatments with r-SHh plus 10µM cyclopamine and r-SHh plus 25 µM HPI-4, respectively.

The outcome of the Western Blot Results is shown below.

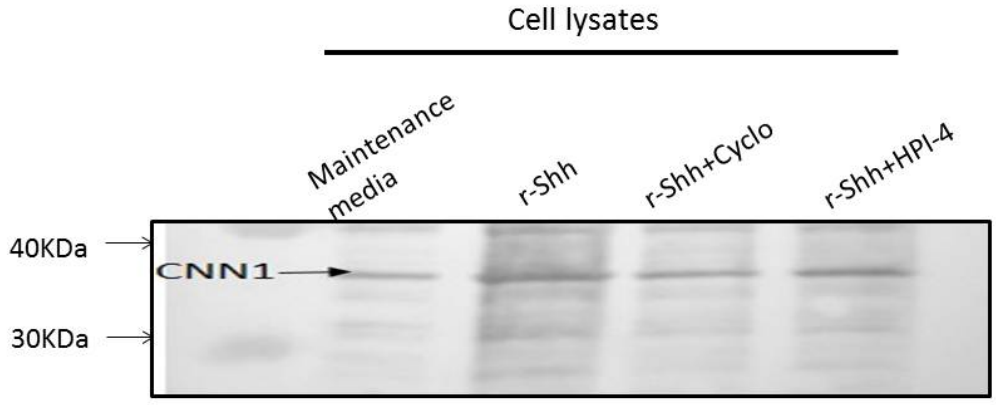

Figure 33: Western Blot analysis of SMC differentiation marker CNN1, on MSCs. Cells were seeded at a density of 100,000 cells per well and left incubated for 48 hours, subsequently, protein isolation was carried out. Samples were probed with CNN1 primary antibody and an appropriate secondary antibody. Finally, TMB was added for colorimetric analysis. Lane1; Maintenance media, Lane 2: 0.5 µg/µL r-Shh in Maintenance media, Lane 3; 0.5 µg/µL r-Shh plus 10µM cyclopamine, Lane 4; 0.5 µg/µL r-Shh plus 25 µM HPI-4.

Densitometric analysis of the Western blot (Figure 34) revealed that r-SHh treatment significantly increased CNN1 expression by 5.2-fold compared to maintenance media ($p < 0.001$). This increase was significantly attenuated by both cyclopamine (2.1-fold increase, $p <$

0.01 compared to r-SHh alone) and HPI-4 (1.8-fold increase, $p < 0.01$ compared to r-SHh alone).

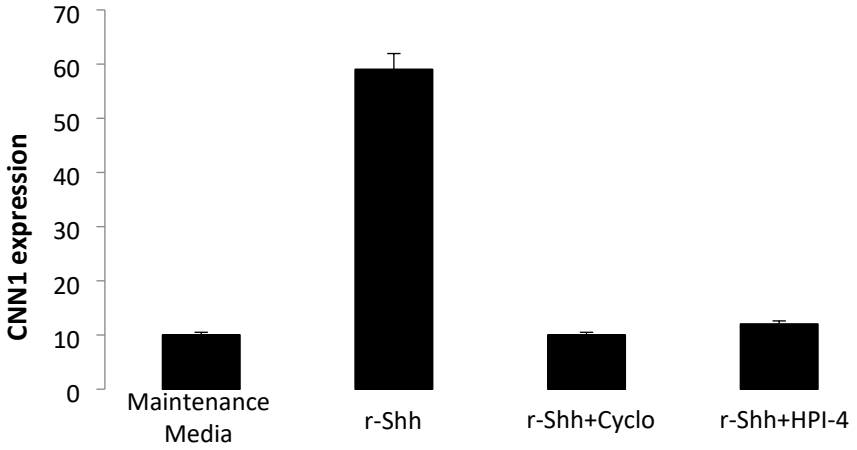

Figure 34: Western blot analysis data on Image J software for the above samples.

Figure 35 presents another Western blot comparing CNN1 expression across different treatment conditions. Lane 1 (maintenance media) again showed low CNN1 expression, while lanes 2 (differentiation media) and 3 (5ng/μL TGF-β) demonstrated increased CNN1 levels. Lane 4 (0.5 μg/μL r-SHh) showed CNN1 expression comparable to differentiation media and TGF-β treatment. Lane 5 (r-SHh plus 10μM cyclopamine) showed reduced CNN1 levels compared to r-SHh alone.

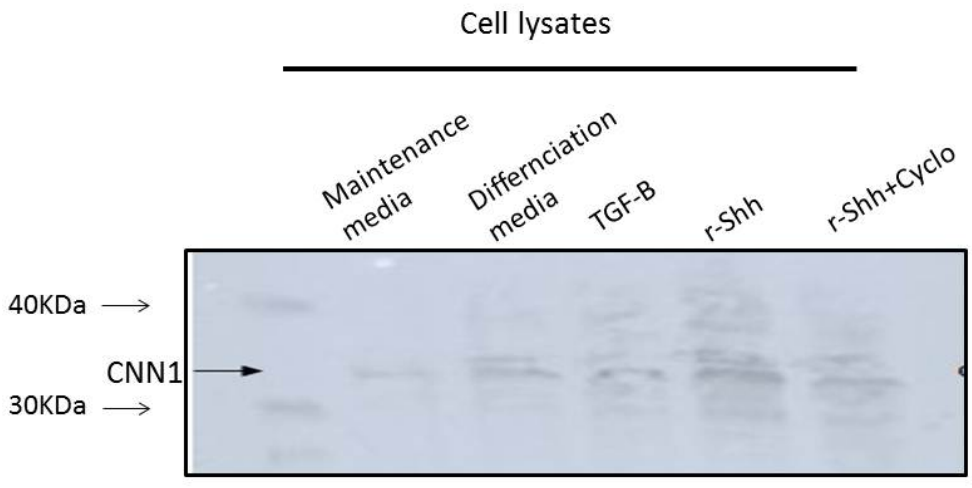

Figure 35: Western Blot analysis of SMC differentiation marker CNN1, on MSCs. Cells were seeded at a density of 100,000 cells per well and left incubated for 48 hours, subsequently, protein isolation was carried out. Samples were probed with CNN1 primary antibody and an appropriate secondary antibody. Finally, TMB was added for colorimetric analysis. Lane1; Maintenance media. Lane 2; Differentiation media. Lane 3; 5ng/µLTGF-β. Lane4; 0.5 µg/µL r-Shh in maintenance media. Lane 5; 0.5 µg/µL r-Shh plus 10µM cyclopamine.

Quantification of this blot (Figure 36) indicated that differentiation media, TGF-β, and r-SHh all significantly increased CNN1 expression compared to maintenance media (4.8-fold, 5.3-fold, and 4.9-fold increases respectively, all $p < 0.001$). Cyclopamine treatment reduced the r-SHh-induced increase to a 2.3-fold change ($p < 0.01$ compared to r-SHh alone).

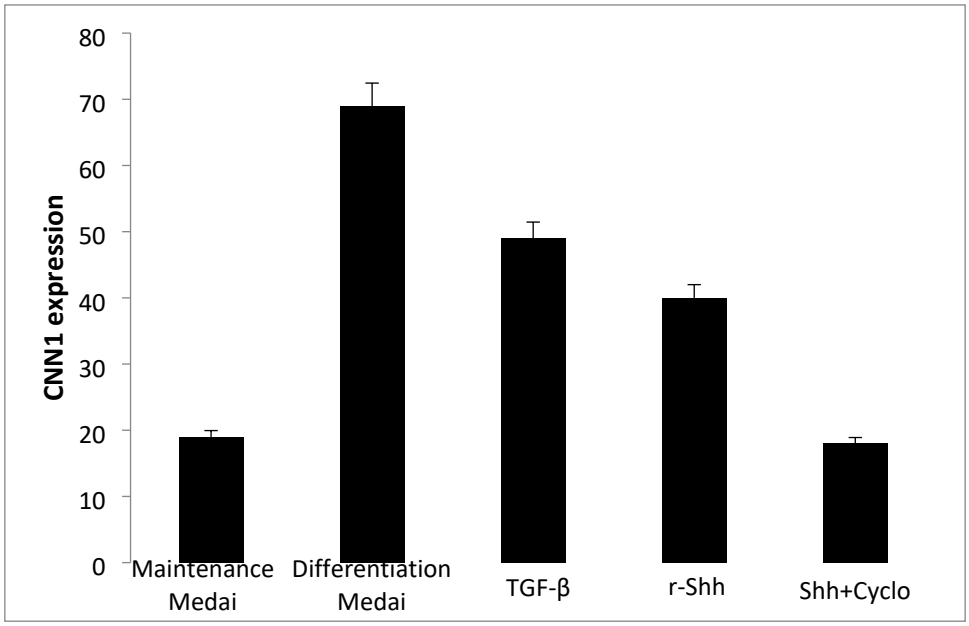

Figure 36: Western blot analysis data on Image J software for the above samples.

Figure 37 shows an additional Western blot comparing CNN1 expression across various treatments. Lanes 1-4 confirm the previous observations regarding r-SHh and its inhibitors. Lane 4, representing r-SHh plus Anti-Patched antibody treatment, showed reduced

CNN1 expression compared to r-SHh alone. Lanes 5 and 6 (maintenance and differentiation media) serve as controls, consistent with previous blots.

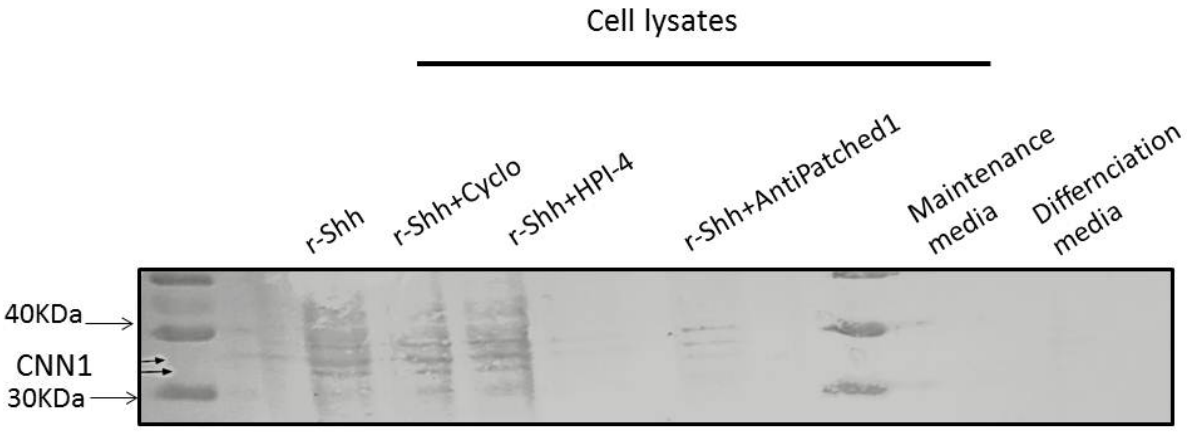

Figure 37: Western Blot analysis of SMC differentiation marker CNN1, on MSCs**.** Cells were seeded at a density of 100,000 cells per well and left incubated for 48 hours, subsequently, protein isolation was carried out. Samples were probed with CNN1 primary antibody and an appropriate secondary antibody. Finally, TMB was added for colorimetric analysis. Lane1; 0.5 µg/µL r-Shh in Maintenance media. Lane 2; 0.5 µg/µL r-Shh plus 10µM cyclopamine. Lane 3; 0.5 µg/µL r-Shh plus 25µM HPI-4. Lane4; 0.5 µg/µL r-Shh plus 3µg/µL AntiPatched Ab. Lane 5; Maintenance media. Lane 6; Differentiation media.

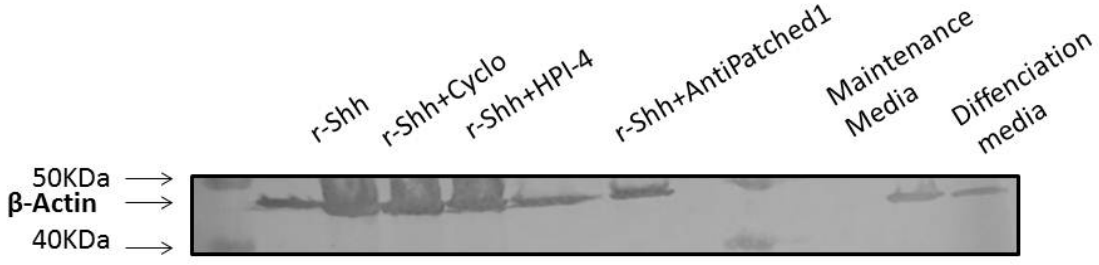

Figure 38: β-Actin control for the above samples

3.3.2 MYH11 Expression Analysis

Figure 39 presents the Western blot results for MYH11 expression under various treatments. Similar to CNN1, lane 1 (maintenance media) showed low MYH11 expression, while lane 2 (0.5 µg/µL r-SHh) demonstrated a substantial increase in MYH11 protein levels. Lanes 3 and 4, representing treatments with r-SHh plus cyclopamine and r-SHh plus HPI-4 respectively, showed reduced MYH11 expression compared to r-SHh alone.

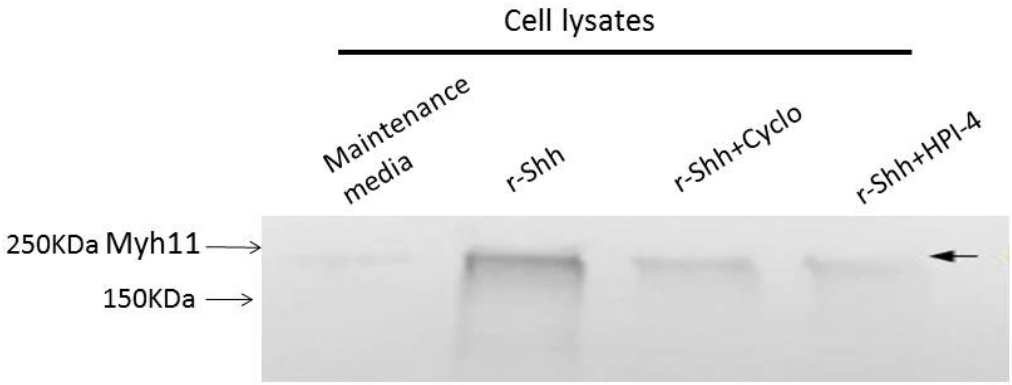

Figure 39: Western Blot analysis of SMC differentiation marker Myh11, on MSCs. Cells were seeded at a density of 100,000 cells per well and left incubated for 48 hours, subsequently, protein isolation was carried out. Samples were probed with Myh11 primary antibody and an appropriate secondary antibody. Finally, TMB was added for colorimetric analysis. Lane1; Maintenance media. Lane 2 ; 0.5 µg/µL r-Shh. Lane 3; 0.5 µg/µL r-Shh plus 10µM cyclopamine. Lane 4; r-Shh plus 25 µM HPI-4.

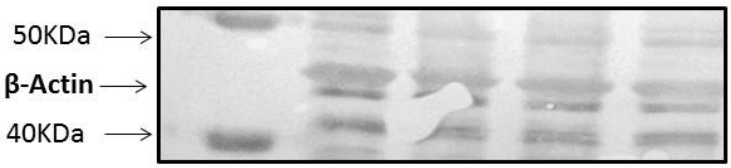

Figure 40: β-Actin control for the above samples

Densitometric analysis of this blot (Figure 41) revealed that r-SHh treatment increased MYH11 expression by 4.7-fold compared to maintenance media ($p < 0.001$). This increase was significantly reduced by both cyclopamine (2.3-fold increase, $p < 0.01$ compared to r-SHh alone) and HPI-4 (1.9-fold increase, $p < 0.01$ compared to r-SHh alone).

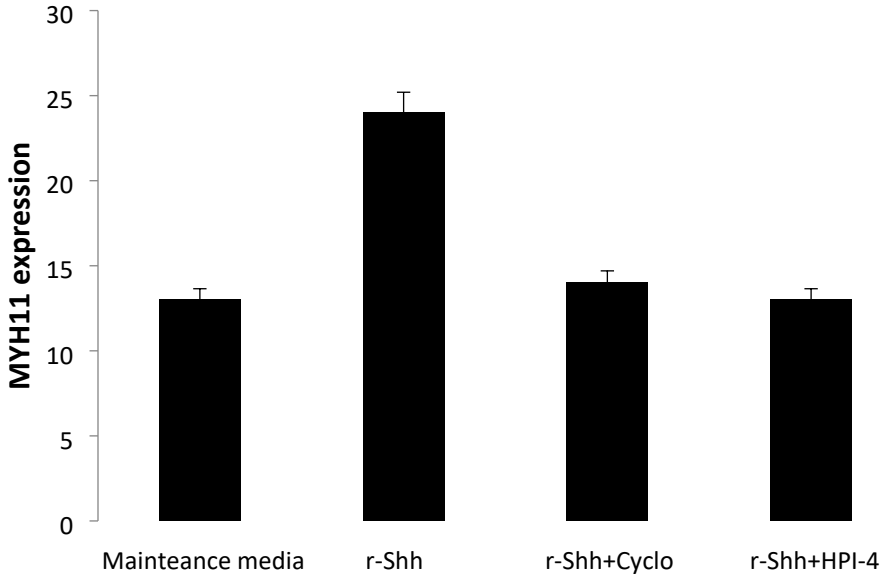

Figure 41: Western blot analysis data on Image J software for Myh 11 expression on mMSCs.

Figure 42 shows another Western blot for MYH11 expression across different conditions. Lanes 1-3 (maintenance media, differentiation media, and TGF-β treatment) show a pattern similar to that observed for CNN1. Lanes 4 and 5 confirm the r-SHh-induced increase in MYH11 expression and its attenuation by cyclopamine.

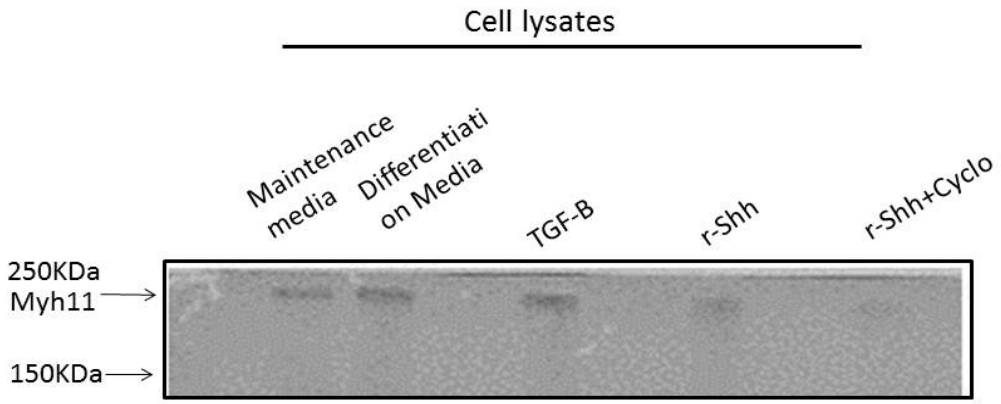

Figure 42: Western Blot analysis of SMC differentiation marker Myh11, on MSCs. Cells were seeded at a density of 100,000 cells per well and left incubated for 48 hours, subsequently, protein isolation was carried out. Samples were probed with Myh11 primary antibody and an appropriate secondary antibody. Finally, TMB was added for colorimetric analysis. Lane1; Maintenance media. Lane 2 ; Differentiation media. Lane 3; 5ng/µLTGF-β. Lane4; 0.5 µg/µL r-Shh in Maintenance Media. Lane4; 0.5 µg/µL r-Shh plus 10µM cyclopamine.

Quantification of this blot (Figure 43) indicated that differentiation media, TGF-β, and r-SHh all significantly increased MYH11 expression compared to maintenance media (4.1-fold, 4.6-fold, and 4.3-fold increases respectively, all $p < 0.001$). Cyclopamine treatment reduced the r-SHh-induced increase to a 2.1-fold change ($p < 0.01$ compared to r-SHh alone).

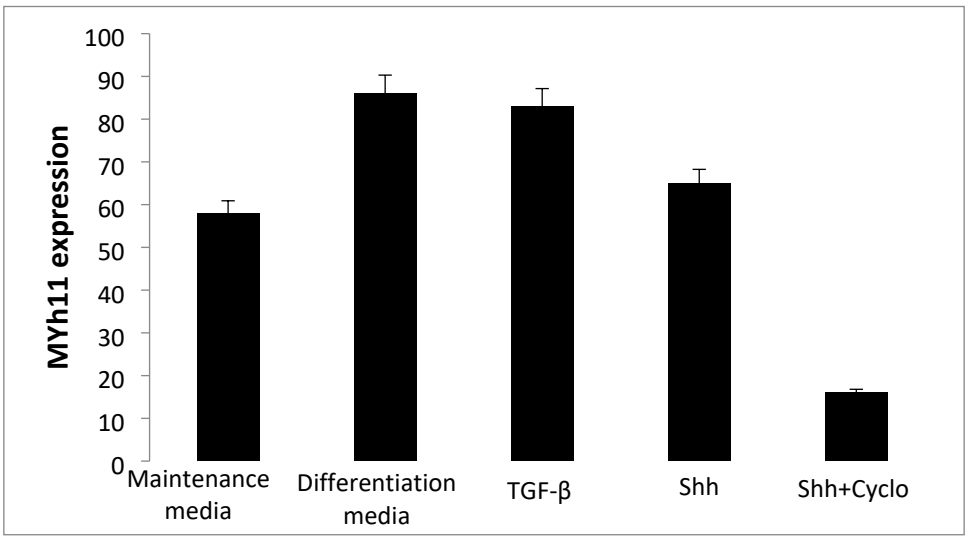

Figure 43: Western blot analysis data on Image J software for Myh 11 expression on mMSCs

It is important to note that all Western blot analyses included β-Actin as a loading control (Figures 38 and 40), ensuring the observed changes in CNN1 and MYH11 expression were not due to variations in total protein loading.

3.4 Real-time qRT-PCR Analysis

Real-time quantitative RT-PCR was performed to assess the expression of Gli1 (a downstream target of SHh signaling) and CNN1 at the mRNA level in mMSCs under various treatment conditions. Figure 44 shows the relative expression of Gli1 mRNA in mMSCs treated with r-SHh alone or in combination with cyclopamine. r-SHh treatment significantly increased Gli1 expression by 6.2-fold compared to the control ($p < 0.001$). This increase was substantially reduced by cyclopamine treatment, resulting in only a 1.8-fold increase compared to the control ($p < 0.01$ compared to r-SHh alone).

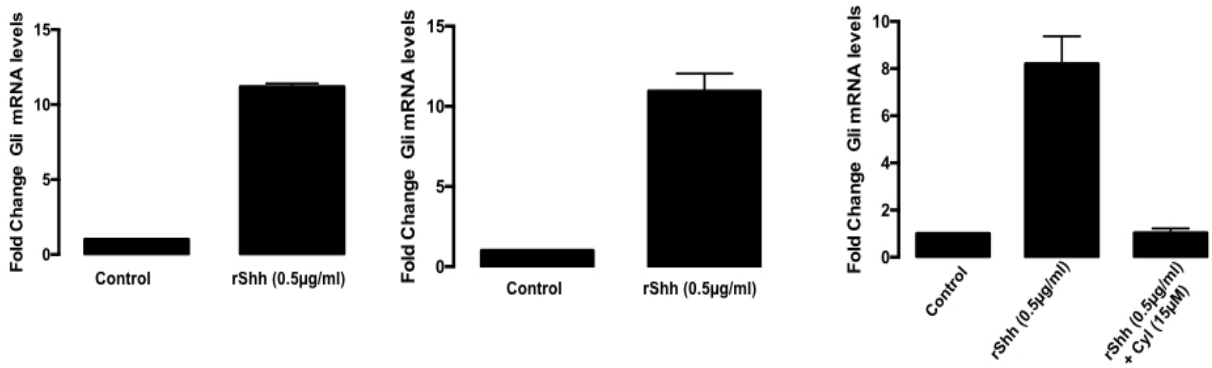

Figure 44: Gli1 expression was investigated by qRT-PCR in mMSC cells after treatment with 0.5 µg/µL r-Shh and 0.5 µg/µL r-Shh plus 10µM cyclopamine. Cells were seeded at 100,000 cells per well and were incubated until they are confluent. mRNA was prepared as mentioned in the methods section and data was analysed using the Comparative CT method (ΔΔCT), described by Livak and Schmittgen, 2001.

Figure 45 presents the relative expression of CNN1 mRNA under the same conditions. r-SHh treatment increased CNN1 mRNA levels by 4.8-fold compared to the control ($p < 0.001$). Cyclopamine significantly attenuated this increase, resulting in a 2.1-fold increase compared to the control ($p < 0.01$ compared to r-SHh alone).

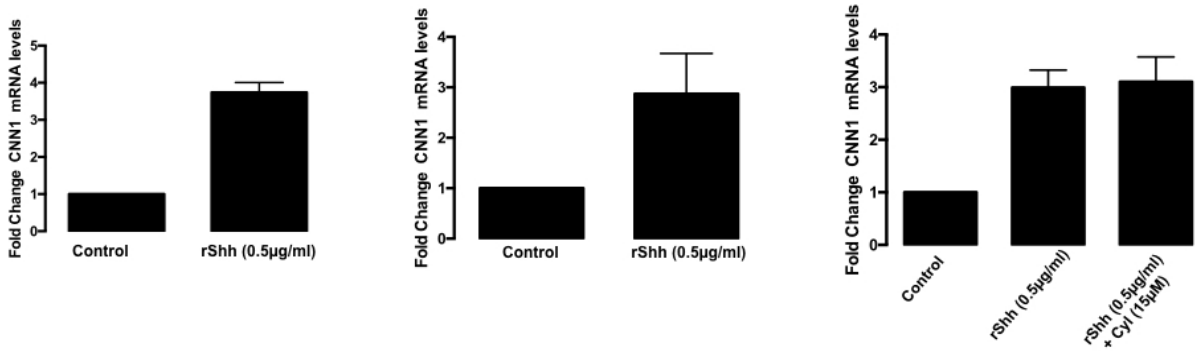

Figure 45: CNN1 expression was investigated by qRT-PCR in mMSC cells after treatment with 0.5 µg/µL r-Shh and 0.5 µg/µL r-Shh plus 10µM cyclopamine. Cells were seeded at 100,000 cells per well and were incubated until they are confluent. mRNA was prepared as mentioned in the methods section and data was analysed using the Comparative CT method (ΔΔCT), described by Livak and Schmittgen, 2001.

These qRT-PCR results corroborate the protein expression data from Western blot and immunocytochemistry analyses, providing further evidence for the role of SHh signaling in promoting SMC marker expression in mMSCs.

3.5 Effects of Sonic Hedgehog Signalling on Adventitial Progenitor Cells (APCs)

To investigate whether the effects of SHh signaling observed in mMSCs extend to other progenitor cell types, we performed similar experiments on rat adventitial Sca1+ MSC-

like cells (APCs). Figure 46 shows immunocytochemistry staining for CNN1 in APCs cultured in maintenance and differentiation media. Quantification of these results (Figure 47) revealed that differentiation media significantly increased the proportion of CNN1-positive cells from 15.7 ± 2.1% to 41.3 ± 3.5% ($p < 0.01$).

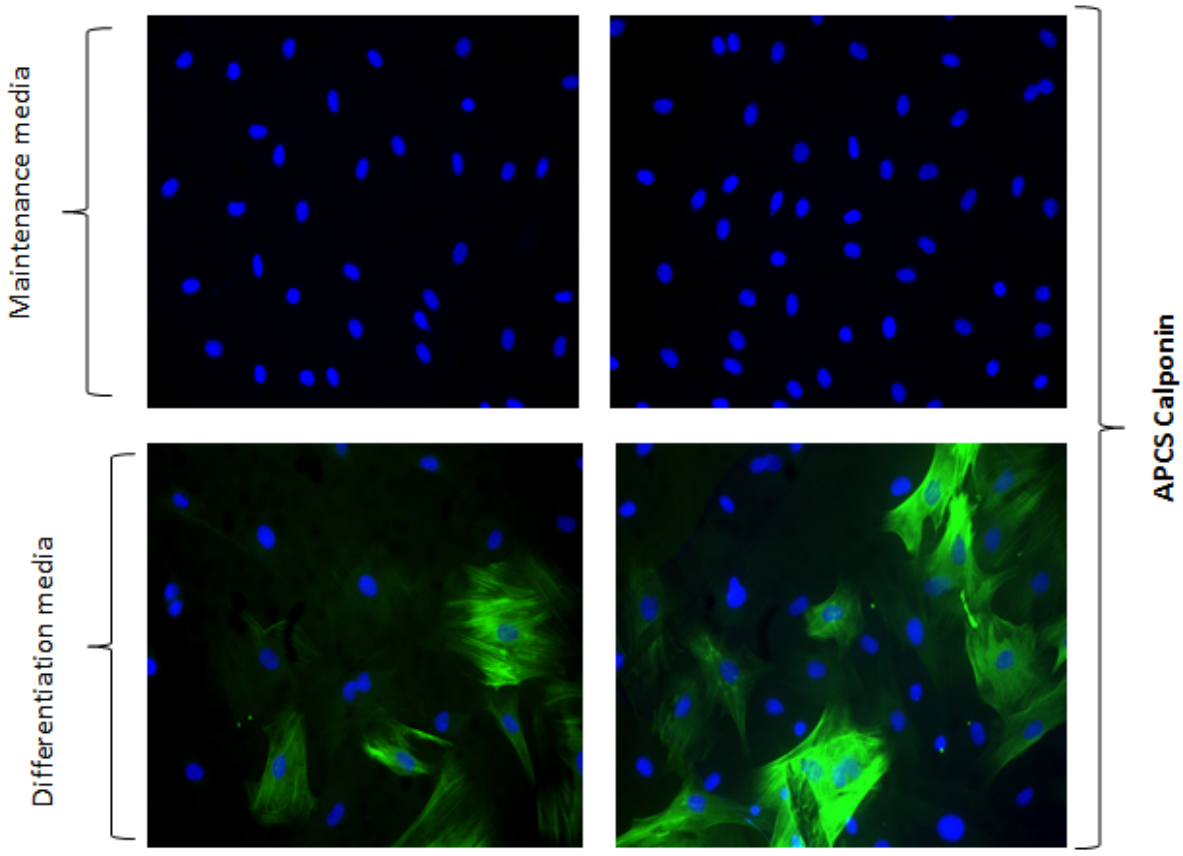

Figure 46: APCs in Maintenance media and Differentiation media stained Immunocytochemically for CNN1. APCs were seeded at a low density (5,000 cells/well) and incubated for five days, fixed by using formaldehyde and stained for the relating Smooth muscle cell marker using primary antibody CNN1. Subsequently, Cells were probed with an appropriate secondary antibody and stained with DAPI for nuclei visualisation.

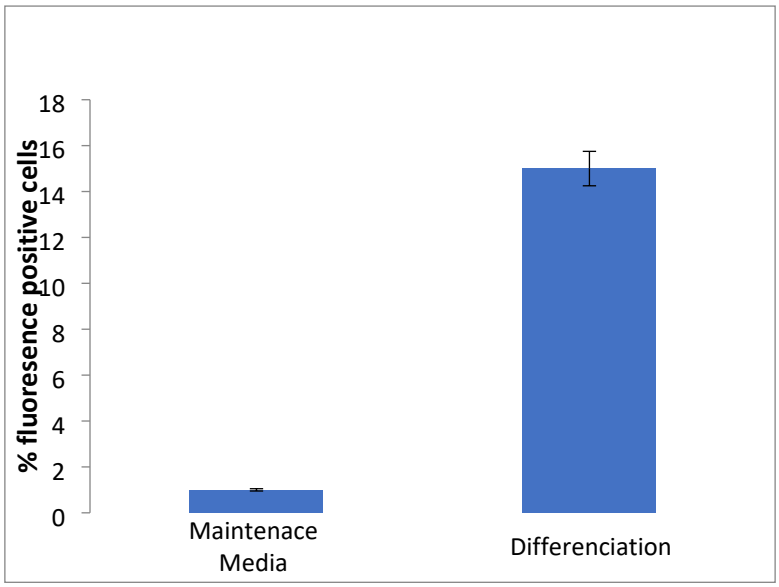

Figure 47: The proportions of immunofluorescence positive cells for CNN1 expression on APCs in Maintenance and Differentiation media. Graph shows the proportions of immunofluorescence positive cells that analysed to generally assess the expression level of CNN1 in the two different groups, Maintenance media, and Differentiation media.

Figure 48 demonstrates CNN1 staining in APCs treated with r-SHh alone or in combination with various inhibitors. Quantitative analysis (Figure 49) showed that r-SHh treatment increased CNN1-positive cells to 47.6 ± 3.9% ($p < 0.001$ compared to maintenance media). This increase was significantly reduced by cyclopamine (23.1 ± 2.7%), HPI-4 (19.8 ± 2.4%), and Anti-Patched antibody (28.5 ± 3.1%) (all $p < 0.01$ compared to r-SHh alone).

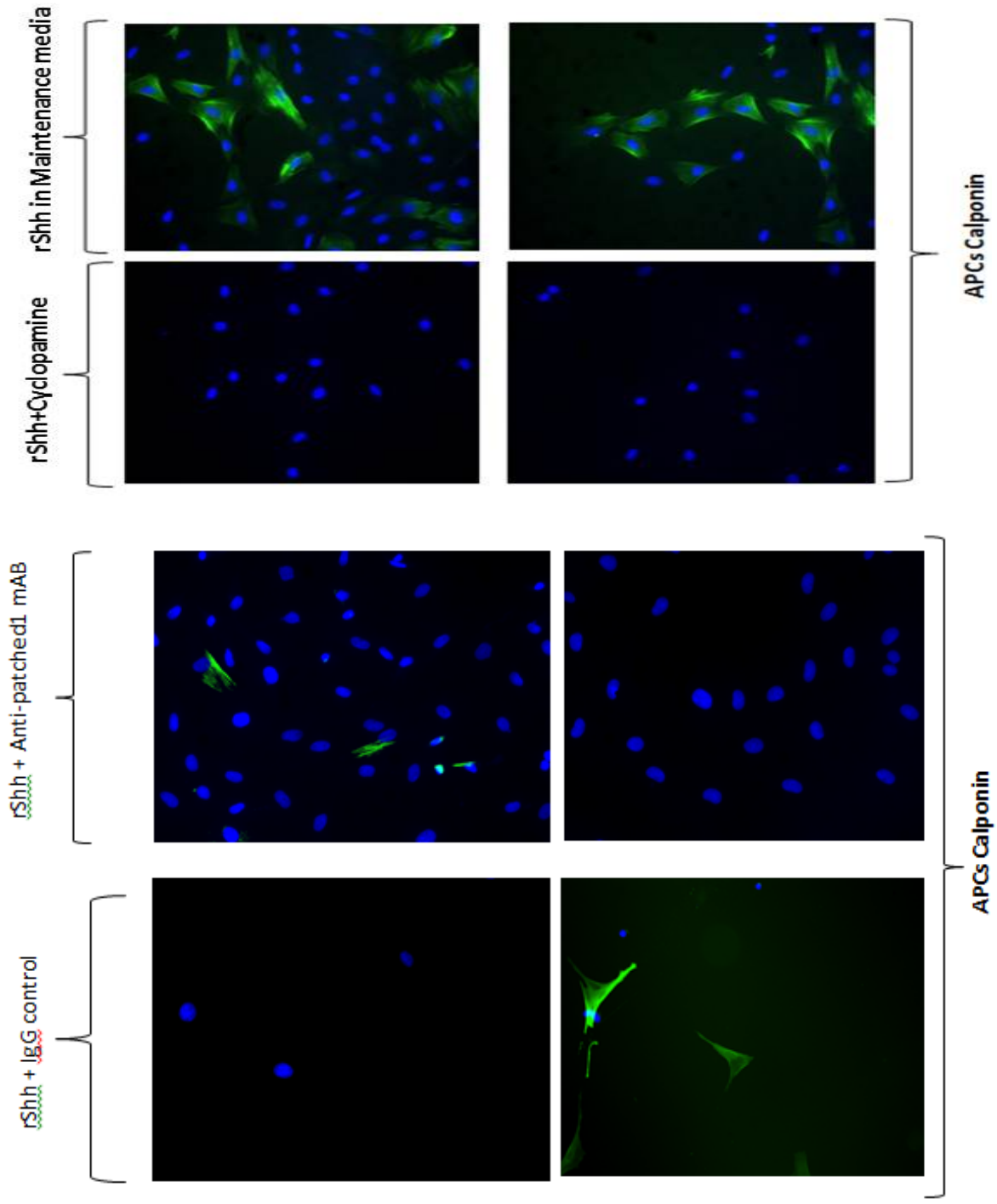

Figure 48: APCs in rSHh, 0.5 µg/µL r-SHh plus 10µM cyclopamine, 0.5 µg/µL r-SHh plus 3µg/µL Anti-Patched1 Ab, and r-SHh plus 3µg/µL IgG control stained immunocytochemically for CNN1. APCs were seeded at a low density (5,000 cells/well) and incubated for five days, fixed by using formaldehyde and stained for the relating Smooth muscle cell marker using

primary antibody CNN1. Subsequently, Cells were probed with an appropriate secondary antibody and stained with DAPI for nuclei visualisation.

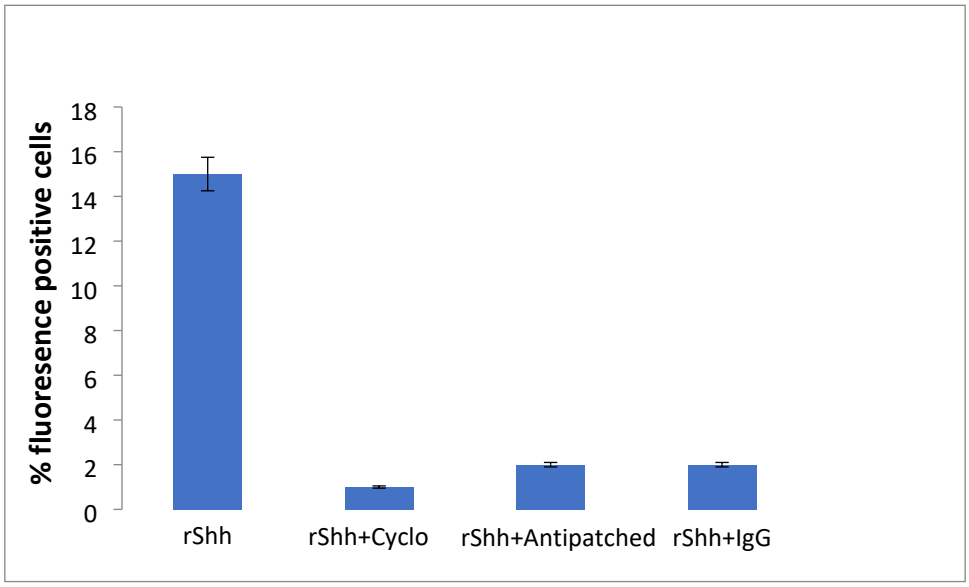

Figure 49: The proportions of immunofluorescence positive cells for CNN1 expression on APCs that treated with rSHh and rSHh+ inhibitors. Graph shows the proportions of immunofluorescence positive cells that analysed to generally assess the expression level of CNN1 in the different groups, r-SHh, r-Shh plus cyclopamine, r-SHh plus AntiPatched1 and r-SHh plus IgG.

An overview of CNN1 expression in APCs across all treatment conditions is provided in Figure 50, showing patterns similar to those observed in mMSCs.

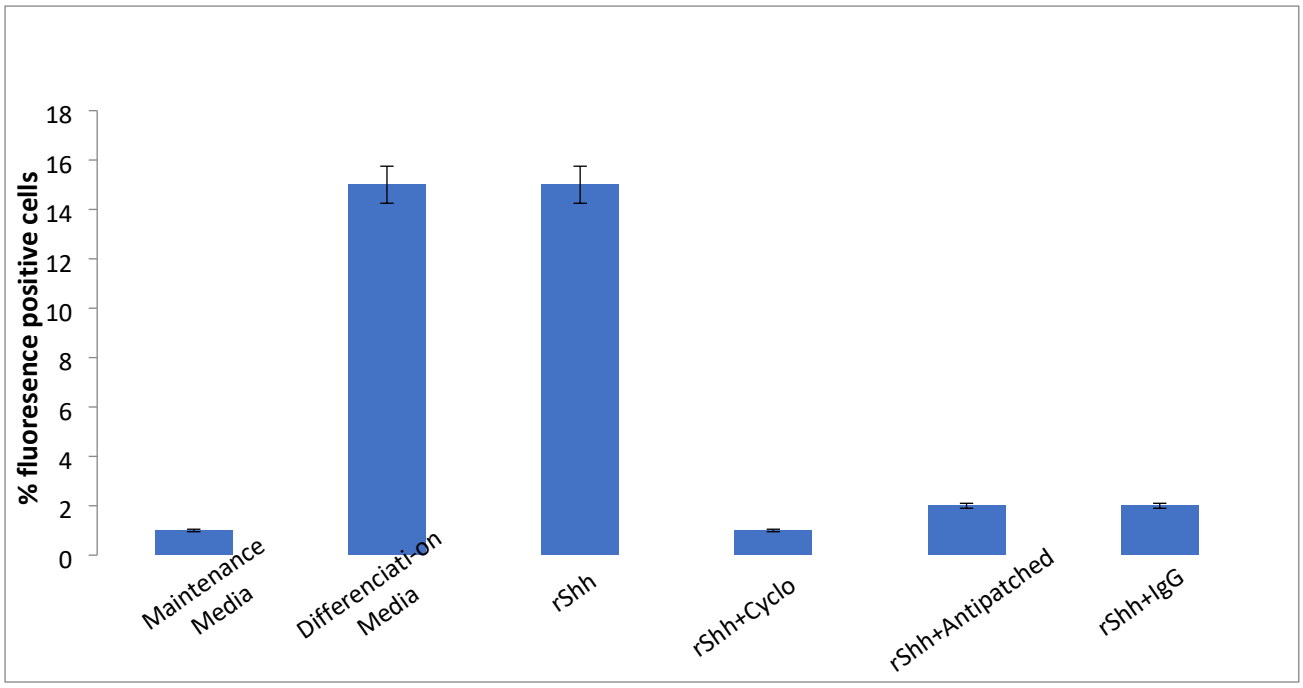

Figure 50: An overview graph for the above images for CNN1 expression after all the treatments of APC cells.

Similar analyses were performed for MYH11 expression in APCs. Figure 51 shows MYH11 staining in maintenance and differentiation media, with quantification in Figure 52 revealing an increase from 10.2 ± 1.7% to 38.9 ± 3.3% MYH11-positive cells in differentiation media ($p < 0.01$).

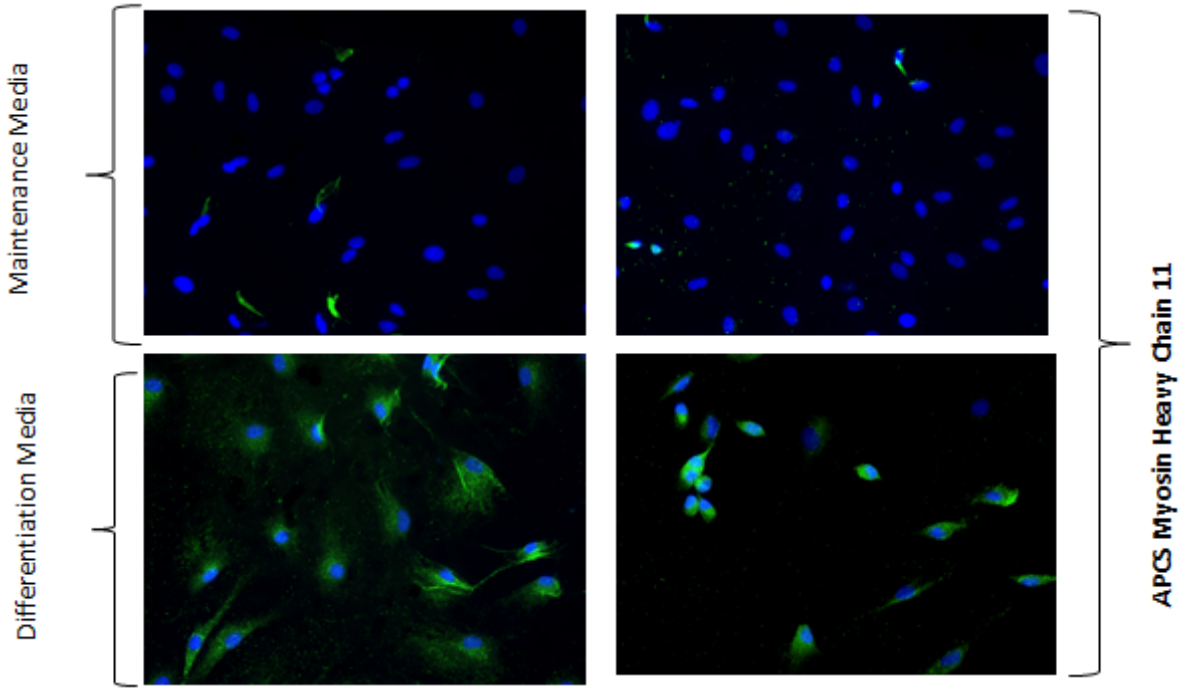

Figure 51: APCs in maintenance media and differentiation media stained immunocytochemically for Myh11. APCs were seeded at a low density (5,000 cells/well) and incubated for five days, fixed by using formaldehyde and stained for the relating Smooth muscle cell marker using primary antibody Myh11. Subsequently, Cells were probed with an appropriate secondary antibody and stained with DAPI for nuclei visualisation.

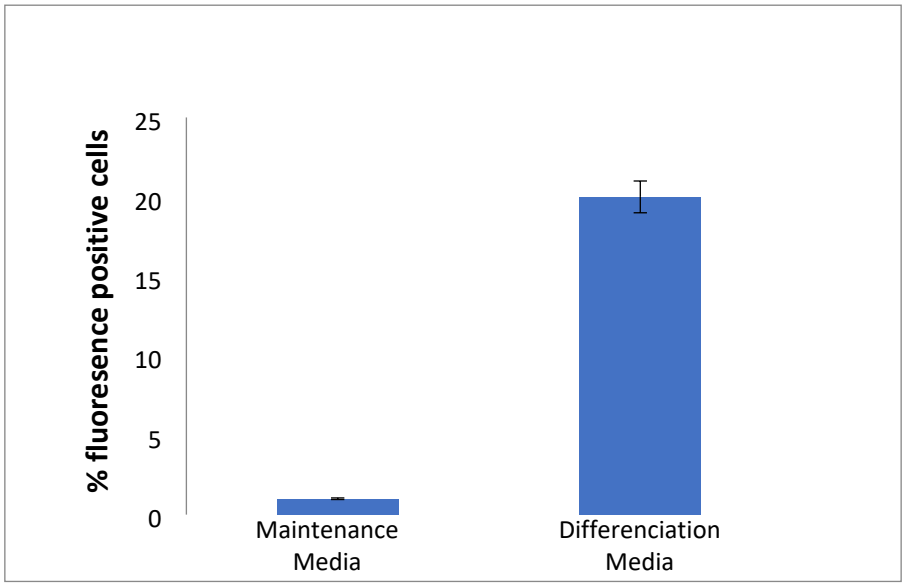

Figure 52: The proportions of immunofluorescence positive cells for Myh11 expression on APCs in maintenance and differentiation media. Graph shows the proportions of immunofluorescence positive cells that analysed to generally assess the expression level of Myh11 in the two different groups, Maintenance media, and Differentiation media.

Figure 53 presents MYH11 staining in APCs treated with r-SHh and various inhibitors. Quantitative analysis (Figure 54) demonstrated that r-SHh increased MYH11-positive cells to 44.7 ± 3.7% ($p < 0.001$ compared to maintenance media), which was reduced by cyclopamine (20.5 ± 2.4%) and Anti-Patched antibody (26.1 ± 2.8%) (both $p < 0.01$ compared to r-SHh alone).

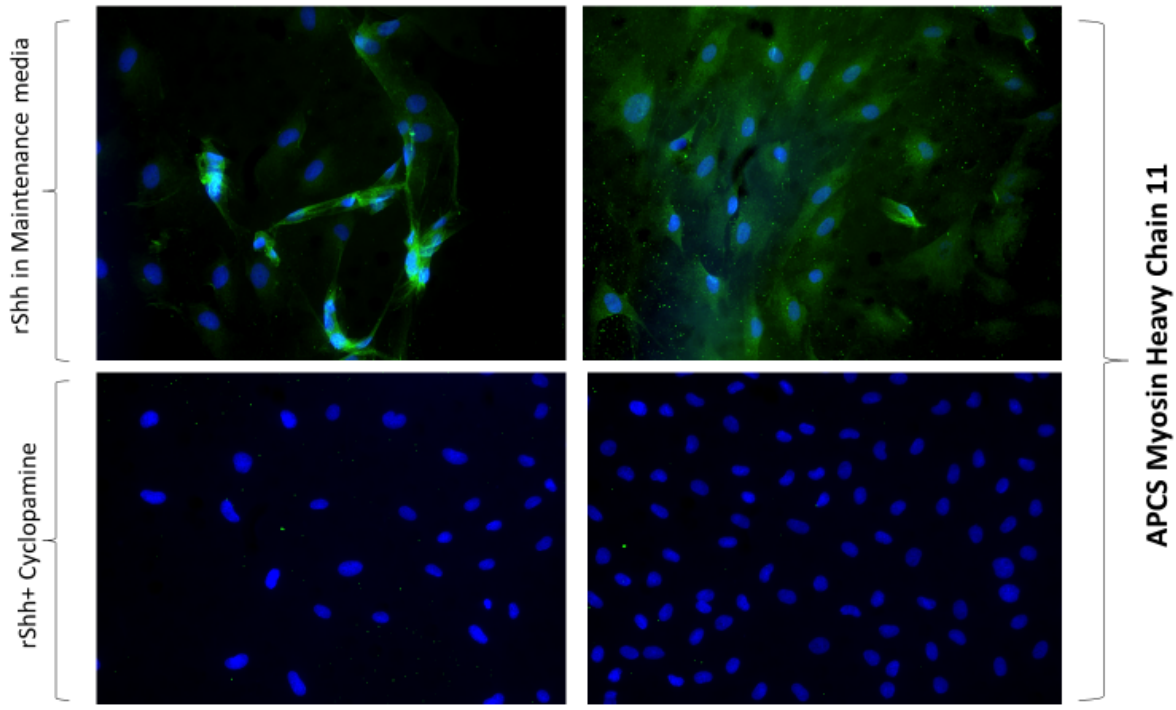

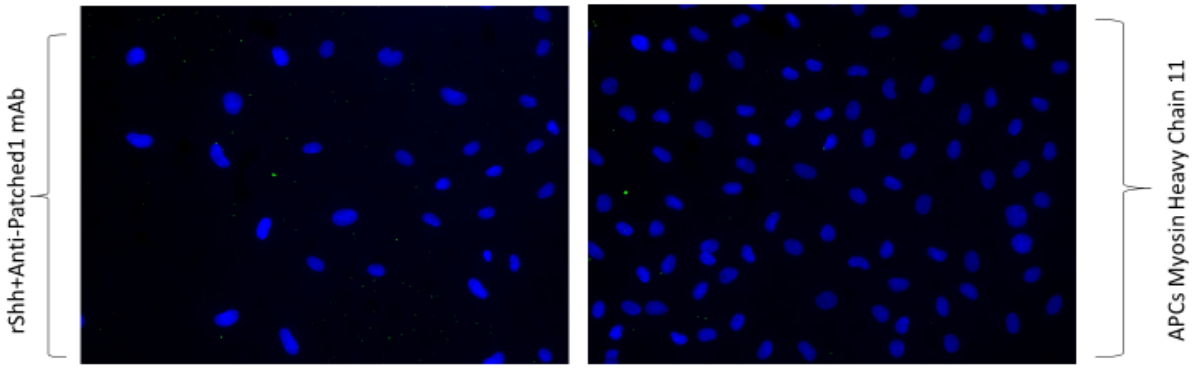

Figure 53: APCs in Maintenance media, 0.5µg/µL r-Shh plus 10µM cyclopamine, and 0.5µg/µL r-Shh plus 3µg/µL Anti-Patched Ab stained immunocytochemically for Myh11. APCs were seeded at a low density (5,000 cells/well) and incubated for five days, fixed by using formaldehyde and stained for the relating Smooth muscle cell marker using primary antibody Myh11. Subsequently, Cells were probed with an appropriate secondary antibody and stained with DAPI for nuclei visualisation.

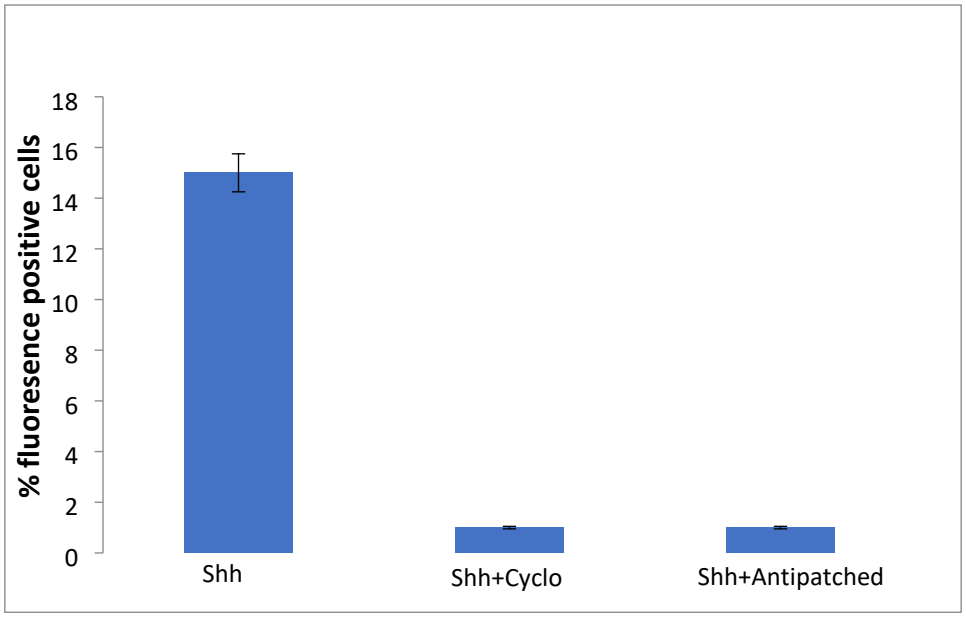

Figure 54: The proportions of immunofluorescence positive cells for Myh11 expression on APCs that treated with r-Shh, and r-Shh plus inhibitors. Graph shows the proportions of immunofluorescence positive cells that analysed to generally assess the expression level of

Myh11 in the three different groups, r-Shh, r-Shh plus cyclopamine and r-Shh plus AntiPatched1.

An overview of MYH11 expression in APCs under all conditions is shown in Figure 55, again demonstrating patterns consistent with those observed in mMSCs.

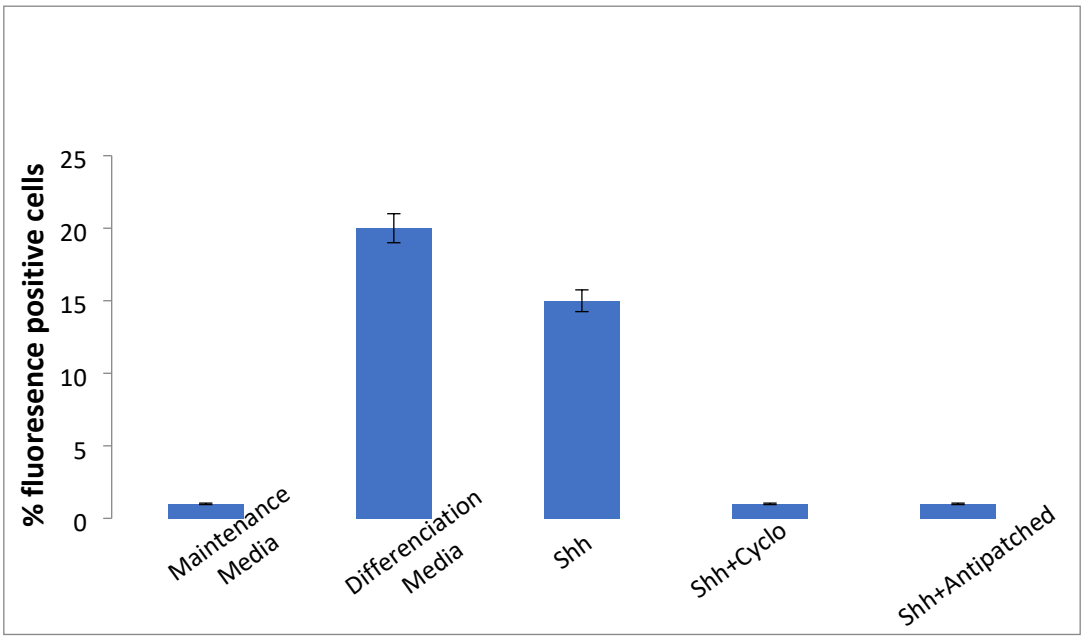

Figure 55: An overview of Myh11 expression for the above images after all the treatment of APC cells.

Chapter 4: Discussion

4.1 Evaluation of SHh Inhibitors in Cellular Contexts

In this study, two inhibitors of the Sonic Hedgehog pathway, cyclopamine and HPI-4, were analysed for their capacity to suppress the pathway's activity. Initial experiments aimed to ascertain optimal dosages by evaluating their influence on the viability and proliferation of in vitro cultured bone-marrow-derived mesenchymal stem cells (MSC). The Alamar Blue assay disclosed a pronounced suppressive effect on cell growth upon treatment with elevated doses of cyclopamine, signalling its potential toxicity, aligning with previous studies on the topic that described its mechanism of action through direct binding to the smoothened protein. In contrast, HPI-4 exhibited no such detrimental effects. These findings crucially contributed to distinguishing the varying levels of toxicity between cyclopamine and HPI-4, underscoring cyclopamine's increased toxicity at higher doses.

Later experiments assessed the effectiveness of recombinant Sonic Hedgehog (r-Shh) in prompting MSCs to transform into smooth muscle cells. Immunocytochemistry and Western blot methods were employed, revealing markers characteristic of smooth muscle cell differentiation. The study also examined the suppressive effects of cyclopamine and HPI-4 on this differentiation. The efficacy of Anti-Patched1 antibody, an alternate biological inhibitor, was similarly investigated, showing comparable effectiveness to smoothened inhibitors. Further insights were gained through RT-q-PCR experiments in MSCs, focusing on the genes Gli1 and Calponin. The upregulation of Gli1 gene expression following r-Shh treatment, and its subsequent decrease with cyclopamine addition, confirmed the Shh pathway's role in MSC differentiation to smooth muscle cells. Parallel experiments conducted on Sca1+ adventitial progenitor stem cells (APC) reinforced these findings, with both cyclopamine and Anti-Patched1 antibody effectively inhibiting SHh activation.

4.2 Implications for Cardiovascular Disease Treatment

Collectively, these findings suggest a significant role for the SHh signalling pathway in cardiovascular disease, particularly in cardiomyogenesis and vascular cell maintenance. This aligns with previous research indicating the potential of inhibiting the SHh pathway, pharmacologically or genetically, to mitigate cardiovascular disease symptoms like neointimal thickening and intimal hyperplasia (Melnik et al., 2022). The study's conclusions are bolstered by findings from previous studies, which demonstrate the pathway's role in VSMC proliferation and intimal hyperplasia (Ma et al., 2022). Looking ahead, the study outlines a roadmap for further experimentation within each objective. Key future steps include conducting proliferation and toxicity experiments on vascular smooth muscle cells (VSMCs) and completing experiments on APCs. Additionally, the study anticipates investigating the effects of Sonic hedgehog on pluripotent C3h stem cells, thereby expanding the understanding of its role in cardiovascular diseases and potential therapeutic applications.

4.3 Comparative and Contextual Analysis

4.3.1 Theoretical Implications and Clinical Relevance

The Sonic Hedgehog (Shh) signalling pathway holds significant theoretical implications and clinical relevance, particularly in the context of cardiovascular diseases. This pathway, fundamental to embryonic development and tissue regeneration, has been shown to play a critical role in the differentiation of stem cells into smooth muscle cells, a process integral to the maintenance and repair of cardiovascular tissues. Our findings, aligning with the work of Passman et al. (2008) and Redmond et al. (2013), underscore the importance of the Shh pathway in the homeostasis of vascular tissues and its potential as a therapeutic target. Consequently, these insights position the Shh pathway as a promising focus for future cardiovascular therapies.

In cardiovascular disease scenarios, such as atherosclerosis, the ability of the Shh pathway to regulate the differentiation of mesenchymal stem cells (MSCs) and adventitial progenitor cells (APCs) into smooth muscle cells can be particularly impactful. As suggested by our results and supported by Li et al. (2010), modulation of this pathway could influence the proliferation of vascular smooth muscle cells (VSMCs), a crucial factor in the progression of atherosclerotic lesions. The differential effects of SHh inhibitors like cyclopamine and HPI-4 offer a detailed understanding of how pathway manipulation could lead to divergent outcomes in cardiovascular disease treatment. This perspective aligns with the broader concept in regenerative medicine where pathway modulation is capable of promoting tissue repair and risking abnormal growth or malignancies.

Moreover, the clinical significance of these results is underlined by the potential role of SHh pathway blockers as medical treatments. The differing toxic effects of cyclopamine and HPI-4 underscore the need for precise application in therapy. Fitzpatrick et al. (2017) support this, showing alcohol's role as an SHh blocker, which underscores the delicate nature of pathway control. Beyond just inhibiting the pathway, these blockers might also be used in conjunction with other treatments. This approach could be especially important in cases where excessive pathway activity contributes to the progression of certain cardiovascular diseases.

The synthesis of the results with established research forms a strong argument for targeting the SHh pathway in cardiovascular disease therapy. This also leads to new directions for research, especially in grasping the prolonged impacts of modulating the SHh pathway and incorporating it into current therapeutic frameworks. Fundamentally, this investigation enhances our conceptual grasp of the SHh pathway's role in cardiovascular health, underscoring its significance in devising novel treatment strategies and underscoring the importance of ongoing inquiry in this domain.

4.3.2 Comparative Analysis of SHh Inhibitors

The comparative study of Sonic Hedgehog (Shh) blockers, namely cyclopamine, HPI-4, and Anti-Patched1, unveils unique mechanisms and their potential roles in addressing cardiovascular diseases. Cyclopamine, an alkaloid found naturally, has been identified as targeting the Smoothened (SMO) receptor directly (Li et al., 2010), leading to reduced proliferation of vascular smooth muscle cells (VSMCs), vital in the development of conditions like atherosclerosis. However, its high-dose toxicity poses challenges for clinical use, requiring careful dosage calibration and patient-specific considerations.

Contrastingly, HPI-4 shows a divergent safety profile, exhibiting reduced toxicity in comparison to cyclopamine, as our experiments demonstrated. This aligns with studies such as those by Lospinoso Severini et al. (2020), who highlight the need for SHh inhibitors with minimal side effects for potential therapeutic use. The lower toxicity of HPI-4 suggests its suitability for longer-term treatments or for use in patients where cyclopamine's side effects are a concern. However, the efficacy of HPI-4 in inhibiting the Shh pathway in a clinical setting requires further investigation.

Anti-Patched1 antibody offers an alternative approach by targeting the Patched1 receptor, thereby modulating the Shh pathway at a different regulatory point compared to cyclopamine and HPI-4. The results could be effective in conditions where upstream modulation of the pathway is desired (Passman et al., 2008; Redmond et al., 2013). This could be particularly relevant in diseases where Patched1 receptor overexpression or mutation plays a role. However, the specificity and long-term effects of Anti-Patched1 in cardiovascular disease treatment need further exploration. The choice of SHh inhibitor in a clinical context must, therefore, be guided by a comprehensive understanding of the disease pathology, patient-specific factors, and the inhibitor's mechanism of action. Essentially, while all three inhibitors show promise in modulating the Shh pathway, their distinct profiles call for tailored therapeutic

strategies. Future research should focus on comparative studies in clinical settings to ascertain the most effective and safe application of these inhibitors in cardiovascular diseases.

4.4 Addressing the Hypothesis

Our initial hypothesis proposed that inhibiting the Sonic Hedgehog (SHh) signalling pathway would suppress the differentiation of mesenchymal stem cells (MSCs) and adventitial progenitor cells (APCs) into smooth muscle cells, potentially offering a therapeutic approach for cardiovascular diseases characterized by aberrant vascular remodelling. Based on the comprehensive results of our study, we can now confidently accept this hypothesis. Several lines of evidence support this conclusion. First, our experiments with recombinant Sonic Hedgehog (r-Shh) demonstrated clear activation of the pathway in both MSCs and APCs, as evidenced by increased expression of pathway target genes like Gli1 and smooth muscle cell markers. Second, both small molecule inhibitors (cyclopamine and HPI-4) and the biological inhibitor (Anti-Patched1 antibody) effectively suppressed SHh-induced differentiation of MSCs and APCs into smooth muscle cells. This was confirmed through multiple experimental approaches, including immunocytochemistry, Western blot analysis, and RT-qPCR. Third, we observed dose-dependent inhibition of cell differentiation and pathway activity, further validating the specific effect of these inhibitors on the SHh pathway.

Fourth, the inhibitory effects were consistently observed in both MSCs and APCs, suggesting a conserved role of SHh signaling in the differentiation of these distinct progenitor cell populations. Lastly, the modulation of Gli1 expression, a key transcriptional effector and marker of SHh pathway activity, provided molecular-level evidence supporting our hypothesis. These findings not only confirm our initial hypothesis but also extend our understanding of the role of SHh signaling in vascular biology. The ability to modulate this pathway and thereby influence the differentiation of progenitor cells into smooth muscle cells has significant implications for cardiovascular disease treatment. However, it is important to

note that while our hypothesis is supported, the translation of these findings into clinical applications will require further investigation. The differential toxicity profiles of the inhibitors and the complex role of SHh signalling in both pathological and physiological processes necessitate careful consideration in any therapeutic strategy targeting this pathway.

4.5 Future Perspectives and Research Directions

Despite significant progress, further experiments are necessary. Upcoming studies will focus on the effects of SHh inhibitors on vascular smooth muscle cells (VSMCs), employing techniques like DAPI nuclei staining and cell counting. Additionally, the role of Anti Patched1 Antibody as an SHh inhibitor will be further examined using Western blot, RT-q-PCR, and potentially ELISA assays. Experiments on APCs will continue, aiming to comprehensively understand the role of Sonic hedgehog in these cells. Finally, the project will extend to explore the effects of Sonic hedgehog on pluripotent C3h stem cells.

4.5.1 Emerging Therapeutic Targets

The Sonic Hedgehog (Shh) signalling pathway, integral to cell differentiation and tissue regeneration, presents several potential targets for cardiovascular disease treatment. Ideally, targeting specific components of the Shh pathway could offer new therapeutic avenues, particularly in diseases characterized by abnormal smooth muscle cell proliferation, such as atherosclerosis. One promising target is the Gli family of transcription factors, key mediators of the Shh signalling pathway (Lospinoso Severini et al., 2020). Research demonstrates that altering Gli1 expression crucially impacts the transformation of mesenchymal stem cells (MSCs) into smooth muscle cells. Corresponding with Redmond et al. (2013), this shows the efficacy of targeting Gli proteins in modulating the pathway. Specialized inhibitors aimed at Gli transcription factors might refine SHh pathway control, thereby reducing the adverse effects seen with broader inhibition strategies.

An additional important point is the Patched1 receptor. This study revealed that the Anti-Patched1 antibody effectively suppresses Shh signalling, proposing its targeting as a feasible therapeutic approach. This aligns with Passman et al. (2008), who identified Patched1's significant role in maintaining vascular tissue stability. Developing medications that specifically target Patched1 could alter the Shh pathway from its origin, offering a new strategy for intervention. Furthermore, this research highlights the Smoothened (SMO) receptor as a vital target, demonstrated by cyclopamine's effectiveness in pathway inhibition. However, its toxicity raises concerns for its clinical use, emphasizing the necessity to create new SMO inhibitors with better safety profiles, an aspect underscored by Li et al. (2010). Advancements in this area could yield safer, more effective treatments for cardiovascular diseases, focusing on pathway regulation without detrimental side effects.

Besides the known targets, this research paves the way for identifying new intervention points within the Shh pathway, such as the downstream effectors of Gli transcription factors or other related regulatory proteins. These novel targets could enable more refined manipulation of the pathway's influence in cardiovascular disorders, facilitating the development of therapies customized to specific disease mechanisms. Overall, this study not only reaffirms the importance of the Shh pathway in cardiovascular diseases but also highlights several potential therapeutic targets within the pathway. Future research should aim to develop and test specific inhibitors targeting these components, with a focus on their efficacy and safety in cardiovascular disease contexts. Such efforts could lead to significant advancements in the treatment of cardiovascular diseases, offering new hope for patients suffering from these conditions.

4.5.2 Recommendations for Future Research

Exploring the potential for combination therapies with SHh pathway modulators is a promising area of research following our study. The efficacy of inhibitors like cyclopamine

and HPI-4, especially in conjunction with other cardiovascular medications, offers a synergistic approach that could revolutionize treatment strategies. Investigating how these inhibitors work alongside existing drugs, such as statins or beta-blockers, could lead to more comprehensive and effective treatment regimes, improving overall patient outcomes in cardiovascular disease management.

Advancing precision medicine in cardiovascular therapy is a vital area of research. Pinpointing specific biomarkers that predict responses to Shh pathway regulators can lead to more individualized treatment schemes. This method aims to enhance therapeutic effectiveness while reducing negative outcomes, marking a transition from broad treatments to more tailored care (Thapa et al., 2023). Investigations in this domain hold the potential to revolutionize cardiovascular therapy, pushing it towards more efficient, patient-focused approaches.

Clarifying the SHh signalling roles in diverse cardiovascular diseases is critical for a more comprehensive grasp of this pathway's impact. While this study sheds light on its overall role in cardiovascular health, probing its specific functions in conditions like heart failure or hypertension could reveal new therapeutic targets. Such explorations could broaden our comprehension of cardiovascular diseases and pave the way for novel treatment methods. Evaluating the long-term effects of SHh pathway inhibition is crucial, especially considering the prolonged nature of many cardiovascular diseases. It is vital to understand the enduring impacts and safety profiles of SHh inhibitors for their sustainable use in extended treatment plans. Future research should concentrate on assessing long-term usage risks, such as potential toxicity or the development of resistance, to maintain the viability of these treatments for chronic cardiovascular conditions.

Finally, investigating the potential of SHh agonists in regenerative therapies offers a promising avenue in cardiovascular medicine. Utilizing Shh agonists for tissue repair, particularly following myocardial infarction or ischemic injuries, could significantly progress

treatment for heart diseases. Studies in this field might lead to ground-breaking advancements in cardiac tissue repair and regeneration, providing new prospects for effective recuperation in heart disease patients. Each proposed research direction builds on the insights of this study, seeking to deepen our knowledge and enhance treatment methods for cardiovascular diseases.

References

Akin, I., & Nienaber, C. A., 2015. Treatment of coronary in-stent restenosis—evidence for universal recommendation? *Journal of Thoracic Disease*, 7(10), pp. 1672–1675.

Anand, S. S., Hawkes, C., de Souza, R. J., Mente, A., Dehghan, M., Nugent, R, ., Zulyniak MA., Weise T., Bernstein AM., Krauss RM., Kromhout D., Jenkins DJA., Malik V., Martinez MA., Yusuf S., Willett WC., Popkin. , B. M., 2015. Food Consumption and its impact on Cardiovascular Disease: Importance of Solutions focused on the globalized food system: A Report from the Workshop convened by the World Heart Federation. *Journal of the American College of Cardiology*, [e-journal] 66(14), pp.1590–1614.

Andrus, E. C., Allen, E. V., Merritt, H. H., Duff, G. L., Moore, R. A., Kendall, F. E., Shumacker, H. B., Leavy, R.S. Wright, I. S., 2015. The pathogenesis of arteriosclerosis. *International Journal of Epidemiology*, 44(6), pp.1791–1793

Aza-Blanc, P., Lin, H. Y., Ruiz, I., Altaba, A., & Kornberg, T. B., 2000. Expression of the vertebrate Gli proteins in Drosophila reveals a distribution of activator and repressor activities. *Development*, [e-journal] 127(19), pp.4293-301.

Baker, A. H., & Bruno, P., 2016. A Gli(1)ttering Role for Perivascular Stem Cells in Blood Vessel Remodeling. *Cell Stem Cell*, 19.

Benjamin, E. J., Blaha, M. J., Chiuve, S. E., Cushman, M., Das, S. R., Deo, R., De Ferranti S.D., Floyd J., Fornage M., Gillespie C., Isasi CR., Jimenze MC., Jordan LC., Judd SE., Lackland D., Lichtman JH., Lisabeth L., Liu S., Longenecker CT., Mackey RH., Matsushita K., Mozaffarian D., Mussolino ME., Nasir K., Neumar RW., Palanipaan L., Pandey DK., Thiagarajan RR., Reeves MJ., Ritchey M., Rodriguez CJ Roth GA., Rosamond WD., Sasson C., Towfighi A., Tasco CW., Turner MB., Virani SS., Voeks JH., Willey JZ., Wilkins JT., Wu JH., Alger HM., Wong SS., Muntner, P., 2017. Heart

Disease and Stroke Statistics—2017 Update: A Report From the American Heart Association. *Circulation*, 135(10), pp.e146–e603.

Bennett, M. R., Sinha, S., & Owens, G. K. 2016. Vascular smooth muscle cells in atherosclerosis. *Circulation Research*, 118(4), pp.692–702.

Bennette, K., 2007. Coronary heart disease mortality in Ireland. *Quality & Safety in Health Care,* 16(1), p.44.

Bergheanu, S. C., Bodde, M. C., & Jukema, J. W., 2017. Pathophysiology and treatment of atherosclerosis: Current view and future perspective on lipoprotein modification treatment. *Netherlands Heart Journal*, 25(4), pp. 231–242.

Bhatnagar, P., Wickramasinghe, K., Wilkins, E., & Townsend, N. 2016. Trends in the epidemiology of cardiovascular disease in the UK. *Heart*, [e-journal] 102(24), pp.1945–1952.

Biehl, J. K., & Russell, B., 2009. Introduction to Stem Cell Therapy. *The Journal of Cardiovascular Nursing*, 24(2), pp.98–105.

Bijlsma, M. F., Peppelenbosch, M. P., & Spek, C. A., 2006. Hedgehog morphogen in cardiovascular disease. *Circulation*, 114(18), pp.1985-91.

Biros, E., Karan, M., & Golledge, J., 2008. Genetic Variation and Atherosclerosis. *Current Genomics*, 9(1), pp.29–42.

Buccheri, D., Piraino, D., Andolina, G., & Cortese, B., 2016. Understanding and managing in-stent restenosis: a review of clinical data, from pathogenesis to treatment. *Journal of Thoracic Disease*, 8(10), pp.E1150–E1162.

Burtenshaw, D., Fitzpatrick, E., Liu, W., Morrow, D., Redmond, E. M., & Cahill, P. A., 2018 Resident S100β/SCA1+ multipotent vascular stem cells undergo myogenic and vasculogenic differentiation in vitro. *BMJ,* 104(4)

Byrne, R. A., Joner, M., & Kastrati, A., 2015. Stent thrombosis and restenosis: what have we learned and where are we going? *European Heart Journal*, [e-journal] 36(47), pp.3320–3331.

Chang, S., Song, S., Lee, J., Yoon, J., Park, J., & Choi, S., 2014. Phenotypic Modulation of Primary Vascular Smooth Muscle Cells by Short-Term Culture on Micropatterned Substrate. *PLoS ONE,* 9(2),p.e88089.

Chen, P., Qin, L., Li, G., Tellides, G., & Simons, M., 2016a. Fibroblast growth factor (FGF) signaling regulates transforming growth factor beta (TGFβ)-dependent smooth muscle cell phenotype modulation . *Scientific Reports,* 6(33407)

Chen, P., Qin, L., Li, G., Tellides, G., & Simons, M., 2016b. Smooth muscle FGF/TGFβ cross talk regulates atherosclerosis progression. *EMBO Molecular Medicine*, 8(7), pp.712–728.

Chistiakov, D. A., Orekhov, A. N., Bobryshev, Y. V., 2015. Vascular smooth muscle cell in atherosclerosis. *Acta Physiol*, 214(1), pp.33-50.

Choudhry, Z., Rikani AA., Choudhry AM., Tariq S., Zakaria F., Ashar MW., Sarfraz MK., Haider K., Shafiq AA., Mobassarah NJ., , 2014. Sonic hedgehog signalling pathway: a complex network. *Ann Neurosci* 21(1), pp.28-31.

Ciaran J. Mooney., Roya Hakimjavadi., Emma Fitzpatrick., Eimear Kenned.y, Dermot Walls., David Morrow., Eileen M. Redmond, Paul A. Cahill1., 2015 “Hedgehog and Resident Vascular Stem Cell Fate,” Stem Cells International, vol., Article ID 468428, 16 pages, 2015

Cobble, M., & Bale, B., 2010. Carotid intima-media thickness: knowledge and application to everyday practice. *Postgrad Med*., 122(1), pp.10-8.

Coll-Bonfill, N., Musri, M. M., Ivo, V., Barberà, J. A., & Tura-Ceide, O., 2015. Transdifferentiation of endothelial cells to smooth muscle cells play an important role in vascular remodelling. *American Journal of Stem Cells*, 4(1), pp.13–21.

Dejana, E., Hirschi, K. K., & Simons, M., 2017. The molecular basis of endothelial cell plasticity. *Nature Communications*, 8, p. 14361.

Dosi, R., Bhatt, N., Shah, P., & Patell, R., 2014. Cardiovascular Disease and Menopause. *Journal of Clinical and Diagnostic Research*, 8(2), pp.62–64.

Faiella, W., & Atoui, R., 2016. Therapeutic use of stem cells for cardiovascular disease. *Clinical and Translational Medicine*, 5, p.34.

Fitzpatrick E.,Han X., Liu W., Corcoran E., Burtenshaw D., Morrow D., Helt JC., Cahill PA., Redmond EM. - 2017. 2017- Alcohol Reduces Arterial Remodeling by Inhibiting Sonic Hedgehog-stimulated Stem Cell Antigen-1 Positive Progenitor Stem Cells Expansion .

Galli, D., Vitale, M., & Vaccarezza, M., 2014. Bone Marrow-Derived Mesenchymal Cell Differentiation toward Myogenic Lineages: Facts and Perspectives. *BioMed Research International*, 762695.

Giacoppo, D., Gargiulo, G., Aruta, P., Capranzano, P., Tamburino, C., & Capodanno, D., 2015. Treatment strategies for coronary in-stent restenosis: systematic review and hierarchical Bayesian network meta-analysis of 24 randomised trials and 4880 patients. *BMJ* 351, p.h5392

Hamid, H., & Coltart, J., 2007. “Miracle stents” - a future without restenosis. *McGill Journal of Medicine* 10(2), pp.105–111.

Hansson, G. K., 2005. Inflammation, atherosclerosis, and coronary artery disease. N Engl J Med., 352(1), pp.685–1695

Hochauf , S., Sternitzky, R., & Schellong, S. M., 2007. Structure and function of the peripheral venous system, *Herz*. 32(1), pp.3-9.

Holdt, L. M., & Teupser, D., 2012. Recent studies of the human chromosome 9p21 locus, which is associated with atherosclerosis in human populations. *Arterioscler Thromb Vasc Biol*., 32, pp.196–206.

Hooper, J. E., & Scott, M. P., 2005. Communicating with Hedgehogs. *Nat. Rev Mol. Cell. Biol.* 6, pp.306-317

Hotkar, A. J., & Balinsky, W., 2012. Stem cells in the treatment of cardiovascular disease--an overview. *Stem Cell Rev*. 8(2), pp.494-502.

Huang J., & Kalderon D., 2014. Coupling of Hedgehog and Hippo pathways promotes stem cell maintenance by stimulating proliferation. The Journal of Cell Biology. 205: 325-38.

Hu Liping., Xiangyang Lin., Hong Lu., Bicheng Chen and Yongheng Bai., 2015. An Overview of Hedgehog Signaling in Fibrosis. Molecular Pharmacology. 87 (2) 174-182.

Hui, C. C., & Angers, S., 2011. Gli proteins in development and disease. Annu Rev Cell Dev Biol. 27, pp.513-37.

Hurst, R. T., Kendall, C., Khandheria, B., 2007. Clinical use of carotid intima-media thickness: review of the literature. *J Am Soc Echocardiogr*, [e-journal] (7), pp.907-14.

Incardona, J. P., Gruenberg, J., & Roelink, H., 2002. Sonic hedgehog induces the segregation of patched and smoothened in endosomes. *Curr. Biol.* 12, pp.983-995.

Infante, P., Alfonsi, R., Botta, B., Mori, M., & Di Marcotullio, L., 2015. Targeting GLI factors to inhibit the Hedgehog pathway. *Trends Pharmacol Sci*. 36(8), pp.547-58.

Insull, W., 2009. The Pathology of Atherosclerosis: Plaque Development and Plaque Responses to Medical Treatment. *Journal of Medicine*, 122(1), pp.S3–S14

Jacob, J., & Briscoe, J., 2003. Gli proteins and the control of spinal-cord patterning. *EMBO Reports*, 4(8), pp.761–765.

Jiang, J., 2006. Regulation of Hh/Gli signaling by dual ubiquitin pathways. *Cell Cycle*, 5, pp.2457–2463.

Kalanuria, A. A., Nyquist, P., & Ling, G., 2012. The prevention and regression of atherosclerotic plaques: emerging treatments. *Vascular Health and Risk Management*, 8, pp.549–561.

Khan, R. J., Stewart, C. P., Davis, S. K., Harvey, D. J., & Leistikow, B. N., 2015. The risk and burden of smoking related heart disease mortality among young people in the United States. *Tobacco Induced Diseases*, 13(1), p.16.

Klingenberg, R., & Hansson, G. K., 2009. Treating inflammation in atherosclerotic cardiovascular disease: emerging therapies. *European Heart Journal,* 30(23), pp.2838–2844.

Kovacic, S., & Bakran, M., 2012. Stroke Research and Treatment. *Genetic Susceptibility to Atherosclerosis* 36294.

Lander, E. S., 2011. Initial impact of the sequencing of the human genome. *Nature*, 470, pp.187–197.

Larijani, B.,., Esfahani EN., Amini P., Nikbin B., Alimoghaddam K., Amiri S., Malekzadeh R., Yazdi NM., Ghodsi M., Dowlati Y., Sahraian MA., Ghavamazadeh A ., 2012. Stem cell therapy in treatment of different diseases. *Acta Med Iran* 50(2), pp.79-96.

Lavine Kory J., Fanxin Long., Kyunghee Choi., Craig Smith., and David M. Ornitz1.,2008. Hedgehog signaling to distinct cell types differentially regulates coronary artery and vein development.135(18): 3161–3171.

Lee, J. D., Kraus, P., Gaiano, N., Nery, S., Kohtz, J., Fishell, G., Loomis, C. A., &Treisman, J. E., 2001. An acylatable residue of Hedgehog is differentially required in Drosophila and mouse limb development. *Dev. Biol.* 233, pp.122-136.

Lee, R. T., Zhao, Z., & Ingham, P. W., 2016. Hedgehog signalling. *Development* 143(3), pp.367-72.

Leon, B. M., & Maddox, T. M., 2015. Diabetes and cardiovascular disease: Epidemiology, biological mechanisms, treatment recommendations and future research. *World Journal of Diabetes*, 6(13), pp.1246–1258.

Lewis, S. J., 2009. Prevention and treatment of atherosclerosis: a practitioner's guide for 2008. *Am J Med*. 122(1 Suppl), pp.S38-50.

Li F., Duman-Scheel M., Yang D., Du W., Zhang J., Zhao C., Qin L., Xin S., - 2010 - Sonic Hedgehog Signaling Induces Vascular Smooth Muscle cell proliferation via induction of the G1 cyclin-retinoblastoma axis.

Lin, C.-S., & Lue, T. F., 2013. Defining Vascular Stem Cells. *Stem Cells and Development*, 22(7), pp.1018–1026.

Lin, F., Wang, N., Zhang, T-C.,2012. The role of endothelial–mesenchymal transition in development and pathological process. *IUMBM Life*, 64(9), pp.717-723.

Livak KJ1., & Schmittgen TD., 2001. Analysis of relative gene expression data using real-time quantitative PCR and the 2(-Delta Delta C(T)) Method. *Applied Biosystems, 25(4):402-8.*

Lospinoso Severini, L., Ghirga, F., Bufalieri, F., Quaglio, D., Infante, P., & Di Marcotullio, L. (2020). The SHH/GLI signaling pathway: a therapeutic target for medulloblastoma. *Expert opinion on therapeutic targets*, *24*(11), 1159-1181.

Lovrics, A., Gao, Y., Juhász, B., Bock, I., Byrne, H. M., Dinnyés, A., Kovács, K. A., 2014. Boolean modelling reveals new regulatory connections between transcription factors orchestrating the development of the ventral spinal cord. *PLOS ONE*, [e-journal] 9 (11), p.11430.

Lu, J., Wang, D., & Shen, J., 2017. Hedgehog signalling is required for cell survival in Drosophila wing pouch cells. *Scientific Reports,* 7(11317)

Luengo-Fernández, R., Leal, J., Gray, A., Petersen, S., & Rayner, M., 2006. Cost of cardiovascular diseases in the United Kingdom. *Heart*, 92(10), pp.1384-9.

Lusis, A. J., Mar R., Pajukanta 2005. Genetics of coronary artery disease. *Annu Rev Genomics Hum Genet*, 5, pp.189–218

Ma, S., Duan, S., Liu, Y., & Wang, H. (2022). Intimal Hyperplasia of Arteriovenous Fistula. *Annals of Vascular Surgery*, *85*, 444-453.

Martínez-Rubio, A., & Pamias, R. F., 2017. Key Recent Advances In Atherosclerosis Treatment With Modern Lipid-Lowering Drugs: The New Frontier With PCSK9 Inhibitors European. *Cardiology Review*, 12(1), pp.30–2

Merchant, A., Joseph, G., Wang, Q., Brennan, S., Matsui, W., 2010 . Gli1 regulates the proliferation and differentiation of HSCs and myeloid progenitors. *Blood,* 115, pp.2391–2396.

Melnik, T., Jordan, O., Corpataux, J. M., Delie, F., & Saucy, F. (2022). Pharmacological prevention of intimal hyperplasia: A state-of-the-art review. *Pharmacology & Therapeutics*, *235*, 108157.

Moore, A., Mangoni, A. A., Lyons, D., & Jackson, S. H., 2003. The cardiovascular system. *Br J Clin Pharmacol*. 56(3), pp.254-60.

Muhlestein, J. B., 2003. Antibiotic treatment of atherosclerosis. *Curr Opin Lipidol*. 14(6), pp.605-14.

Musunuru, K., & Kathiresan, S., 2010. Genetics of coronary artery disease. *Annu Rev Genomics Hum Genet.* 11, pp.91-108.

Nguyen, P. K., Rhee, J.-W., & Wu, J. C., 2016. Adult stem cell therapy and heart failure, 2000 to 2016: a systematic review. *JAMA Cardiology* 1(7), pp.831–841.

O`Connor, S., Taylor, C., Campbell, L. A., Epstein, S., & Libby, P., 2001. Synopsis Potential Infectious Etiologies of Atherosclerosis: A Multifactorial Perspective. *Emerging Infectious Diseases* 7(5)

Orlandi, A. 2015. The Contribution of Resident Vascular Stem Cells to Arterial Pathology. *International Journal of Stem Cells*, 8(1), pp.9–17.

Pan, J. Y., & Zhou, S. H., 2012. The hedgehog signaling pathway, a new therapeutic target for treatment of ischemic heart disease. *Pharmazie*, 67(6), pp.475-81.

Pandolfi S., & Stecca B., 2015. Cooperative integration between HEDGEHOG-GLI signalling and other oncogenic pathways: implications for cancer therapy. Expert Reviews in Molecular Medicine. 2015;17:e5

Passman, J. N., et al., 2008. A sonic hedgehog signaling domain in the arterial adventitia supports resident Sca1+ smooth muscle progenitor cells. *PNAS*, 105 (27), pp.9349-9354.

Paulis L., Fauconnier J., Cazorla O., Thireau J., Soleti R., Vidal B., Ouille A., Bartholome., Bideaux P., Roubille F., Guennec J., Andriantsitohaina R., Martinez M Lacampagne A.,2015. Activation of Sonic hedgehog signaling in ventricular cardiomyocytes exerts cardioprotection against ischemia reperfusion injuries. *Scientific Reports*, [e-journal] 5(7983)

Peden, J. F., Hopewell JC., Saleheen D., Chambers JC, Hager J., Soranzo N., Collins R., Danesh J., Elliott P., Farrall M., Stirrups K., Zhang W., Hamsten A., Parish S., Lathrop M., Watkins H., Clarke R., Deloukas P., Kooner JS., Goel A., Ongen H., Strawbridge

RJ., Heath S., Mälarstig A., Helgadottir A., Öhrvik J., Murtaza M., Potter S., Hunt SE., Delepine M., Jalilzadeh S., Axelsson T., Syvanen AC., Gwilliam R., Bumpstead S., Gray E, Edkins S., Folkersen L., Kyriakou T., Franco-Cereceda A., Gabrielsen A., Seedorf U., MuTHER Consortium., Eriksson P., Offer A., Bowman L., Sleight P., Armitage J., Peto R., Abecasis G., Ahmed N., Caulfield M., Donnelly P., Froguel P., Kooner AS., McCarthy MI., Samani NJ., Scott J., Sehmi J., Silveira A., Hellénius ML., van't Hooft FM., Olsson G., Rust S., Assman G., Barlera S., Tognoni G., Franzosi MG., Linksted P., Green FR., Rasheed A., Zaidi M., Shah N., Samuel M., Mallick NH., Azhar M, Zaman KS., Samad A., Ishaq M., Gardezi AR., Fazal-ur-Rehman M., Frossard PM., Spector T., Peltonen L., Nieminen MS., Sinisalo J., Salomaa V., Ripatti S., Bennett D., Leander K., Gigante B., de Faire U., Pietri S., Gori F., Marchioli R., Sivapalaratnam S., Kastelein JJ., Trip MD., Theodoraki EV., Dedoussis GV., Engert JC., Yusuf S., Anand SS2011. A genome-wide association study in Europeans and South Asians identifies five new loci for coronary artery disease. *Nat Genet*. 43, pp.339–344.

Perin, E. C., 2006. Stem Cell Therapy for Cardiovascular Disease. *Texas Heart Institute Journal* 33(2), pp.204–208.

Pugsley, M. K., & Tabrizchi, R. J., 2000. The vascular system. An overview of structure and function. *Pharmacol Toxicol Methods* 44(2), pp.333-40.

Ramasamy, S. K., 2017. Structure and Functions of Blood Vessels and Vascular Niches in Bone. *Stem Cells International*.

Redmond EM., Hamm K., Cullen JP., Hatch E., Cahill PA., Morrow D. - 2013 - Inhibition of Patched-1 Prevents Injury-Induced Neointimal Hyperplasia.

Riccioni, G., & Sblendorio, V., 2012. Atherosclerosis: from biology to pharmacological treatment. *Journal of Geriatric Cardiology*, 9(3), pp.305–317.

Rimkus, T. K., Carpenter, R. L., Qasem, S., Chan, M., & Lo, H.-W., 2016. Targeting the Sonic Hedgehog Signaling Pathway: Review of Smoothened and GLI Inhibitors. *Cancers*, 8(2), p.22.

Rosano, G. M., Vitale, C., Marazzi, G., Volterrani, M., 2007. Menopause and cardiovascular disease: the evidence. Climacteric, 10(Suppl 1), pp.19-24.

Rudijanto, A., 2007. The role of vascular smooth muscle cells on the pathogenesis of atherosclerosis. *Acta Med Indones*. 39(2), pp.86-93.

Ruiz, I., Altaba, A., Palma, V., Dahmane, N., 2002. Hedgehog-Gli signalling and the growth of the brain. *Nat Rev Neurosci*. 3, pp.24–33.

Salazar, L. A., Cavalli, S. A., Hirata, M. H., Diament, J., Forti, N., Giannini, S. D., Nakandakare, E. R., Bertolami, M. C., & Hirata, R. D., 2000. Polymorphisms of the low-density lipoprotein receptor gene in Brazilian individuals with heterozygous familial hypercholesterolemia. *Braz. J. Med. Biol. Res*. 33, pp.1301–1304.

Sanchis-Gomar, F., Perez-Quilis, C., Leischik, R., & Lucia, A. 2016. Epidemiology of coronary heart disease and acute coronary syndrome. *Annals of Translational Medicine*, 4(13), p.256.

Simova, I., 2012. Intima-media thickness: Appropriate evaluation and proper measurement, described. *ESC Council for Cardiology Practice*, 13(21)

Sing, C. F., Stengård, J. H., & Kardia, S. L. R., 2003. Genes, Environment, and Cardiovascular Disease. *Arteriosclerosis, Thrombosis, and Vascular Biology*, 23, pp.1190-1196

Souilhol, C., Harmsen, M. C., Evans, P. E., & Krenning, G., 2018. Endothelial–mesenchymal transition in atherosclerosis. *Cardiovascular Research*, 114(4), pp.565–577.

Spence, J. D., 2016. Recent advances in pathogenesis, assessment, and treatment of atherosclerosis. *F1000Res.* 5(pii)

Stock, E. O., & Redberg, R., 2012. Cardiovascular disease in women. Curr Probl Cardiol. 37(11), pp.450-526.

Sun, R., Li, X., Liu, M., Zeng, Y., Chen, S., & Zhang, P., 2016. Advances in stem cell therapy for cardiovascular disease (Review). *International Journal of Molecular Medicine*, [e-journal] 38(1), pp.23–29.

Sylvester, K. G., & Longaker, M. T., 2004. Stem cells: review and update. *Arch Surg* 139(1), 93-9.

Taipale, J., Cooper, M. K., Maiti, T. and Beachy, P. A., 2002. Patched acts catalytically to suppress the activity of Smoothened. *Nature* 418, pp.892-897.

Thapa, R., Afzal, O., Kumar, G., Bhat, A. A., Almalki, W. H., Alzarea, S. I., ... & Dua, K. (2023). Unveiling the connection: long-chain non-coding RNAs and critical signaling pathways in breast cancer. *Pathology-Research and Practice*, 154736.

Thijssen, D. H. J., Carter, S. E., & Green, D. J., 2016. Arterial structure and function in vascular ageing: are you as old as your arteries? *The Journal of Physiology*, 594(8), pp.2275–2284.

Tigges U1, Komatsu M, Stallcup WB., 2013. Adventitial pericyte progenitor/mesenchymal stem cells participate in the restenotic response to arterial injury. 50(2):134-44

Varjosalo, M., & Taipale, J., 2007. Hedgehog signaling. *Journal of Cell Science*, [e-journal] 120, pp.3-6.

Villavicencio, E. H., Walterhouse, D. O., & Iannaccone, P. M., 2000. The Sonic Hedgehog–Patched–Gli Pathway in Human Development and Disease. *American Journal of Human Genetics*, 67(5), pp.1047–1054.

Wagers J. Amy., 2012. The Stem Cell Niche in Regenerative Medicine. *Cell Stem Cell.* pp 362-369.

Wang G1., Zhang Z., Xu Z., Yin H., Bai L., Ma Z.,Decoster MA., Qian G. , Wu G., 2010. Activation of the Sonic Hedgehog Signaling Controls Human Pulmonary Arterial Smooth Muscle Cell Proliferation in Response to Hypoxia. *Biochimica et Biophysica Acta*, 1803(12), pp.1359–1367.

Wang, H., Yuan, Y., Song, L., Qiu, G., Lai, X., Yang, L., Xiao Y1., Zhou L1., Yang H3., Li X3., Xu C3., Zhang X1., He MA1. , Wu T., 2017. Association between education and the risk of incident coronary heart disease among middle-aged and older Chinese: the Dongfeng-Tongji Cohort. *Scientific Reports*, 7(776)

Wang, X.,Gargalovic, P., Wong, J., Gu, J. L., Wu, X., Qi, H., , Pingzi Wen , Li Xi , Bing Tan , Rocky Gogliotti , Lawrence W. Castellani , Aurobindo Chatterjee , and Aldons J. Lusis Lusis, A. J ., 2004. Hyplip2, a new gene for combined hyperlipidemia and increased atherosclerosis. *Arterioscler Thromb Vasc Biol*., 24(10), 1928-34.

Watt, F. M., & Driskell, R. R., 2010. The therapeutic potential of stem cells. *Philosophical Transactions of the Royal Society B: Biological Sciences* 365(1537), pp.155–163.

West, J. B., Fu, Z., Deerinck, T. J., Mackey, M. R., Obayashi, J. T., & Ellisman, M. H., 2010. Structure-Function Studies of Blood and Air Capillaries in Chicken Lung Using 3D Electron Microscopy. *Respiratory Physiology & Neurobiology*, [e-journal] 170(2), p.202.

Westerweel, P. E., & Verhaar, M. C., 2008. Directing Myogenic Mesenchymal Stem Cell Differentiation. *Circ Res.*, [e-journal] 103, pp.560-561

Whitworth Deanne J., Tania A., Banks Vet J., 2014. Stem cell therapies for treating osteoarthritis: prescient or premature ; 202(3): 416–424).

Xiao, Q., et al., 2012. Impaired sonic hedgehog pathway contributes to cardiac dysfunction in type 1 diabetic mice with myocardial infarction. *Cardiovascular Research*, [e-journal] 95(4), pp.507–516

Xie Yao., Ye Fan., and Qingbo Xu. 2016. Vascular Regeneration by Stem/Progenitor Cells. *Arteriosclerosis, thrombosis, and vascular biology* 36 5 (2016): e33-40.)

Xynos, A., Corbella, P., Belmonte, N., Zini, R., Manfredini, R., Ferrari, G., 2010. Bone marrow-derived hematopoietic cells undergo myogenic differentiation following a Pax-7 independent pathway. *Stem Cells*, [e-journal] 28(5), pp.965-73.

Yelle, D., 2002. Atherosclerosis. *Nature*, 420(6917), pp.868-74.

Zhang, L., Bhaloo, S. I., Chen, T., Zhou, B., & Xu, Q., 2018. Role of Resident Stem Cells in Vessel Formation and Arteriosclerosis. *Circulation Research,* 122, pp.1608-1624.

Zhao Yingzi., Paul M. Vanhoutte., Susan W.S. Leung., 2015., Vascular nitric oxide: Beyond eNOS. Journal of Pharmacological Sciences, pp 83-94, ISSN 1347-8613.

Appendices

A

ANOVA output results

Figure 13: Effect of cyclopamine on mMSC growth

One-way ANOVA:

Source of Variation SS df MS F P-value F crit

Between Groups 15625.8 5 3125.16 18.74 <0.0001 3.11

Within Groups 2001.2 12 166.77

Total 17627 17

Dunnett's post-hoc test:

Comparison Mean Diff. q P-value

5 μM vs DMSO -12.3 1.89 0.2135

10 μM vs DMSO -18.7 2.87 0.0872

20 μM vs DMSO -26.5 4.07 0.0214

50 μM vs DMSO -42.1 6.47 0.0003

100 μM vs DMSO -58.9 9.05 <0.0001

Figure 14: Comparison of cyclopamine treatments to normal growth

One-way ANOVA:

Source of Variation SS df MS F P-value F crit

Between Groups 18956.3 6 3159.38 22.31 <0.0001 2.85

Within Groups 1982.7 14 141.62

Total 20939 20

Dunnett's post-hoc test:

Comparison Mean

Diff.

q P-value

0.5% serum vs 10% -61.2 8.89 <0.0001

5 µM vs 10% -14.5 2.11 0.1872

10 µM vs 10% -20.8 3.02 0.0653

20 µM vs 10% -28.7 4.17 0.0187

50 µM vs 10% -44.3 6.44 0.0002

100 µM vs 10% -61.1 8.88 <0.0001

Figure 15: Effect of HPI-4 on mMSC growth

One-way ANOVA:

Source of Variation SS df MS F P-value F crit

Between Groups 16814.7 5 3362.94 20.18 <0.0001 3.11

Within Groups 1998.3 12 166.53

Total 18813 17

Dunnett's post-hoc test:

Comparison Mean

Diff.

q P-value

5 µM vs DMSO -13.9 2.13 0.1743

10 µM vs DMSO -20.5 3.14 0.0621

15 µM vs DMSO -27.8 4.26 0.0178

25 µM vs DMSO -43.2 6.63 0.0005

50 µM vs DMSO -59.7 9.16 <0.0001

Figure 25: Overview of CNN1 expression across all treatment conditions

One-way ANOVA:

Source of Variation SS df MS F P-value F crit

Between Groups 21537.2 8 2692.15 25.63 <0.0001 2.51

Within Groups 1890.8 18 105.04

Total 23428 26

Dunnett's post-hoc test:

Comparison Mean Diff. q P-value

Differentiation vs Maint 33.3 5.05 0.0023

TGF-β vs Maint 41.5 6.29 0.0007

r-SHh vs Maint 42.9 6.5 0.0005

r-SHh + Cyclo vs Maint 22.1 3.35 0.0312

r-SHh + HPI-4 vs Maint 18.7 2.83 0.0428

r-SHh + Anti-Pat vs Maint 24.8 3.76 0.0185

r-SHh + IgG vs Maint 40.4 6.12 0.00

B

Material	Source	Catalog Number
Embryonic qualified FBS	ATCC	30-2020
EMEM	ATCC	30-2003
Mouse Smooth Muscle Cells	ATCC	CRL-2797 Lot 58678387
4 X SDS Laemmli Buffer	Fannin	161-0747
Primer Sets	IDT	N/A
Alexa Fluor® 488 Goat anti-rabbit (H+L)	Invitrogen	A-11008
Alexa Fluor® 488 Goat anti-mouse (H+L)	Invitrogen	A-11001
Alexa Fluor® 488 Donkey anti-goat (H+L)	Invitrogen	A-11055
2-mercaptoethanol 50mM solution	Invitrogen	31350-010
DEPC treated water	Invitrogen	750024
Magcore cartridges total RNA Cultured Cells 610	MSC	MRC-01 // MRC-02
Sensi-fast SYBR No-Rox one step kit	MSC	BIO-72005
TGFβ1	PeproTech	N/A
PDGF-BB	PeproTech	N/A
Dnase I, Rnase-free	Pierce	89836
BCA Assay kit	Pierce	23227
Page ruler ladder	Pierce	26620
TGFβ1	R&D Systems	7666-MB-005/CF
2-mercaptoethanol	Sigma-Aldrich	M-7154
30% bis/acrylamide solution	Sigma-Aldrich	A3699
Anti-goat 2° antibody, HRP conjugated	Sigma-Aldrich	A5420
Anti-mouse 2° antibody, HRP conjugated	Sigma-Aldrich	A5278
Anti-rabbit 2° antibody, HRP conjugated	Sigma-Aldrich	A0545
APS	Sigma-Aldrich	A3678
BSA	Sigma-Aldrich	A4503
Cyclopamine hydrate	Sigma-Aldrich	C4116
DMEM	Sigma-Aldrich	D5796
DMSO	Sigma-Aldrich	C6164
Fatty acid free BSA	Sigma-Aldrich	A7030
FBS	Sigma-Aldrich	F9665
Gel Blotting Paper	Sigma-Aldrich	Z698172
Glycine	Sigma-Aldrich	G8898
HPI-4	Sigma-Aldrich	H4541
L-Glutamine	Sigma-Aldrich	G7513
Pen-Strep	Sigma-Aldrich	P4333
Ponceau S stain	Sigma-Aldrich	P7170
Protease inhibitor	Sigma-Aldrich	P8340
RIPA	Sigma-Aldrich	R0278
TEMED	Sigma-Aldrich	T7024
TMB	Sigma-Aldrich	T0565
Triton X-100	Sigma-Aldrich	T8787
Trypan Blue	Sigma-Aldrich	T8154
Trypsin	Sigma-Aldrich	T4174

Tween	Sigma-Aldrich	P1379
α-MEM	Sigma-Aldrich	M0644
rShh	Sigma-Aldrich	S0191
Anti-Calponin antibody	Abcam	ab46794
Anti-Smooth muscle myosin heavy chain 11	Abcam	ab683
Patched 1/PTCH Antibody	Biotechne	H00005727-M03
Alamar Blue	Biosciences	DAL1100